ROBUST STRING STABILITY OF VEHICLE PLATOONS WITH COMMUNICATION

A Dissertation

by

SHYAMPRASAD KONDURI

Submitted to the Office of Graduate and Professional Studies of
Texas A&M University
in partial fulfillment of the requirements for the degree of

DOCTOR OF PHILOSOPHY

Chair of Committee,	Prabhakar R. Pagilla
Committee Members,	Swaroop Darbha
	Sivakumar Rathinam
	Suman Chakravorty
Head of Department,	Andreas A. Polycarpou

August 2017

Major Subject: Mechanical Engineering

ABSTRACT

This work investigates longitudinal spacing policies and vehicular communication strategies that can reduce inter-vehicular spacing between the vehicles of automated highway platoons, in the presence of parasitic actuation lags. Currently employed platooning technologies rely on the vehicle's onboard sensors for information of the neighboring vehicles, due to this they may require large spacing between the vehicles to ensure string stability in the presence of uncertainties, such as parasitic actuation lags. More precisely, they require that the minimum employable time headway ($h_{\min}$) must be lower bounded by $2\tau_0$ for string stability, where τ_0 is the maximum parasitic actuation lag. Recent studies have demonstrated that using vehicular communication one may be able to employ smaller spacing between vehicles while ensuring robustness to parasitic lags. However, precise results on the extent of such reduction are sparse in the literature . In this work, platoon string stability is used as a metric to study controllers that require vehicular communication, and find the amount of *reduction in spacing* such controllers can offer.

First, the effects of multiple vehicle look ahead in vehicle platoons that employ a Constant Spacing Policy (CSP) based controller without lead vehicle information in the presence of parasitic lags is studied and string instability of such platoons is demonstrated. A robustly string stable CSP controller that employs information from the leader and the immediate predecessor is considered to determine an upper bound on the allowable parasitic lag; for this CSP controller, a design procedure for the selection of controller gains for a given parasitic lag is also provided. For a string of vehicles adopting a Constant Time Headway Policy (CTHP), it is demonstrated that the minimum employable time headway can be further decreased via vehicular communication in the following manner: (1) if the position, velocity and acceleration of the immediate predecessor vehicle is used, then the

minimum employable time headway $h_{\min}$ can be reduced to τ_0; (2) if the position and velocity information of r immediately preceding vehicles is used, then $h_{\min}$ can be reduced to $4\tau_0/(1+r)$; (3) furthermore, if the acceleration of 'r' immediately preceding vehicles is used, then $h_{\min}$ can be reduced to $2\tau_0/(1+r)$; and (4) if the position, velocity and acceleration of the immediate and the r-th predecessors are used, then $h_{\min} = 2\tau_0/(1+r)$. Note that cases (3) and (4) provide the same lower bound on the minimum employable time headway; however, case (4) requires much less communicated information. Representative numerical simulations that are conducted to corroborate the above results are discussed.

Vehicle formations employing ring structured communication strategies are also studied in this work and a combinatorial approach for developing ring graphs for vehicle formations is proposed. Stability properties of the platoons with ring graphs, limitations of using ring graphs in platoons, and methods to overcome such limitations are explored. In addition, with ring communication structure, it is possible to devise simple ways to reconfigure the graph when vehicles are added to or removed from the platoon or formation, which is also discussed in this work. Further, experimental results using mobile robots for platooning and two-dimensional formations using ring graphs are discussed.

To my parents

Konduri Chandra Mouli and Konduri Durga,

and my wife

Rajanala Rachana,

ACKNOWLEDGMENTS

I would like to express my sincerest gratitude to my advisor, and dissertation committee chairman Prof Prabhakar R. Pagilla for his supervision, and support that has made this work possible. His encouragement is one of the main driving factors in starting this work. Working under his guidance has been a wonderful learning experience both professionally and personally. I have learnt a lot from his courses in control theory, which I will be using for the rest of my professional life.

I would like to express my gratitude to Dr. Swaroop Darbha for his invaluable inputs throughout my graduate studies, that has resulted in improving this work significantly. I would like to thank Dr. Sivakumar Rathinam and Dr. Suman Charavorty for being a part of my committee and for their inputs in improving this dissertation. I thank Dr. Rhinehart and Dr. Lucca from OSU and Dr. Girish Chowdhary from UIUC for their insights during the initial stages of this work.

I want to thank Dr. McAdams and the Mechanical Department staff, especially Sandy Havens for all her help in keeping up with the forms and other paper work.

I want to specially thank my wife Rachana for being the beacon of my sanity and for giving me the much needed push to begin my work towards a Ph.D. She is more than patient in putting up with my charades and was a constant motivation. I would be nothing but a nobody without her by my side. She has constantly encouraged me in my pursuits both academically and personally.

I want to thank my brothers in arms Konduri Aditya and Orlando Cobos for their constant support and encouragement, and for the countless hours spent on discussing issues ranging from university parking problems to philosophical issues in life and work. I want to thank my colleagues at TAMU Mitch, Angel, Yalun, and those at OSU Emilio Gabino,

Kedar, Sandeep and Rakshit. It has been a joy working with them. I also want to give a special thanks to Cynthia, Gabo and Izzie for all the love and for the delicious Ecuadorian food.

I am indebted to my parents Chandra Mouli and Durga, and to my brother Subramanyam for their support throughout my endeavors. My fathers gyan has helped me during troubling times in my life. I also want to thank Rachana's family for their support. Last but not the least, I wish to thank all my friends.

CONTRIBUTORS AND FUNDING SOURCES

Contributors

This work was supported by a dissertation committee consisting of Professor Prabhakar R. Pagilla, Prof. Swaroop Darbha, Prof. Sivakumar Rathinam of the Department of Mechanical Engineering and Prof. Suman Chakravorty of the Department of Aerospace Engineering.

All the work conducted for the dissertation was completed by the student independently.

Funding Sources

Graduate study was supported by a fellowship and a graduate assistantship from Oklahoma State University, and graduate reasearch assistantship at Texas A&M University.

TABLE OF CONTENTS

Page

LIST OF FIGURES

FIGURE Page

LIST OF TABLES

TABLE Page

1. INTRODUCTION

Vehicular platoons have been studied extensively in the literature for the past several decades, as they are expected to decrease travel times, increase fuel efficiency and highway capacity, and decrease accidents caused by human errors. Information flow between the vehicles and spacing policies employed to maintain the inter-vehicular spacing play a vital role in maintaining the platoon, and as a result there has been significant ongoing research in these areas. In particular, one is interested in finding suitable communication strategies and developing controllers that are scalable to increases in the platoon size. Ideally, reducing the spacing between the vehicles in the platoon would increase highway capacity and fuel efficiency. However, if the vehicles are very close to each other, the reaction time to account for any transient disturbances is reduced, and this can lead to collisions [1]. The selection of the desired spacing distance and maintaining stability of the platoon for that spacing is further complicated when one also has to ensure robustness to system uncertainties, such as parasitic lags and time delays. Current technologies where vehicles use only their onboard sensors for information tend to employ larger inter-vehicular spacing to account for system uncertainties; this may not provide adequate improvement in highway capacity or fuel efficiency [2]. The focus of this work is on the investigation of spacing policies, communication strategies, and controller designs that can aid in reducing inter-vehicular spacing while ensuring robustness to parasitic lags.

1.1 Autonomous Transportation

Autonomous Vehicles (AVs) are poised to become the next major advancement in the evolution of vehicular transportation, thanks to the heavy investment from industries in passenger and cargo sectors. Traditionally, autonomous transportation systems have been frequently employed in mass transportation with a limited area of operation, such as air-

ports and public transport systems. Examples include terminal transit systems in airports, such as Dallas, Dubai, Newark, London Heathrow, etc. [3], and metro transit systems in cities, such as Milan, Copenhagen, London, Turi, etc [4]. There are also examples of personal autonomous vehicles around the world, some of them are Personal Rapid Transit (PRT) system at the Heathrow Airport [5], the LUTZ project at Milton Keyes in UK [6], the Uber autonomous taxis in Pittsburgh, USA, the Google autonomous car, etc. Although such projects are successful their operational scope and region is limited. For instance the PRT system at Heathrow Airport, uses personal autonomous pods that travel in fixed paths similar to airport trains. There have been some efforts to bring fully autonomous or semi autonomous vehicles onto roadways and highways, examples of such efforts are the PATH program in California (USA) [7] and SARTRE in Europe [8]. At the core of these efforts is a vehicle capable of autonomous motion.

Many commercially available cars have at least some level of autonomy or autonomous features, such as cruise control systems, blind spot and rear monitoring systems, etc. Some models offer more semi-autonomous functions, such as parking assistance, obstacle detection and haptic feedback, autonomous braking, automated lane keeping, etc. There are some latest vehicles in the market that offer very advanced autonomous driving features, such as the Tesla's Autopilot system, Audi and Volvo autonomous driving systems [9]. With improvements in processor size and processing capabilities, sensor and communication systems, autonomous transportation is closer than ever for the reach of common people. The time horizons set by government regulators and industry experts indicate that commercial sales of level 4 autonomous (highly autonomous) vehicles are expected to begin around 2020 and level 5 (fully autonomous) vehicles are expected to be commercially available between 2023-2025 [10]. This in-turn has increased the interest from industry and academia towards solving the problems involved in commercializing autonomous transport systems.

A bulk of the research and implementation efforts in automated transportation has focused on commercial trucking or freight transport [11, 12]. There are several reasons for this: possibility of increase in the highway capacity, operational safety, and the improvements in fuel efficiency of the freight transport. Furthermore, in many countries, trucks and freight transport vehicles are more regulated than passenger vehicles, and commercial trucks are used more frequently than regular passenger cars. The Environmental Protection Agency (EPA) estimates that the freight transport accounts for a sizable share of carbon emissions and fuel consumption compared to other types of road vehicles [13]. Any small reduction in fuel consumption of individual trucks will decrease the overall fuel consumption of the industry. With this in mind several countries and labs around the world have focused on studying Autonomous Highway Systems (AHS) [2, 7, 8, 11]. There are efforts from the automobile industry to develop fully autonomous trucks, such as the Volvo and Daimler self driving truck tested in Europe and Otto's self driving truck in USA. There are also efforts in setting up the infrastructure for autonomous highway travel [2, 11].

Research on AHS covers a wide variety of theoretical and practical problems, such as road infrastructure, vehicle localization, environment sensing, vehicle control, autonomous cruise control (ACC), cooperation between individual vehicles, vehicle to vehicle communication, vehicle longitudinal and lateral control, etc [1, 11, 14, 15]. Substantial progress has been made in these areas over the past few decades, evidence of which can be seen from the road tests conducted in [7, 8, 16].

1.2 Vehicle Platoons

One of the key areas of research is the autonomous highway platoons, where multiple autonomous vehicles are bound together in the form of platoons. Traditionally, the term 'platoon' was used to refer vehicles traveling in a single lane with a fixed distance between them. However, many recent studies use the term platoon to refer to any string of auto-

mated vehicles on the highway. Vehicles in the platoon are expected to travel together at the same speed and with a fixed or varying spacing between each other. A typical setup

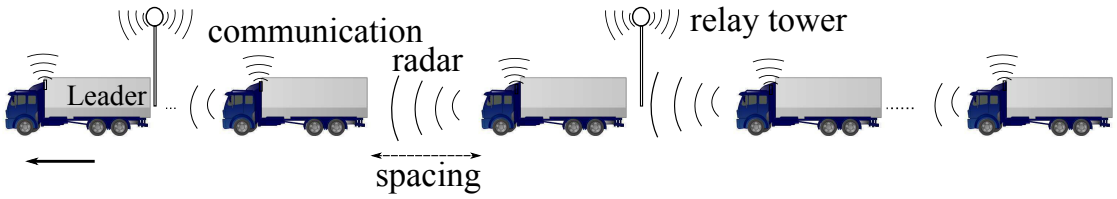

Figure 1.1: A typical setup of vehicles in platoon

of autonomous vehicles traveling in a platoon is shown in Figure 1.1. The vehicles are equipped with an array of onboard sensors, such as GPS, radar, sonar, etc. In more recent setups the vehicles are also equipped with short range V2V communication equipment. The highway may also be setup with special infrastructure, such as the information relay towers, traffic cameras, etc. Some of the challenges of vehicle platoons include: grouping vehicles into a platoon, specifying the spacing between individual vehicles and their speed, dealing with vehicle entry and exit in and out of the platoon, etc [2, 17]. As mentioned earlier, the key goals of platooning vehicles are that each vehicle maintains a speed consistent with rest of the platoon and a safe distance from its neighboring vehicle, which in general is the vehicle that is immediately ahead of it, called the preceding or predecessor vehicle. A spacing policy and an associated controller are used by every vehicle for this purpose. The spacing policy dictates the desired inter-vehicular spacing between the vehicles and the associated controller uses information about the vehicle's own state and that of the preceding vehicle to generate the control input. Control input is usually applied as a desired acceleration to the vehicle.

Depending on how the spacing between the vehicles is determined, the spacing policies fall into two broad categories a Constant Spacing Policy (CSP) and a Variable Spacing

Policy (VSP). In a CSP, each vehicle is controlled to maintain a desired constant following distance irrespective of the velocity of the vehicles in the platoon. Several types of CSP based controllers are discussed in [18], such as a basic CSP controller, CSP controller with acceleration feedback, CSP controller with multiple vehicle feedback, etc. Some other works from the literature that also discuss CSP controllers are [15, 19–21]. It is known that *some* CSP based controllers may lead to string instability especially in the absence of the lead vehicle information [22]. A VSP based controller has the potential to circumvent string instability with onboard information only. In a VSP, the desired following distance of a controlled vehicle changes with its speed. Chief among the VSPs is the Constant Time Headway Policy (CTHP) [23], where the desired following distance of a controlled vehicle varies linearly with its speed and the constant of proportionality is referred to as the time headway (h_w). At zero speed the spacing between the vehicles is minimum and it increases with the speed of the vehicles. Smaller time headway is desirable as this translates to higher capacity and efficiency [2, 12]. Therefore, selecting a time headway that is as small as possible while ensuring safe and comfortable operation of the vehicles is essential for platoons using CTHP controllers.

Many other types of variable spacing policies have been explored throughout the literature. A constant safety factor based policy was adopted in [24]. An exponential nonlinear spacing law was used in [25] and its performance was compared to the CSP and CTHP controllers. A delay based spacing policy was discussed in [14]. A nonlinear variable spacing policy was used in [26]. In this dissertation only the CSP and CTHP are employed as these are the most commonly used in the literature.

Controllers utilize the desired spacing obtained from the spacing policy and the actual spacing obtained from sensors or communication or a combination of both, to compute the control input. They are designed to satisfy two important requirements: the individual vehicle stability and the platoon string stability. Vehicle stability ensures that each vehicle

follows the preceding vehicle at a desired distance in the absence of any external disturbances. String stability is the ability of the controller to attenuate disturbances in spacing errors as they propagate upstream in the vehicle string. If the platoon is not string stable, then a disturbance on a vehicle (e.g: change in velocity) is amplified as it propagates upstream to the following vehicles (especially at the tail of the platoon); this may in-turn lead to collisions, jerky vehicle response, uncomfortable and unsafe driving experience for passengers. String stability is a commonly used performance metric for studying the transient behavior of the platoon while designing longitudinal spacing controllers for AVs.

String stability was studied extensively in the literature starting from the 1970s [18, 23, 27–30]. Several authors in the past have presented formal and mathematical definitions of string stability in vehicle platoons [19, 23, 27, 31]. Some of the initial definitions for string stability in the context of vehicle platoons are provided in [27, 28]. A more formal definition of string stability is given in [32]. It is known from prior research at California PATH that string stability and high throughput can be guaranteed with CSP based controllers if the velocity of a reference vehicle is broadcast to all vehicles in a platoon and employed as feedback in all following vehicles. This would require that every vehicle needs to communicate with the lead vehicle of the platoon, which may not be efficient over long distances. Instead of the reference vehicle information, vehicles in the platoon may utilize information of multiple immediate predecessors within their communication range. However, it was also shown primarily using numerical simulations that if the controllers were to use information from multiple immediate predecessors, then the platoon *may* only be weakly string stable [22]. It is known that controllers employing CTHP are in general string stable [19].

Traditional vehicle control systems, such as the Adaptive Cruise Control (ACC) system rely only on onboard sensors [2, 33], and employ CTHP controllers owing to their string stability. In [34], it was shown that employing a small headway may result in string

instability in the presence of parasitic actuation/sensing lags; in particular, it was shown that if τ_0 is the maximum parasitic lag and h_w is the time headway, then string stability can be maintained only if $h_w \geq 2\tau_0$. Typical values of time headway considered in truck platooning are in the range of $0.5 - 1$ s, which at a speed of 65 mph (≈ 30 m/s) equate to a physical spacing of $15 - 30$ m. Therefore, the additional constraints due to parasitic lags cause the vehicles to be too far apart. Further, it was shown that even if most of the vehicles on the highway are equipped with ACC systems this would not improve the efficiency of traffic movement and in some scenarios ACC may also cause instabilities [35, 36]. Thus, the main drawback of ACC systems is that the desired spacing between vehicles must be large to maintain string stability. For this reason researchers have started looking for methods to improve ACC systems in an effort to reduce time headway.

Intuitively, if the vehicle's controller has knowledge of what the predecessor vehicle is about to do then it may be possible to react more quickly to the changes. For example, if the vehicle knows that the predecessor vehicle is about to reduce speed, then it can also start reducing the speed or take other necessary actions. This is the idea behind cooperation between the vehicles in the platoon that are equipped with ACC systems, and this strategy is referred to as the Cooperative Adaptive Cruise Control (CACC). In the CACC system controllers use information obtained from the sensors as well as from the Vehicle to Vehicle (V2V) and/or Infrastructure to Vehicle (I2V) communication. CACC is a fairly new idea which is extensively studied in the recent literature partly due to the advancements in the communication technologies at the disposal of the automotive industry. A detailed and formal definition of the concepts involved in CACC of vehicle platoons is presented in [2] and a review of the existing literature is presented in [1]. A platoon of cars using CACC was the focus of study in [37] where the authors have found that using CACC with a CTHP controller produces string stable platoons when using homogeneous vehicles in the platoon. The authors acknowledged that string stability of the platoons with

CACC needs further investigation, especially in regard to the comparison of performance of various spacing controllers.

While CTHP was initially proposed for AVs to circumvent the need for vehicular communication, the use of V2V and I2V communications when employing CTHP may seem paradoxical and this point was not clearly articulated in the literature [38]. Recently, the *necessity* for using communication when employing CTHP in trucks was recently highlighted by Ploeg [16], who noticed string instability without V2V or I2V communication in a platoon of three trucks when employing a time headway of about 0.35 seconds. The authors in [33] used string stability as a metric to show that using predecessor vehicle's acceleration can reduce the employable time headway from $2\tau_0$ while ensuring string stability. Other platoon experiments and numerical simulations also seem to suggest that employing the acceleration information of immediately preceding vehicles can help reduce the employable time headway in CTHP [2, 19, 33, 37, 39].

With the recent advances in V2V and I2V communications, and consequently the investigations into CACC systems, a natural question arises in the context of autonomous vehicles (AVs): what traffic safety and throughput benefits can be guaranteed through the use of V2V and I2V communications? Several other works have demonstrated the advantages of using V2V communication in other areas of vehicle platooning. The benefits of using V2V communication among AVs for collision avoidance via an emergency lane change maneuver are discussed in [40]. In an emergency braking scenario, inter-vehicular communication aids coordination amongst vehicles in a platoon leading to a reduction in the probability of a collision, expected number and severity of collisions [41]. In [42, 43], the authors reported that information from upstream vehicles results in a reduction of collisions and pileups. A safety factor called Deceleration based Surrogate Safety Measure (DSSM) was computed and transferred to downstream vehicles in [44]. Some studies have investigated the effect of the limitation of communication on platoon string stability.

For example, in [45], some design guidelines on selection of controllers and operational parameters were presented by considering the effect of delays and sampling in communication channels.

However, most of the literature on longitudinal spacing controllers have only demonstrated the benefits of communication using numerical simulations or experiments with a few exceptions, such as [33]. In this context some of the problems include: can a CACC system utilizing CSP controllers guarantee string stability, what kind of spacing policy will provide most benefits, how does uncertainty in the communication affect the performance, etc. Although some forms of CSP controllers were already shown to benefit from using communication (i.e., the leader or reference vehicle information), prior research and numerical results also suggest that V2V communication does not help many other forms of CSP based controllers in guaranteeing string stability [18]. It is of importance to investigate how robust the string stability of CTHP controllers is when communication is used to gain additional information; that is, how does one characterize the improvements on selection of time headway for CTHP controller when communication is available. Selection of the smallest time headway for a CTHP controller in CACC systems with string stability guarantee is still an open problem.

It is also of interest to study if any unconventional information flow between vehicles can provide additional benefits. Conventional information flow in the platoons has always been from the front of the platoon to the back, i.e., the leader to the upstream. The only common exception is the bidirectional communication where the vehicles use information from their predecessor and follower vehicles. Vehicular communication can be useful in creating other types of information exchange which *may* be more beneficial. A ring type communication is like a predecessor follower type communication with an additional communication link between the lead vehicle and the tail vehicle of the platoon. Ring graphs have been considered in the literature mainly for cyclic pursuits around an equilib-

rium point [46, 47]. Each vehicle is modeled as a kinematic unicycle to study equilibrium formations and global behavior. The use of ring communication graphs to maintain vehicle platoons was investigated in [48], and a platoon solution to guarantee stability is derived using a simple coordination control law based on the ring interconnection. Ring graphs with vehicle platoons were also studied in [49] where the scalability of the controller is discussed along with some experimental validation. Some more recent studies that use ring graphs in vehicle formations can be found in [25] and [26]. Unlike predecessor follower type graphs, ring graphs may also be useful in 2D and 3D formations where maintaining the formation shape is of utmost importance. Traditionally vehicles in the formation rely on information from all the vehicles within their neighborhood, however this will require exchange of substantial amount of information. In such scenarios ring graphs may be useful to maintain tight formations. Clearly, the advantages, limitations and design considerations when using ring graphs for communication should be further explored.

The results from recent literature motivate the prospective users to employ additional information that can only be obtained using V2V or I2V communication to improve the highway capacity, passenger safety, comfort and efficiency of the autonomous vehicle platoons. However, there are several questions that need to be addressed before full scale implementation of such systems, such as what kind of information is beneficial, is information from communication beneficial for all the controllers utilizing CSP or CTHP, and can the improvements in performance be quantified, etc. In the context of CTHP, the following are addressed in this work: is it possible to reduce the minimum time headway if V2V communication is used? If yes, then by what factor?

1.3 Contributions

A key contribution of this research is to outline and quantify the advantages of using vehicular communication in the longitudinal spacing control of the vehicles in a platoon.

Multiple information exchange methods that require V2V communication are studied to determine how and what information will impact the time headway. For CSP controllers the effect of using information from multiple predecessors on string stability is investigated. A majority of this work is geared towards investigating CTHP controllers. String stability in the presence of parasitic lags for platoons using CTHP controllers, that employ immediate predecessor acceleration information, multiple predecessors information and immediate predecessor/follower information, is studied to find the effect of this additional information on minimizing the time headway. Ring type information flow and its effect on the control of a platoon or formation is also studied. The individual contributions are listed below.

- When the platoon uses a CSP controller with information from 'r' immediate predecessor vehicles, then the platoon is not robustly string stable.
- If the CSP controller uses information from the immediate predecessor and the leader of the platoon, then the platoon is robustly string stable. A bound on the maximum parasitic lag, which is as a function of controller gains, under which robust string stability can be maintained is determined [50].
- When the platoon uses a CTHP controller with the position, velocity and acceleration information of the immediately preceding vehicle, then the lower bound on the minimum employable time headway is equal to the parasitic lag value τ [51].
- If the CTHP controller employs the position, velocity and acceleration information of 'r' immediate predecessors, then the minimum employable time headway is $2\tau/(1+r)$.
- If the CTHP controllers employs information from only the immediate and the 'r^{th}' predecessors, then the minimum employable time headway is $2\tau/(1+r)$ [51].

- In the absence of vehicular communication, predecessor vehicle brake light status may be used to improve time headway.

- If ring communication is used with the CTHP controller, then the platoon is stable irrespective of the size of the platoon. Furthermore, vehicles can be added to or removed from the platoon without affecting the platoon string stability. For large platoons and formations in two- and three-dimensions, ring communication graphs may be obtained by modeling the problem as a special case of the Traveling Salesman Problem (TSP) [52, 53].

The rest of this document is organized as follows. A detailed background of the problem, including a brief overview of the vehicle dynamics, definition of string stability and methods used to analyze it, is presented in Chapter 2. Prior analysis of string stability when using CSP and CTHP controllers is also discussed in this chapter. Results pertaining to the CSP controller with multiple predecessor vehicle information, and CSP controller with leader information, along with a controller design procedure are presented in Chapter 3. Chapter 4 involves the analysis of CTHP controllers and their respective improvements in the minimum employable time headway. Numerical studies that involve use of predecessor brake light information in ACC systems and information quantization in vehicular communication are presented in Chapter 5. Ring graphs for communication, stability of platoons, reconfiguration, and experimental validation using mobile robots are discussed in Chapter 6. A summary of the dissertation along with conclusions drawn and future research directions are presented in Chapter 7.

2. VEHICLE PLATOONS AND SPACING POLICIES

In this chapter, a brief review of a commonly employed vehicle model, spacing policies and string stability analysis methods from the literature is presented. First, the dynamic model for individual vehicles that is used for the analysis of the control laws is discussed in the Section 2.1, followed by a discussion on the information flow models and the spacing policies employed in the vehicle platoons. In Section 2.2 the string stability and robust string stability of a platoon are defined and two common methods employed in the literature for the analysis of string stability are discussed. Some prior results pertaining to the string stability of platoons with CSP and CTHP controllers are discussed later in Section 2.2.1.

2.1 Vehicle Dynamics

Consider a platoon of N homogeneous vehicles moving in a single lane on a highway. Let i ($i = 1,\ 2,\ 3, \cdots,\ N$) represent the index of vehicle in the platoon. Let x represent the longitudinal position of the vehicle, and let each vehicle be a body of mass m with tire friction p and aerodynamic drag coefficient of c. A commonly used vehicle model for the longitudinal position control of the vehicle is [18],

$$ma_i(t) + cv_i^2(t) = \hat{u}_i(t) - p_i \tag{2.1}$$

where a, v and $\hat{u}$ are the acceleration, velocity and the control input of the vehicle, and the subscript i denotes that the variable corresponds to the i^{th} vehicle of the platoon. Other models that also account for the length of the vehicle, location of its center of gravity, etc., were considered in the literature; for example see [15, 16, 54]. The above dynamic model

can be simplified by using the following control input,

$$\hat{u}_i(t) = cv_i^2(t) + mu_i(t) + p_i.$$

Then the simplified dynamic model of the i^{th} vehicle is,

$$a_i(t) = u_i(t), \tag{2.2}$$

where u_i is the augmented or the synthetic input of the i^{th} vehicle. A typical longitudinal position control architecture for AVs is shown in Figure 2.1 [15, 55]. The upper controller uses information from the predecessor(s) feedback and the desired spacing to compute the control input u_i (usually in the form of a desired acceleration or a velocity set point). The lower level controller adjusts the engine throttle or wheel brakes to track the set point. Due to the limitations on the bandwidth, there is a parasitic actuation lag associated with the acceleration or deceleration tracking. Failure to account for such parasitic lags may result in the saturation of control input which can cause undesired behavior. Hence, the upper level controller is designed such that the desired response is guaranteed robustly in the presence of these bandwidth limitations.

For simplicity, one can approximate the behavior of the engine and the brake dynamics as a first order perturbation to the simple vehicle model in equation (2.2). The perturbed model of the vehicle is as follows,

$$\tau\dot{a}_i(t) + a_i(t) = u_i(t), \tag{2.3}$$

where τ is the parasitic actuation lag. It is assumed that τ is *uncertain* and that $\tau \in (0, \tau_0]$. Longitudinal spacing controllers are used in the upper level and they require two components, (1) information of neighboring vehicles, and (2) spacing policy, as shown in

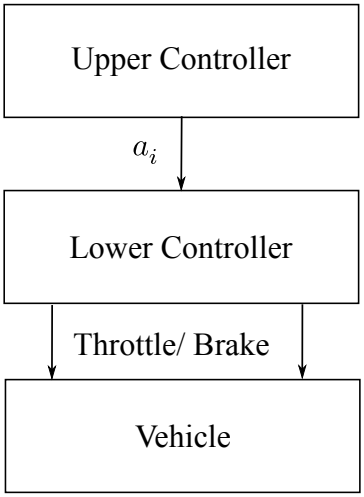

Figure 2.1: Longitudinal control structure of the vehicle in AVs.

Figure 2.2.

2.1.1 Information Flow Graphs

Information used by the longitudinal spacing controller may include the position, velocity and sometimes the acceleration of the neighboring vehicles, and it may be obtained using onboard sensors or vehicular communication. Graph theory is frequently employed to represent and analyse the information exchange among the vehicles in the platoon. The graphs that are used to represent the information exchange are called the information flow graphs. One of the most commonly used information flow graph in vehicle platoons is the predecessor follower (PF) graph or the path graph shown in Figure 2.3. Another common information flow graph consists of every vehicle exchanging information from both the predecessor and the follower vehicle; it is called the bidirectional information flow graph, shown in Figure 2.4.

In large platoons a controller may obtain information from vehicles that are further downstream using vehicular communication. An example of such an information flow graph is the Leader Predecessor Follower (LPF) graph shown in Figure 2.5, where each

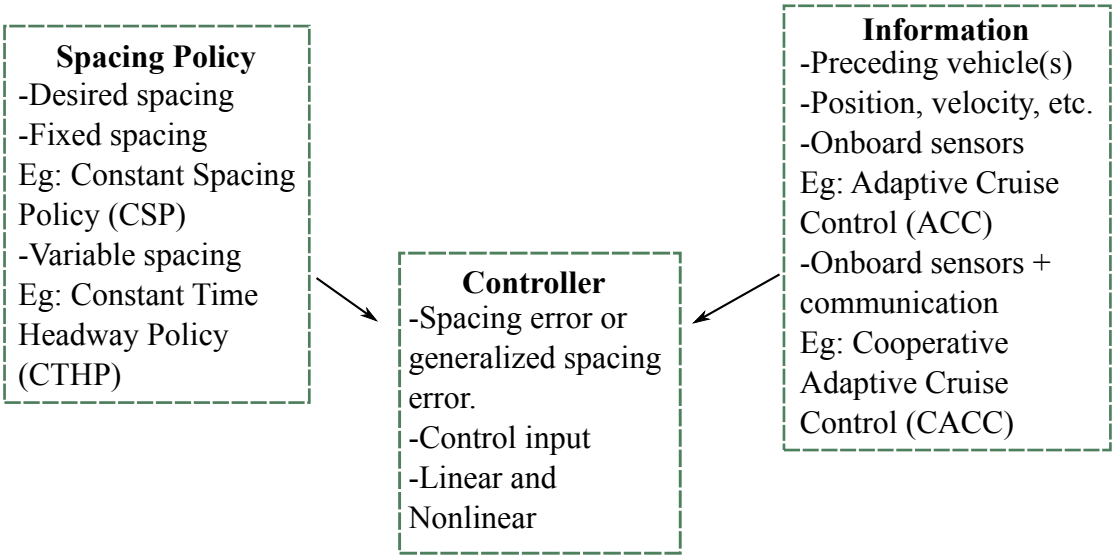

Figure 2.2: Components of longitudinal spacing controllers.

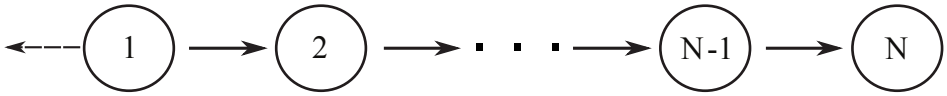

Figure 2.3: Vehicle platoon with predecessor follower type information flow, solid arrows indicate the direction of information flow

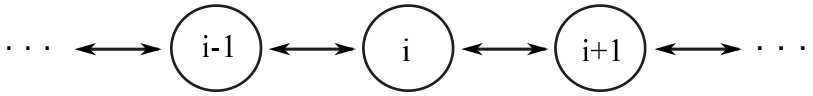

Figure 2.4: Vehicle platoon with bi-directional information flow

vehicle obtaines information from its own predecessor as well as the leader of platoon. Another example of such an information flow graph is shown in Figure 2.6, where every vehicle obtains information from three predecessor vehicles. It was demonstrated in multiple studies that information exchange plays an important role in the stability and string stability of the platoon [56–58].

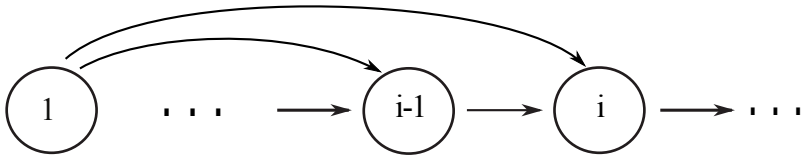

Figure 2.5: Platoon of vehicles with information flow from the platoon leader and predecessor (LPF)

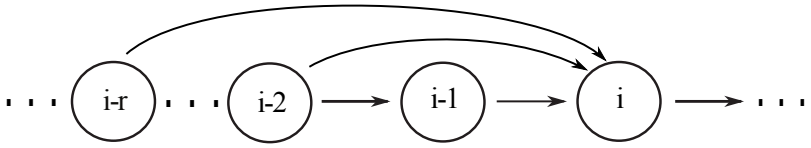

Figure 2.6: Vehicle platoon with predecessor follower type information flow from 'r' predecessor vehicles.

2.1.2 Spacing Policies and Controllers

In this section some controllers that employ the CSP and CTHP are discussed. Consider the string of vehicles shown in Figure 2.7, where d is the minimum spacing or the standstill spacing between the vehicles. For CSP controllers, d is the desired spacing and for the CTHP controllers it is the desired standstill spacing.

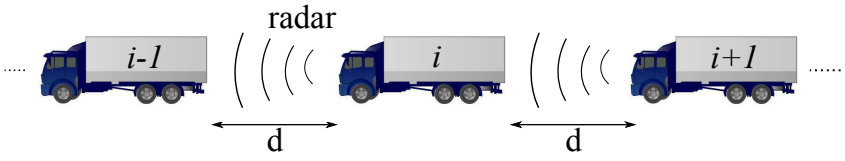

Figure 2.7: String of vehicles using controller with CSP.

The spacing error (e_i) of the i^{th} vehicle is the difference between the actual and desired

longitudinal spacing between the i^{th} vehicle and its predecessor.

$$e_i = x_i - x_{i-1} + d. \tag{2.4}$$

The generalized or velocity dependent spacing error is defined as,

$$\delta_i = e_i + h_w v_i = x_i - x_{i-1} + d + h_w v_i, \tag{2.5}$$

The objective of the CSP controllers is to regulate the spacing error to zero, where as, the objective of CTHP controllers is to regulate the generalized spacing error to zero.

Consider a CSP controller that employs the position and the velocity information of the predecessor vehicle [18],

$$u_i = -k_v(v_i - v_{i-1}) - k_p(x_i - x_{i-1} + d), \tag{2.6}$$

where k_v and k_p are the positive controller gains associated with velocity and position feedback, respectively. In the absence of parasitic lags, the governing equation for the spacing error of the i^{th} vehicle is obtained by substituting the control law from (2.6) in the vehicle dynamics (2.2) and simplifying.

$$\ddot{e}_i + k_v\dot{e}_i + k_p e_i = k_v\dot{e}_{i-1} + k_p e_{i-1}. \tag{2.7}$$

Taking the Laplace transform of the above governing equation, results in the transfer function describing the propagation of the spacing error from $(i-1)^{th}$ vehicle to that of i^{th} vehicle.

$$\frac{E_i(s)}{E_{i-1}(s)} = H(s) = \frac{k_v s + k_p}{s^2 + k_v s + k_p}, \quad \forall\, i \geq 2. \tag{2.8}$$

Notice that the above transfer function is valid only for vehicles with index 2 through N,

because the first vehicle of the platoon is the leader and is independent. The CSP controller that also employs the acceleration of the predecessor is,

$$u_i = k_a a_{i-1} - k_v(v_i - v_{i-1}) - k_p(x_i - x_{i-1} + d). \tag{2.9}$$

More generalized forms of the above control law can be formulated that utilize multiple vehicles in the feedback.

A simple CTHP controller is [18, 23]

$$u_i = -k_v(v_i - v_{i-1}) - k_p\delta_i, \tag{2.10}$$

where k_v, k_p are the positive gains. The above controller results in the following error propagation equation,

$$\delta_i(s) = \frac{k_v s + k_p}{s^2 + (k_v + k_p h_w)s + k_p}\delta_{i-1}(s) := H(s)\delta_{i-1}(s). \tag{2.11}$$

Notice that the above transfer function is reduced to the CSP transfer function in equation (2.8), if the time headway is zero. One can also design CTHP controllers that employ the acceleration information of the predecessor or the information from 'r' immediate predecessor vehicles. The gains in the above CSP and CTHP controllers are selected to ensure vehicle stability and platoon string stability. The string stability of a platoon and some known results of string stability of the above CSP and CTHP controllers are discussed next.

2.2 String Stability

String stability is the ability of the vehicles to attenuate the spacing errors caused by external disturbances as they propagate upstream (increasing vehicle index) in the vehicle

string. The following definition of string stability is from [18].

Definition 1. *A string of vehicles is string stable if, given* $\gamma > 0$, *there exists* $\delta > 0$ *such that whenever*

$$\max\left[\|e_i(0)\|_\infty, \|\dot{e}_i(0)\|_\infty, \|\sum_{j=1}^{i} e_j(0)\|_\infty, \|\sum_{j=1}^{i} \dot{e}_j(0)\|_\infty\right] < \delta \implies \sup_i \|e_i\|_\infty < \gamma,$$

and weakly string stable if,

$$\max\left[\|e_i(0)\|_1, \|\dot{e}_i(0)\|_1\right] < \delta \implies \sup_i \|e_i\|_\infty < \gamma$$

The definition implies that for a string of vehicles if the maximum error of all the initial errors of the vehicles in the string is bounded, then the maximum error in time as well as in vehicle index should also be bounded. It is customary in the study of string stability to assume that the string is of infinite length. This is because a finite length string, the errors may always be bounded by a finite value. An extension of string stability is the robust string stability which is defined as follows,

Definition 2. *A string of vehicles is robustly string stable in presence of parasitic lag* τ_0, *if the vehicles are string stable according to Definition 1 for all* $\tau \in [0, \tau_0]$.

Analytical methods to investigate the string stability of a vehicle string vary in literature [15, 18, 58]. Two methods of analysis are discussed next.

(1) Frequency Domain Method [18]: This method involves the study of the peak magnitude of the error propagation transfer function. The method is briefly discussed in the following. A detailed discussion of this method can be found in [15, 18]. The following definitions of norms are used in the analysis,

$$\|f\|_1 := \int_0^\infty |f(t)|dt, \quad \|f\|_\infty := \sup_{t\geq 0} |f(t)|.$$

where $f(t)$ is a linear piecewise continuous function.

Consider the spacing error propagation equation from the $(i-1)^{th}$ vehicle to the i^{th} vehicle

$$E_i(s) = H(s)E_{i-1}(s). \tag{2.12}$$

Using the inverse Laplace transform, the error propagation in time domain will be,

$$e_i(t) = h(t) * e_{i-1}(t)$$

where $*$ is the convolution operator and $h(t)$ is the impulse response of transfer function $H(s)$. From linear control theory it is known that,

$$\|e_i\|_\infty = \|h * e_{i-1}\|_\infty \leq \|h\|_1 \|e_{i-1}\|_\infty.$$

Thus, for string stability a necessary and sufficient condition is,

$$\|h(t)\|_1 < 1. \tag{2.13}$$

Computing the above norm is a tedious task. Also from linear systems theory [59], it is known that,

$$|H(0)| \leq \|H\|_\infty \leq \|h\|_1,$$

where,

$$H(0) = \left| \int_0^\infty h(t)dt \right|.$$

If the impulse response $h(t)$ does not change sign (i.e., non-negative) then,

$$|H(0)| = \left| \int_0^\infty h(t)dt \right| = \int_0^\infty |h(t)|dt = \|h(t)\|_1.$$

Therefore, when $h(t) \geq 0$,

$$|H(0)| = \|H\|_\infty = \|h\|_1,$$

and the string stability of the vehicles can be investigated in the frequency domain by studying the magnitude of $H(s)$, if its impulse response $h(t)$ is non-negative.

$$\|H(j\omega)\|_\infty \leq 1, \;\; h(t) \geq 0 \tag{2.14}$$

The above condition is both necessary and sufficient to guarantee string stability and has been widely used in the string stability analysis. The above analysis can also be extended to the case of multiple vehicle feedback.

Consider the following spacing error propagation equation,

$$E_i(s) = H_1(s)E_{i-1}(s) + H_2(s)E_{i-2}(s) + \cdots + H_r(s)E_{i-r}(s),$$

where 'r' is the number of preceding vehicles in the string that influence the i^{th} vehicle spacing error. The underlying characteristic polynomial for spacing errors is the following difference equation,

$$P(z) = z^r - \sum_{l=1}^{r} H_l(j\omega)z^{r-l}. \tag{2.15}$$

The spectrum of the above polynomial describes the string stability of the vehicle string. Hence, if $|z| < 1$, the platoon is string stable. A *sufficient condition* for $|z| \leq 1$ is given by [22],

$$|H(j\omega)| \leq 1 \tag{2.16}$$

Notice that if the vehicle has feedback only from its predecessor then the above polynomial becomes,

$$P(z) = z - H(j\omega),$$

and the condition for string stability reduces to (2.14). Although this method is widely used in the literature, it requires that the impulse response of the error propagation transfer function be non-negative in order to ensure the existence of feedback gains that guarantee string stability.

(2) Spatial Invariance Method: This method relies on the the spatial invariance of the error propagation in the vehicle string. The differential equation governing the spacing errors can be discretized along the index of the vehicles in the string [27, 58, 60]; this discrete equation describes the propagation of error along the vehicle index.

Let $X_i = [e_i, v_i, a_i]^T$ be the state vector representing the vehicle i, and

$$\hat{X}(t) = [X_{-\infty}(t), \cdots, X_i(t), \cdots, X_{\infty}(t)],$$

denote the infinite length vehicle platoon. The vehicle dynamics in equation (2.3) can be rewritten as,

$$\begin{pmatrix} \dot{e}_i \\ \dot{v}_i \\ \dot{a}_i \end{pmatrix} = \begin{pmatrix} v_i - v_{i-1} \\ a_i \\ \frac{1}{\tau}(-a_i + u_i) \end{pmatrix} \tag{2.17}$$

The following bilinear $\mathcal{Z}$-transformation is used to transform the above representation into a discretized state equation.

$$\tilde{X}(z,t) := \mathcal{Z}[\hat{X}(t)](z) = \sum_{i=-\infty}^{\infty} X_i(t) z^{-k}, \tag{2.18}$$

where, $z = e^{j\theta}$, $\theta \in [0, 2\pi]$. Thus, the spatially discretized state equation of the platoon

is,

$$\frac{d}{dt}\begin{pmatrix}\tilde{e}(z,t)\\ \tilde{v}(z,t)\\ \tilde{a}(z,t)\end{pmatrix} = \underbrace{\begin{bmatrix}0 & 1-z^{-1} & 0\\ 0 & 0 & 1\\ 0 & 0 & \frac{1}{\tau}\end{bmatrix}}_{\tilde{A}(z)}\begin{pmatrix}\tilde{e}(z,t)\\ \tilde{v}(z,t)\\ \tilde{a}(z,t)\end{pmatrix} + \underbrace{\begin{bmatrix}0\\ 0\\ \frac{1}{\tau}\end{bmatrix}}_{\tilde{B}(z)}\tilde{u}(z,t). \tag{2.19}$$

It is very important to note that the difference equation represents a space shift and it is still a continuous function of time as evidenced by the presence of the time variable in the equation. Also, it is assumed that the states and inputs in the above state space are square summable [58]. The string stability can be investigated by studying the eigenvalues of the above system. The following lemma from [58] is used to determine the string stability.

Lemma 1. *The system shown in* (2.19) *is asymptotically stable if and only if the following statements are true,*

1. *Real* $\lambda(\tilde{A}(e^{j\theta})) \leq 0, \quad \forall \quad \theta \in [0, 2\pi]$, *and*

   Real $\lambda(\tilde{A}(e^{j\theta})) = 0$ *for at most a countable number of* $\theta \in [0, 2\pi]$.

2. $\sup_{\theta\in[0,2\pi],t\geq 0} \|e^{\tilde{A}(e^{j\theta})t}\| < \infty$.

where λ *denotes the eigenvalues of matrix* $\tilde{A}$.

Therefore, according to the above lemma, in order for the platoon to be string stable, the eigenvalues of the system matrix $\tilde{A}(e^{j\theta})$, for a given $\theta \in [0, 2\pi]$ should lie in the open left half plane with at most one eigenvalue on the imaginary axis, and further, the eigenvalues should all be distinct. Since the state space representation is formed by spatial discretization, satisfying the above lemma guarantees error convergence along the index of the vehicles in the string.

2.2.1 String stability of CSP and CTHP controllers

String stability of CSP controllers with PF and LPF information flow graphs was studied a great deal in the literature, especially in [18, 22]. Substituting $s = j\omega$ in the error propagation transfer function from (2.8) and taking the infinity norm of $H(j\omega)$,

$$||H(j\omega)||_\infty^2 = \frac{k_p^2 + k_v^2\omega^2}{(k_p - \omega^2)^2 + \omega^2 k_v^2}.$$

For sufficiently small frequencies, i.e., $0 < \omega < \sqrt{2k_p}$,

$$|H(j\omega)| > 1.$$

Therefore, the system is not string stable and any small error in one of the vehicles may be amplified as it propagates through the platoon. Using similar analysis it can also be shown that the platoon using the controller using predecessor acceleration (2.9), may be *weakly* string stable when $k_a = 1$. The notation "weak" string stability refers to the case when spacing errors may attenuate or remain the same with the increase in vehicle index. It was reported that the platoon employing such controller lacks any robustness to uncertainties such as parasitic lags. Numerical simulations were primarily used to show these results.

If a vehicle can access the information of leader, it was shown in the literature that the platoon using a CSP controller which employs information from the reference and predecessor vehicles is string stable [19, 22]. Moreover, it was also shown that string stability is also robust to the presence of small uncertainties, such as parasitic lags in the vehicles [22]. In this work an upper bound on such parasitic lags in terms of controller gains is determined, which is then used to provide a controller design process.

It is also known that CTHP controller (2.10) can guarantee string stability [19]. Substituting $s = j\omega$ in the error propagation transfer function from (2.11) and taking the infinity

norm of $H(j\omega)$,

$$||H(j\omega)||_\infty^2 = \frac{k_p^2 + k_v^2\omega^2}{(k_p - \omega^2)^2 + \omega^2(k_v + k_p h_w)^2}.$$

Clearly, $\|H(j\omega)\|_\infty \leq 1$ for any non-zero h_w. When $\tau > 0$ the error propagation equation becomes,

$$\delta_i(s) = \frac{k_v s + k_p}{\tau s^3 + s^2 + (k_v + k_p h_w)s + k_p}\delta_{i-1}(s) := H(s)\delta_{i-1}(s).$$

Define the minimum employable time headway ($h_{\min}$) as the minimum time headway for which the platoon is string stable for every $\tau \in [0, \tau_0]$. From the above error propagation transfer function, [34]

$$h_{\min} = 2\tau_0. \tag{2.20}$$

However, as noted before this is too restrictive in many practical scenarios. Several studies have indicated that using vehicular communication may improve (reduce) the minimum employable time headway. For instance the following Semi-Autonomous ACC (SAACC) was considered by Rajamani and Zhu in [33],

$$u_i = -k_1 a_{i-1} - k_2 a_i - k_3 \dot{e}_i - k_4 e_i - k_5 v_i \tag{2.21}$$

They demonstrated that the minimum employable time headway can be reduced to

$$h_{\min} = \frac{\tau}{-k_1}, \;\; k_1 < 0.$$

Other studies have used numerical and vehicular experiments to demonstrate the benefits of communication. While studying vehicle string with communication delays in acceleration information, the authors of [39] have showed that when one employs two predecessor vehicles' information in the feedback, the minimum employable time headway can be re-

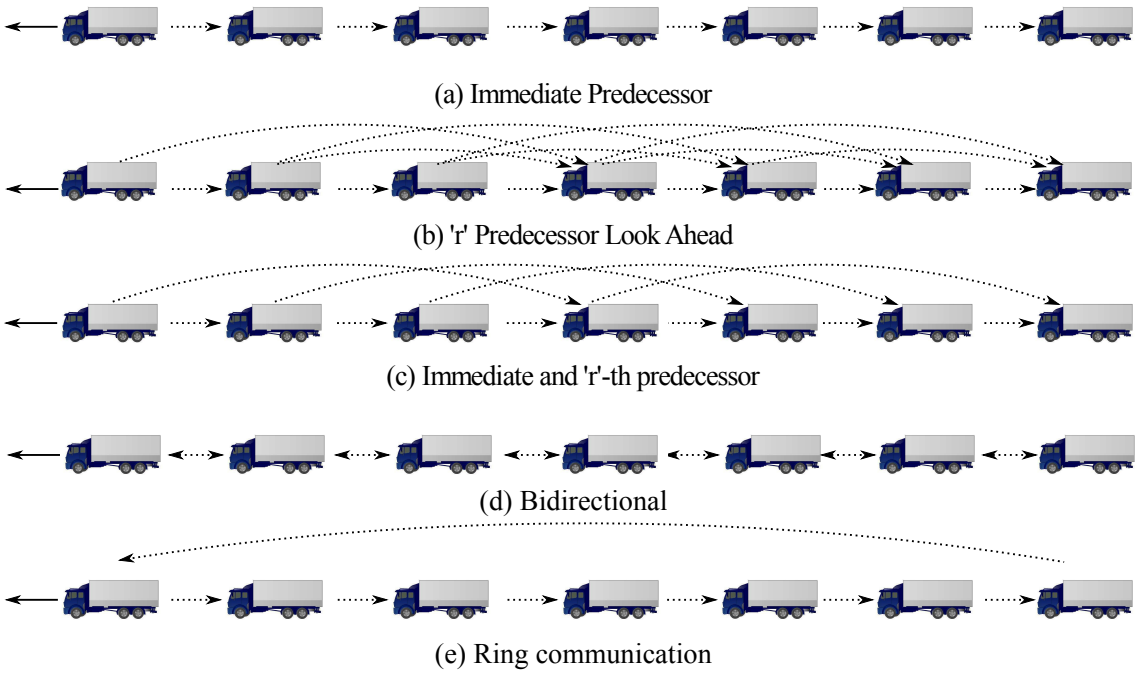

Figure 2.8: Information flow structures investigated, direction of travel (solid), information flow (dotted)

duced to $h_{\min} = 4\tau/3$. Using the information of immediate predecessor and follower in the feedback, the author of [55] were able to show that the time headway can be reduced by about 30%. With the exception of [33], none of the results on CTHP provide any analytical bounds on $h_{\min}$. In the following chapters, the string stability analysis methods discussed are utilized to study different types of CSP and CTHP controllers that rely on vehicular communication. The information flow graphs that require communication that are considered in the rest of this work are shown in Figure 2.8.

3. CONSTANT SPACING CONTROLLERS*

In this chapter, the analysis of string stability of controllers based on the CSP is presented. String instability of a CSP controller that uses information from 'r' predecessor vehicles is established using perturbation analysis in Section 3.1. A CSP controller which uses the LPF information is investigated in Section 3.2 to find a bound on the maximum allowable parasitic lags which will ensure string stability. This bound on the parasitic lag is used to propose a design procedure for selecting control gains for CSP with LPF information is presented in Section 3.2.2. Numerical simulations are presented and discussed in Section 3.3.

3.1 CSP With 'r' Predecessor Information

Let every vehicle in the platoon has access to the information of 'r" immediate preceding vehicles (shown in Figure 2.8(b)). The value of 'r' may be selected depending on the capabilities of the communication instruments and the spacing between vehicles. The corresponding CSP control input can be written as

$$u_i = \sum_{l=1}^{r} \left(k_{al} a_{i-l} - k_{vl}(v_i - v_{i-l}) - k_{pl} \left(x_i - x_{i-l} + \sum_{p=\max[0,i-l+1]}^{i} d_p \right) \right), \quad (3.1)$$

where the subscript $i-l$ denotes that the variable is defined between vehicles i and l. Note that for the control action that employs information from 'r' predecessors, if $i \leq r$, then the i-th vehicle control input utilizes only information from $i-1$ vehicles ahead of it. The

*Parts of this chapter have been reprinted from "Vehicle Platooning with Multiple Vehicle Look-Ahead Information", Shyamprasad Konduri, Prabhakar R. Pagilla and Swaroop Darbha, to be presented in IFAC World Congress 2017.

governing equation of the spacing error when using the above control law is,

$$\tau\frac{d}{dt}\ddot{e}_i + \ddot{e}_i + \sum_{l=1}^{r}(k_{vl}\dot{e}_i + k_{pl}e_i) = \sum_{l=1}^{r}\left(k_{al}\ddot{e}_{i-l} + k_{vl}\dot{e}_{i-l} + k_{pl}e_{i-l}\right). \tag{3.2}$$

Let

$$H_l(s) = \frac{k_{al}s^2 + k_{vl}s + k_{pl}}{\tau s^3 + s^2 + \sum_{l=1}^{r}(k_{vl}s + k_{pl})}.$$

Taking the Laplace transform of (3.2), the error propagation equation can be written as,

$$E_i(s) = \sum_{l=1}^{r} H_l(s)E_{i-l}(s). \tag{3.3}$$

Using perturbation theory it can be shown that the platoon is not string stable. The following theorem summarizes this result [50].

Theorem 1. *A platoon of N vehicles with individual vehicle dynamics given by (2.3) and with the control input given in equation (3.1) is not robustly string stable for any finite r.*

Proof. Considering the spacing errors to be states of a spatially discrete system, the following characteristic polynomial describes the spacing error dynamics when the lead vehicle performs a sinusoidal acceleration maneuver at a frequency ω:

$$P(z) = z^r - \sum_{l=1}^{r} H_l(j\omega)z^{r-l}. \tag{3.4}$$

If the platoon is not string stable then at least one of the roots of $P(z)$ will lie outside the unit circle for non zero parasitic lags.

There are three cases to consider: (1) $\sum_{l=1}^{r} k_{al} < 1$, (2) $\sum_{l=1}^{r} k_{al} > 1$, and (3) $\sum_{l=1}^{r} k_{al} = 1$. In each of the three cases, an approach that relies on perturbation analysis is used to show that the platoon is string unstable. In particular, it is shown that the root at $z = 1$ moves outside the unit circle for either sufficiently small values of ω or $\frac{1}{\omega}$. Note that

since $\sum_{l=1}^{r} H_l(0) = 1$, $P(1) = 0$; thus, there is a root at $z = 1$.

Case (1): The change of the root at $z = 1$ with ω around $\omega = 0$ will be evaluated. Since there is no drop in the degree of the polynomial as ω varies, the roots are continuous functions of ω.

Let $z(\omega) = R(\omega)e^{j\theta(\omega)}$. Denote y' and y'' as the first and second derivatives of the variable y with respect to ω. The first and the second derivatives of z with respect to ω at $(\omega = 0, R(\omega) = 1)$ are given by

$$z'(0) = R'(0) + j\theta'(0), \tag{3.5}$$

$$z''(0) = R''(0) - (\theta'(0))^2 + j(\theta''(0) + 2R'(0)\theta'(0)). \tag{3.6}$$

Also, consider the Taylor series expansion of $R(\omega)$ around $\omega = 0$,

$$R(\omega) = R(0) + \omega R'(0) + (\omega^2/2)R''(0) + h.o.t.$$

The derivative of $P(z(\omega))$ with respect to ω is given by setting $P'(z(\omega)) = 0$:

$$P'(z) = rz^{r-1}z' - \sum_{l=1}^{r} \left(H_l^{'} z^{r-l} + H_l(r-l)z^{r-l-1}z' \right).$$

Evaluating $P'(z)$ at $\{z, \omega\} = \{1, 0\}$, and setting it equal to zero results in $z'(0) = 0$. This implies that $R'(0) = 0$ and $\theta'(0) = 0$. Since this does not provide any indication of how the root changes with respect to ω around $\omega = 0$, consider the second derivative of $P(z)$:

$$P''(z) = rz^{r-1}z'' + r(r-1)z^{r-2}(z')^2 - \sum_{l=1}^{r} \Big(H_l^{''} z^{r-l} + 2H_l^{'}(r-l)z^{r-l-1}z'$$
$$+ H_l(r-l)(r-l-1)z^{r-l-2}(z')^2 + H_l(r-l)z^{r-l-1}z'' \Big). \tag{3.7}$$

Evaluating $P''(z)$ at $\{z, \omega\} = \{1, 0\}$ and setting it equal to zero,

$$\begin{aligned} rz''(0) - \sum_{l=1}^{r} H_l^{''}(0) - \sum_{l=1}^{r}(r-l)H_l(0)z''(0) = 0 \\ \implies z''(0) = \frac{\sum_{l=1}^{r} H_l^{''}(0)}{r - \sum_{l=1}^{r}(r-l)H_l(0)} = \frac{\sum_{l=1}^{r} H_l^{''}(0)}{\sum_{l=1}^{r-1} lH_l(0)}. \end{aligned} \tag{3.8}$$

Let

$$K_p := \sum_{l=1}^{r} k_{pl}, \qquad K_v := \sum_{l=1}^{r} k_{vl}.$$

From $H_l(j\omega)$ one can determine

$$H_l(0) = \frac{k_{pl}}{K_p},\ H_l'(0) = \frac{j(k_{vl}K_p - k_{pl}K_v)}{K_p^2},\ H_l''(0) = \frac{2(H_l(0) - k_{al}) - 2H_l'(0)K_v j}{K_p}.$$

which in turn gives

$$\sum_{l=1}^{r} H_l(0) = 1,\ \sum_{l=1}^{r} H_l^{'}(0) = 0,\ \text{and},\ \sum_{l=1}^{r} H_l^{''}(0) = \frac{2\left(1 - \sum_{l=1}^{r} k_{al}\right)}{K_p}.$$

Hence, $z''(0)$ is real and positive when $\sum_{l=1}^{r} k_{al} < 1$. Therefore, $R''(0) > 0$ which implies that there is a root with magnitude greater than one for small ω. Thus, the platoon is not string stable when $\sum_{l=1}^{r} k_{al} < 1$ at low frequencies.

Case (2): If $\sum_{l=1}^{r} k_{al} > 1$, then let $\lambda = \frac{1}{\omega}$; further, define $\bar{H}_l(\lambda) := H(\frac{1}{\lambda})$. Clearly, for $\tau = 0$,

$$\bar{H}_l(\lambda) = \frac{k_{al} + k_{vl}\lambda + k_{pl}\lambda^2}{1 + \sum_{l=1}^{r} k_{vl}\lambda + \sum_{l=1}^{r} k_{pl}\lambda^2}.$$

Rewriting $P(z)$ in terms of λ,

$$P(z) = z^r - \sum_{l=1}^{r} \bar{H}_l(\lambda) z^{r-l}.$$

Let $K_a = \sum_{l=1}^{r} k_{al} > 1$. Consider $\lambda = 0$ and note that $\sum_{l=1}^{r} \bar{H}_l(0) = \sum_{l=1}^{r} k_{al} > 1$. Clearly,

$$P(1) = 1 - \sum_{l=1}^{r} \bar{H}_l(0) < 0,$$

and

$$P(K_a) = K_a^r - \sum_{l=1}^{r} k_{al} K_a^{r-l} > K_a^r - \sum_{l=1}^{r} k_{al} K_a^{r-1} = K_a^r - K_a^r = 0.$$

Hence, when $\lambda = 0$, $P(z)$ is a real polynomial and has a real root between 1 and $K_a > 1$ and is not Schur consequently. The above argument presumes $k_{al} > 0$; if this were not the case, then for sufficiently large real values of z, the term z^r dominates other terms and the polynomial $P(z)$ will be positive for all such values. Even in this case, the polynomial $P(z)$ will have a real positive root outside the unit disk. Therefore, when $\lambda = 0$, one root of $P(z)$ lies outside the unit disk. From the continuity of roots with respect to the coefficients, for sufficiently small values of λ (or equivalently, sufficiently large values of ω), the polynomial $P(z)$ has a root outside the unit disk and consequently the platoon is not string stable.

Case (3): When $\sum_{l=1}^{r} k_{al} = 1$ and $\tau = 0$, notice that for every s, $z = 1$ is always a root of the polynomial

$$P(z) = z^r - \sum_{l=1}^{r} \frac{k_{al} s^2 + k_{vl} s + k_{pl}}{s^2 + \sum_{l=1}^{r} k_{vl} s + \sum_{l=1}^{r} k_{pl}} z^{r-l}.$$

Next fix *any* s and vary τ, to examine the perturbation of the root at $z = 1$ using the approach for case 1. Let y' denote $\frac{dy}{d\tau}$ in this case. In order to make the dependence of $H_l(s)$ on τ explicit, write

$$H_l(s, \tau) = \frac{k_{al} s^2 + k_{vl} s + k_{pl}}{\tau s^3 + s^2 + \sum_{l=1}^{r} k_{vl} s + \sum_{l=1}^{r} k_{pl}}.$$

Differentiating the characteristic polynomial with respect to τ yields:

$$rz^{r-1}z' - \sum_{l=1}^{r} H_l(s,\tau)(r-l)z^{r-l-1}z' - \sum_{l=1}^{r} H_l'(s,\tau)z^{r-l} = 0.$$

When $z = 1$ and $\tau = 0$, simplifying the above equation yields:

$$z'(0) = \frac{-s^3}{\sum_{l=1}^{r} l(k_{al}s^2 + k_{vl}s + k_{pl})}.$$

Further, when $s = j\omega$, the real part of $z'(0)$ denoted by $\Re(z'(0))$ is given by:

$$\Re(z'(0)) = \frac{\omega^4(\sum_{l=1}^{r} lk_{vl})}{(\sum_{l=1}^{r} l(k_{pl} - k_{al}\omega^2)^2 + \omega^2(\sum_{l=1}^{r} lk_{vl})^2} > 0.$$

Expressing $z(\tau)$ in the polar form as $R(\tau)e^{j\theta(\tau)}$, from the above equation $\Re(z'(0)) = R'(0) > 0$, indicating that for any sufficiently small $\tau_0 > 0$, the root of the characteristic equation will be outside the unit circle. □

Therefore, based on the above theorem, the platoon is not robustly string stable with feedback from 'r' predecessor vehicles, irrespective of the use of predecessor acceleration feedback in the controller.

3.2 With Leader and Predecessor Information

When the vehicle utilizes information from only its predecessor and the platoon leader (shown in Fig. 2.5), then the control input may be written as follows:

$$u_i = k_{a1}a_{i-1} - k_{v1}(v_i - v_{i-1}) - k_{p1}(x_i - x_{i-1} + d_i) \\ k_{aL}a_L - k_{vL}(v_i - v_L) - k_{pL}(x_i - x_L + d_{i-L}) \quad (3.9)$$

where the subscript L denotes the variable corresponds to the leader vehicle, d_{i-L} denotes the spacing between vehicle i and the leader, and all the gains $k_{a1}, k_{v1}, k_{p1}, k_{aL}, k_{vL}, k_{pL}$ are non-negative. It was shown in [18] that the platoon is string stable and is also robust to the presence of a sufficiently small parasitic lag.

3.2.1 String Stability Analysis

The objective of this section is to find the range of parasitic lags for which this controller is robustly string stable by utilizing the requirements for platoon string stability. The following theorem provides this result.

Theorem 2. *Let $K_v = k_{v1} + k_{vL}$ and $K_p = k_{p1} + k_{pL}$. A platoon of N vehicles with individual vehicle dynamics governed by (2.3) and the control input as given by (3.9) with $k_{vL} \geq \sqrt{2K_p}$ is string stable for parasitic lags satisfying $\tau \in [0, \tau_0]$ with*

$$\tau_0 = \frac{1 - k_{a1}^2}{2K_v}. \tag{3.10}$$

Proof. Substituting the control input (3.9) into Eq. (2.3) will result in the following governing equation for the spacing error dynamics:

$$\tau \dddot{e}_i + \ddot{e}_i + (k_{v1} + k_{vL})\dot{e}_i + (k_{p1} + k_{pL})e_i = k_{a1}\ddot{e}_{i-1} + k_{v1}\dot{e}_{i-1} + k_{p1}e_{i-1}.$$

Taking the Laplace transformation of the above spacing error governing equation will result in the following error propagation equation:

$$E_i(s) = H(s)E_{i-1}(s) = \frac{k_{a1}s^2 + k_{v1}s + k_{p1}}{\tau s^3 + s^2 + K_v s + K_p} E_{i-1}(s) \tag{3.11}$$

For stability using the Routh-Hurwitz criteria, we have the following conditions:

$$K_v > 0,\ K_p > 0, \text{ and } K_v > \tau K_p.$$

An upper bound on τ is obtained from the above conditions:

$$\tau < \frac{K_v}{K_p}. \tag{3.12}$$

Consider,

$$\|H_p(j\omega;\tau)\|_\infty^2 = \frac{(k_{p1} - k_{a1}\omega^2)^2 + k_{v1}^2\omega^2}{(K_p - \omega^2)^2 + \omega^2(K_v - \tau\omega^2)^2}.$$

Then, $\|H_p(j\omega;\tau)\|_\infty \leq 1$ will imply that

$$(k_{p1} - k_{a1}\omega^2)^2 + k_{v1}^2\omega^2 \leq (K_p - \omega^2)^2 + \omega^2(K_v - \tau\omega^2)^2. \tag{3.13}$$

Upon simplification the above equation results in,

$$\tau^2\omega^6 + \omega^4(1 - k_{a1}^2 - 2K_v\tau) + \omega^2(K_v^2 - k_{v1}^2 + 2k_{a1}k_{p1} - 2K_p) - k_{p1}^2 + K_p^2 \geq 0. \tag{3.14}$$

For the above inequality to be satisfied for all ω,

$$\begin{aligned} \tau^2 &\geq 0 \\ 1 - k_{a1}^2 - K_v\tau &\geq 0 \\ K_p^2 - k_{p1}^2 \geq 0 \implies K_p &\geq k_{p1} \\ K_v^2 - k_{v1}^2 + 2k_{a1}k_{p1} - 2K_p &\geq 0 \end{aligned} \tag{3.15}$$

To show the last inequality, consider $k_{vl}^2 \geq 2K_p$. Then,

$$k_{vL}^2 + 2k_{vL}k_{v1} \geq 2K_p,$$
$$k_{vL}^2 + 2k_{vL}k_{v1} + k_{v1}^2 \geq k_{v1}^2 + 2K_p,$$
$$K_v^2 - k_{v1}^2 \geq 2K_p.$$

Since k_{a1} and k_{p1} are non-negative,

$$K_v^2 - k_{v1}^2 + 2k_{a1}k_{p1} - 2K_p \geq 0. \tag{3.16}$$

Therefore, for the inequality (3.14) to be satisfied,

$$1 - k_{a1}^2 - 2K_v\tau \geq 0.$$

This provides the following bound on the lag:

$$\tau \leq \frac{1 - k_{a1}^2}{2K_v}. \tag{3.17}$$

Notice that for τ to be non-negative, from the above relation one also needs

$$1 - k_{a1}^2 \geq 0 \implies |k_{a1}| \leq 1 \tag{3.18}$$

Since $k_{vl} \geq \sqrt{2K_p}$, then $K_v \geq \sqrt{2K_p}$. Thus,

$$\frac{K_v}{K_p} = \frac{K_v^2}{K_pK_v} \geq \frac{2K_p}{K_pK_v} = \frac{2}{K_v}. \tag{3.19}$$

Further, since $1 - k_{a1}^2 \leq 1$,

$$\frac{1 - k_{a1}^2}{2K_v} < \frac{2}{K_v} \leq \frac{K_v}{K_p}. \tag{3.20}$$

Therefore, the bound given by (3.17) is smaller than (3.12), and $\tau_0 = \dfrac{1 - k_{a1}^2}{2K_v}$. □

Notice that $k_{a1} \leq 1$ is one of the requirements for any $\tau \geq 0$. To maximize the allowable lag, it is clear that one must choose small values for k_{a1} and K_v. Also notice that in the proof the bound $k_{vL} \geq \sqrt{2K_p}$ is used to show that the inequality in (3.14) is satisfied, however there may be other combinations of gains K_v and K_p which will also ensure that the conditions are satisfied.

Remark 1. *The bound on τ given by equation (3.10) of the above theorem is obtained using a sufficient condition for string stability. Thus, there is a possibility that one can have a $\tau > \frac{1-k_{a1}^2}{2K_v}$ and the platoon is still string stable. Although the derived bound on τ is not tight, it is the best bound known and quite useful for designing controller gains such that the platoon is string stable.*

3.2.2 Design Procedure

This section presents a procedure for the design of a controller shown in equation (3.9) for a known range of parasitic lags in the system. Consider the lag $\tau \in (0, \tau_0]$. Designing the controller involves choosing the vehicle gains such that they satisfy conditions in equations (3.10) and (3.16)-(3.18); from these equations the following guidelines choosing the controller gains are extracted.

- Since the gains are same for all the vehicles, and k_{aL} does not effect the spacing error propagation (described in equation (3.11)), start by setting the gain associated with lead vehicle acceleration feedback to zero, i.e.,

$$k_{aL} = 0 \tag{3.21}$$

- From equation (3.10) one needs,

$$1 - k_{a1}^2 \geq 2\tau K_v.$$

However, from (3.18) it is required that $k_{a1} \leq 1$. Hence, to increase the flexibility in choosing the value of K_v (and consequently K_p), choose the predecessor acceleration gain to be zero, i.e.,

$$k_{a1} = 0, \tag{3.22}$$

leading to

$$1 \geq 2\tau K_v$$

Thus, one can choose velocity gains such that,

$$K_v = 1/2\tau. \tag{3.23}$$

- For the choice of position gains (K_p), consider the feedback gains of predecessor vehicle and lead vehicle velocities to be at a ratio of α, then with (3.23),

$$\frac{k_{vL}}{k_{v1}} = \alpha$$

$$\implies k_{v1} = \frac{1}{2(1+\alpha)\tau}, \text{ and} \tag{3.24}$$

$$k_{vL} = \frac{\alpha}{2(1+\alpha)\tau}. \tag{3.25}$$

Combining (3.25) with the condition in (3.15) will result in

$$K_p \leq \frac{\alpha^2}{8(1+\alpha)^2\tau^2}.$$

Therefore, the position feedback gains can be chosen such that,

$$K_p = \frac{\alpha^2}{8(1+\alpha)^2\tau^2}. \tag{3.26}$$

- Any choice of k_{p1} and k_{pL} chosen to satisfy the above equation will also satisfy the final condition (3.15).

Therefore, the choice of the controller gains given in equations (3.21)-(3.26) will ensure that the platoon is string stable in the presence of a parasitic lag τ. Note that one can still find gains satisfying all the conditions from Theorem 2 even by choosing non-zero values for the acceleration gain k_{a1}; however, this may reduce the velocity and position feedback gains resulting in larger settling times.

3.3 Numerical Simulations

Numerical simulations were conducted to corroborate the results of Theorems 1 and 2. A 15 vehicle platoon is considered for this purpose. The following parameter values are used: inter-vehicular spacing, $d_i = 5$ m; desired platoon velocity, $v_0 = 29$ m/s (≈ 65 mph); and PF information flow with $r = 2$. For simplicity, the gain values for all the controllers were chosen to be equal. Zero initial spacing errors are considered with velocity of vehicles equal to desired velocity. For all the simulations, the lead vehicle undergoes a speed change maneuver which results in the velocity profile as shown in Figure 3.1 and the corresponding input acceleration profile is shown in Figure 3.2.

The evolution of the vehicle spacing errors utilizing two vehicle look ahead, with $\sum_{j=1}^{r} k_{ak}$ equal to zero, less than 1 ($k_{ak} = 0.1$), and equal to 1 ($k_{ak} = 0.5$) are shown in the Figures 3.3-3.5 and their corresponding control inputs are shown in Figures 3.6-3.8. A non-zero parasitic lag of 0.1 seconds is chosen in the simulations [33]. The spacing errors of the second vehicle has a higher overshoot, which is attenuated by the vehicle

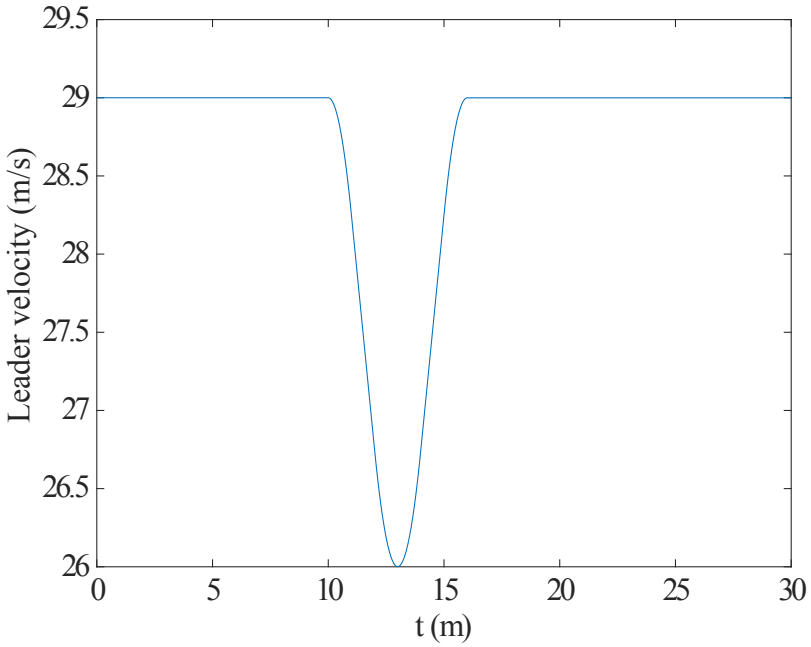

Figure 3.1: Leader velocity profile employed in simulations

with index 3; this is due to the presence of the lead vehicle feedback for both the vehicles with index 2 and 3. Since the leader information is available for both vehicles 2 and 3, the platoon from the leader to vehicle 3 is string stable, following the results of Section 3.2. However, from vehicle index 4 to 15, the leader information is not available and the control input is computed solely based on the information from the two immediate predecessors. Hence, the spacing errors are amplified from vehicle 4 to vehicle 15 following the result of Theorem 1. Notice that the overshoot of tail vehicles increases with the number of vehicles irrespective of the acceleration gain. Also, when the acceleration gain is close to unity, the response of vehicles at the tail of the platoon is highly oscillatory. This behavior is observed for all the numerical simulations with different number of vehicles. For example see the spacing error evolution of platoon with 25 vehicles with acceleration feedback gain $K_a = 1$ shown in Fig. 3.9. Notice that the magnitude of oscillations increases with

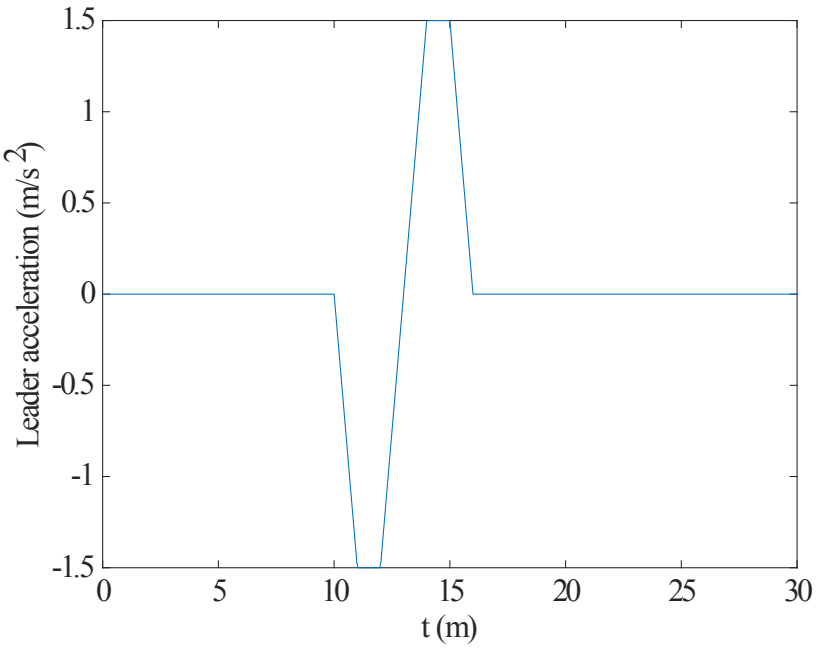

Figure 3.2: Leader acceleration profile employed in simulations

the number of vehicles. Furthermore, the evolution of the control input when $K_a = 1$ indicates that the vehicle behavior is jerky and passengers at the tail-end of the platoon may experience high acceleration and deceleration cycles.

3.3.1 Platoon with Leader and Predecessor Feedback

For the platoon of vehicles that are subjected to parasitic lags, when the leader information is available to all the following vehicles, the behavior of the upper bound on lag τ with respect to the velocity feedback gains K_v for different values of k_{a1} is shown in Fig. 3.11. For simplicity the velocity feedback gains are selected equal, i.e, $k_{v1} = k_{vL}$. Three values of k_{a1} are considered and the bound is computed using (3.10). From these numerical simulations, one can observe that the allowable lag is maximized when one chooses smaller values for both K_v and k_{a1}. Further, even for a large k_{a1} (with $k_{a1} < 1$) one can increase the bound on lag by decreasing the value of K_v.

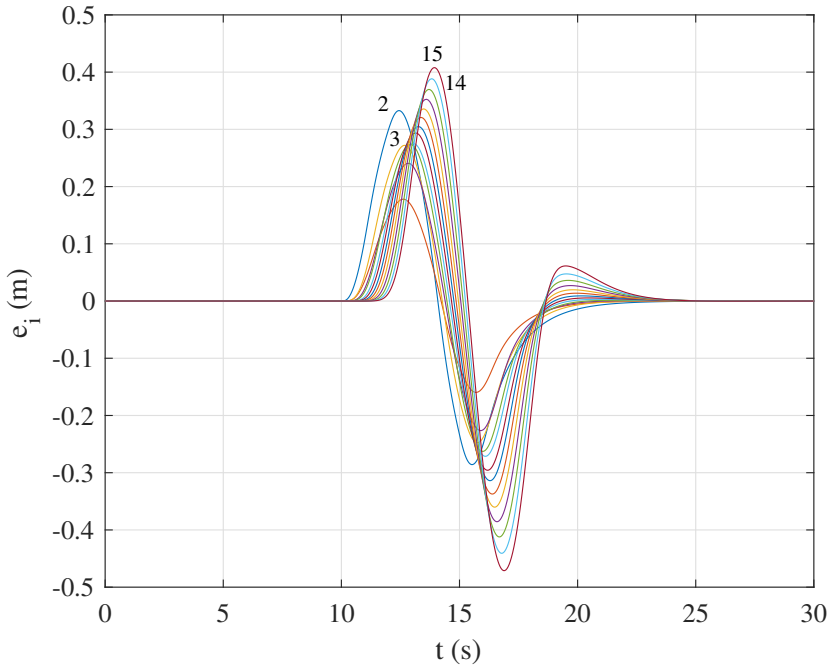

Figure 3.3: Evolution of spacing errors with $K_a = 0$

Simulations were also conducted using the design procedure discussed in Section 3.2.2. The same platoon of 15 vehicles is chosen with a parasitic lag in the range $\tau = (0, 0.1)$. Gains were chosen such that $k_{p1} = k_{pL} = k_p$ and $k_{v1} = k_{vL} = k_v$. Then, according to the design procedure, we obtain $k_p = 1.56$, $k_v = 2.5$ and $k_{aL} = k_{a1} = 0$. Utilizing these gain values in the controller, the evolution of spacing errors of vehicles in the platoon are shown in Figures. 3.12 - 3.14.

The evolution of spacing errors of follower vehicles indexed 2 to 15 is shown in Figure. 3.12. The largest spacing error is for the first follower vehicle shown by index 2, and the spacing error decreases with the increase in the vehicle index number. Therefore, the platoon is string stable to the gains chosen in accordance to the conditions provided by Theorem 2.

As noted earlier the design procedure discussed in the previous section is *a* method.

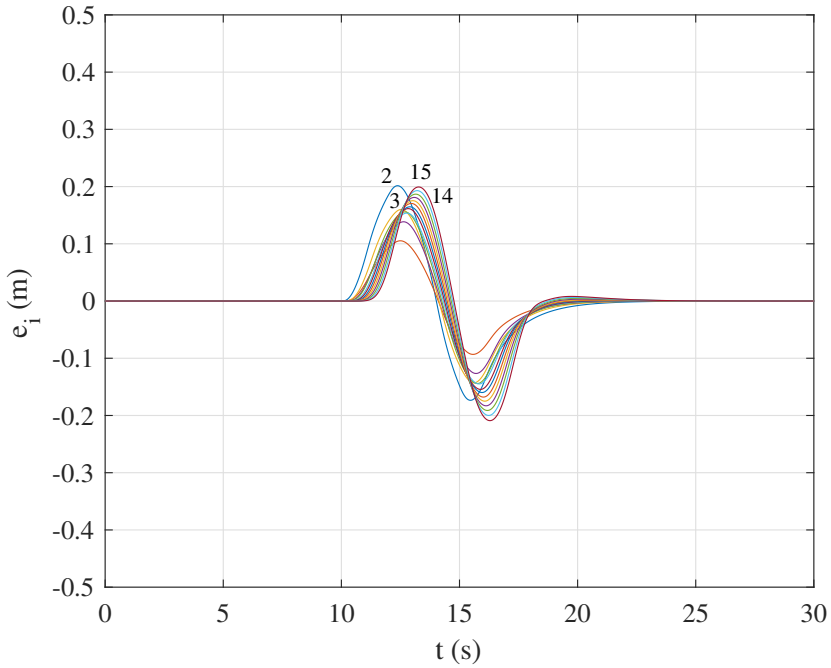

Figure 3.4: Evolution of spacing errors with $K_a = 0.4$

It is possible that the platoon can be string stable even if one were to choose non-zero acceleration feedback gains. The spacing errors of vehicles for the example scenario with acceleration feedback gains $k_{aL} = k_{a1} = 0.2$ and $k_{aL} = k_{a1} = 0.4$ are shown in Figures 3.13 and 3.14. As the acceleration feedback gain values increase from 0 to 0.4, the overshoot in spacing errors for the following vehicles is reduced. This is expected as the acceleration feedback in the control input results in a more tightly bound platoon. However, since the platoon is string stable even without the acceleration feedback, the inclusion of acceleration feedback is not necessary for string stability.

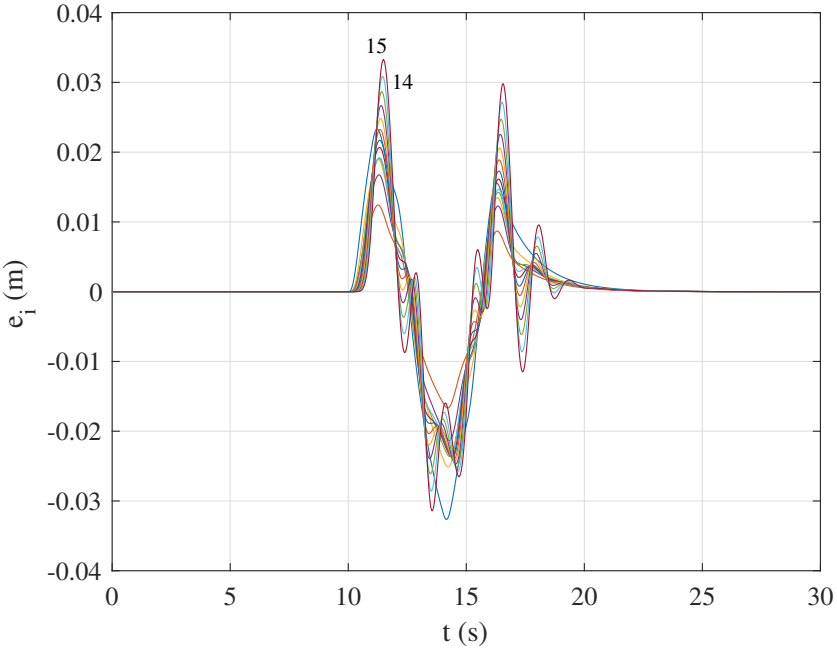

Figure 3.5: Evolution of spacing errors with $K_a = 1$

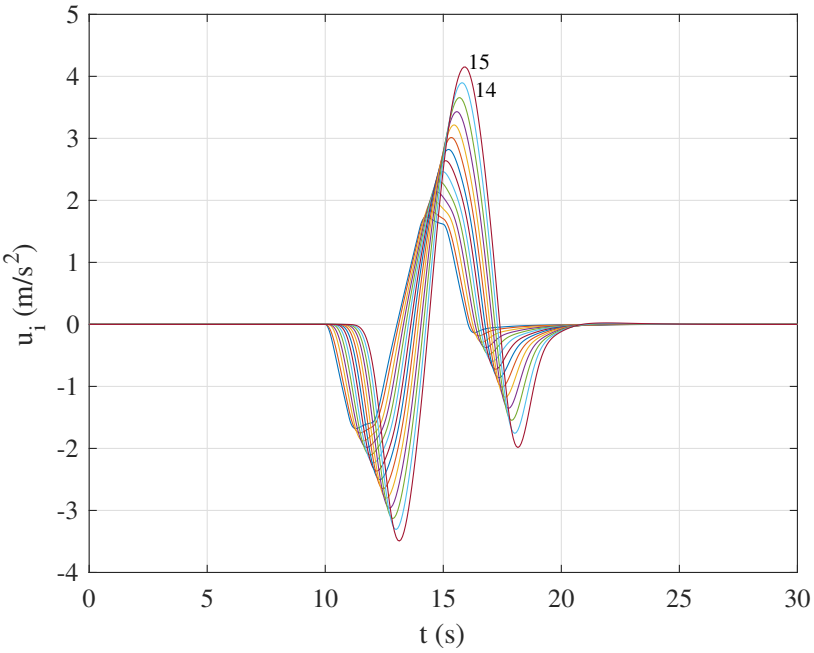

Figure 3.6: Control effort for platoon of 15 vehicles with $K_a = 0$

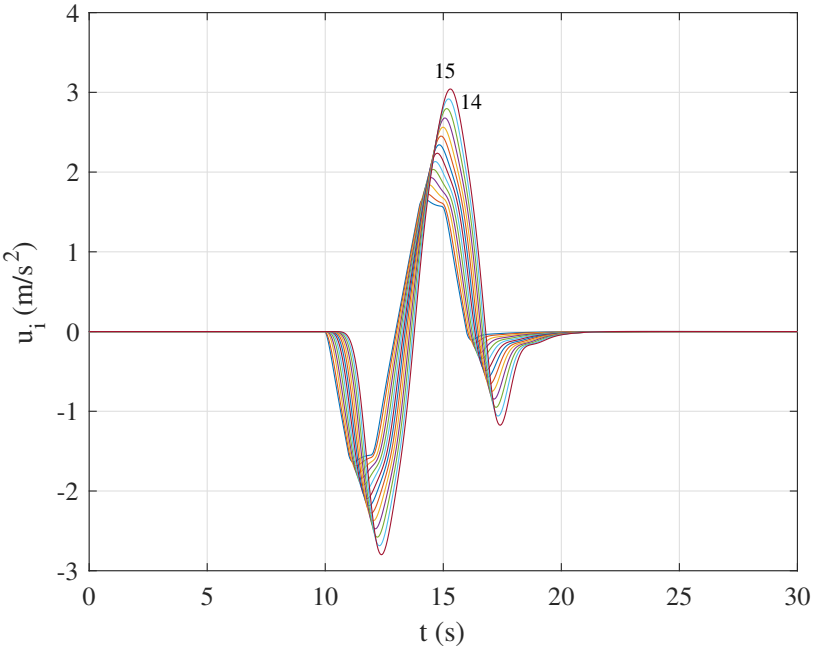

Figure 3.7: Control effort for platoon of 15 vehicles with $K_a = 0.4$

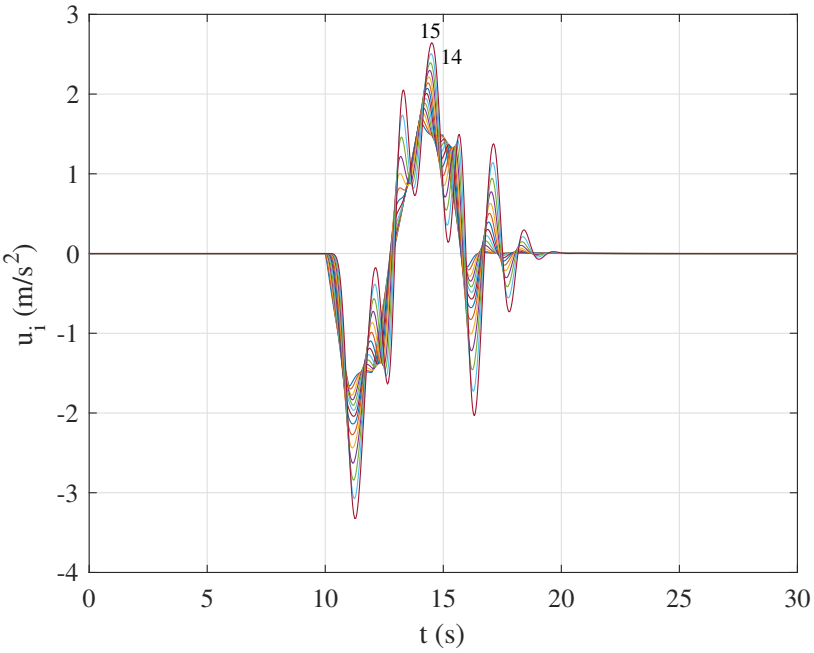

Figure 3.8: Control effort for platoon of 15 vehicles with $K_a = 1$

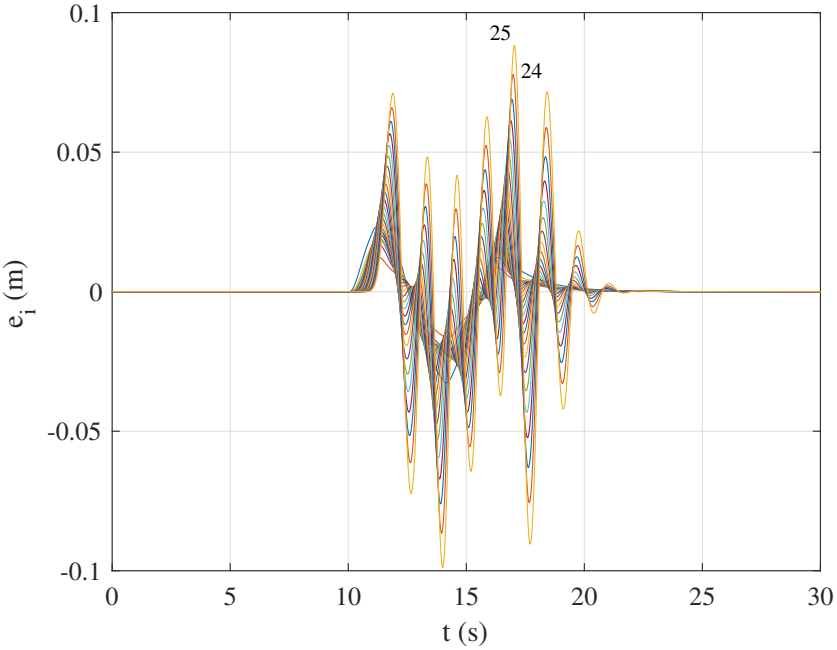

Figure 3.9: Evolution of spacing error using a r predecessor CSP controller with $K_a = 1, N = 25$

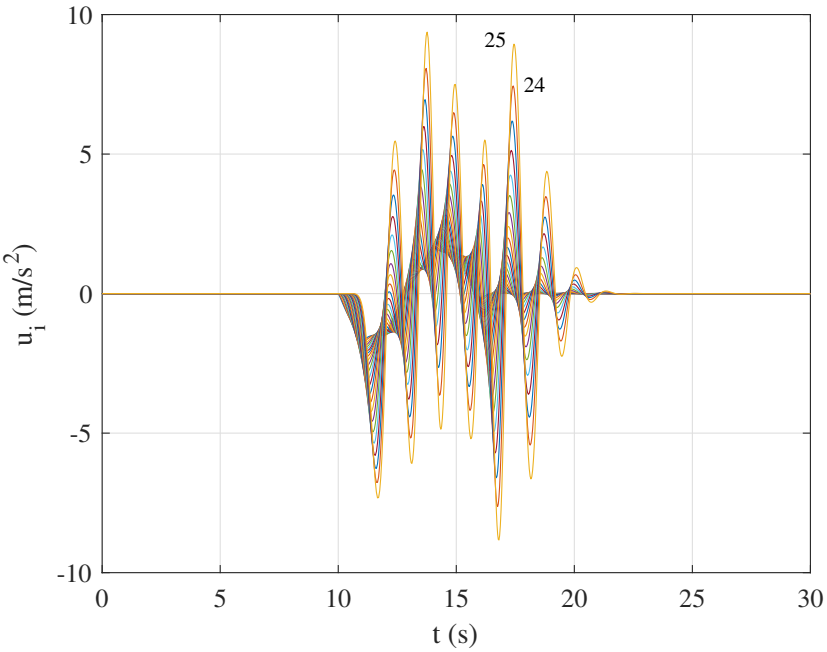

Figure 3.10: Evolution of control effort using a r predecessor CSP controller with $K_a = 1, N = 25$

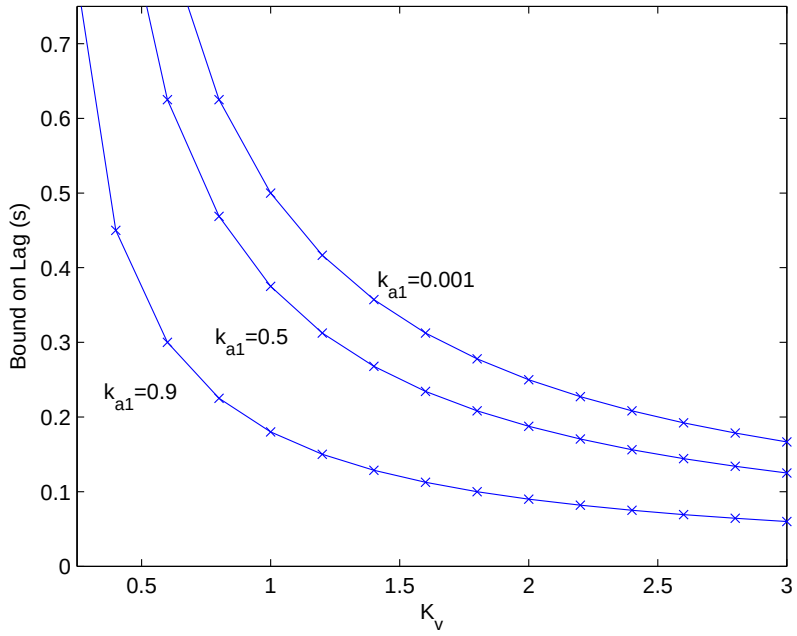

Figure 3.11: Relationship between maximum allowable parasitic lag and the cummulative velocity feedback gain (τ_0 vs. K_v) with LPF CSP controller.

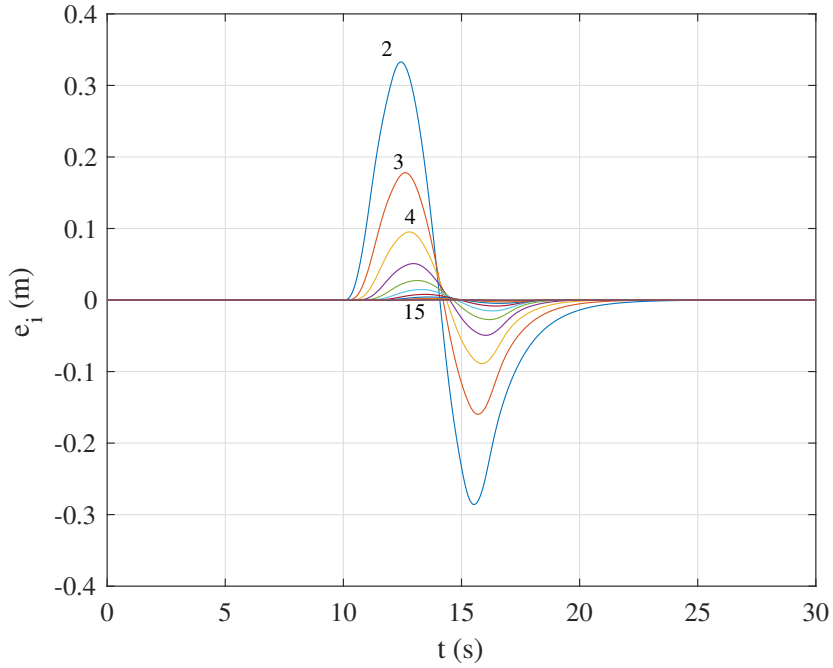

Figure 3.12: Evolution of spacing errors in a platoon of 15 vehicles with LPF information.

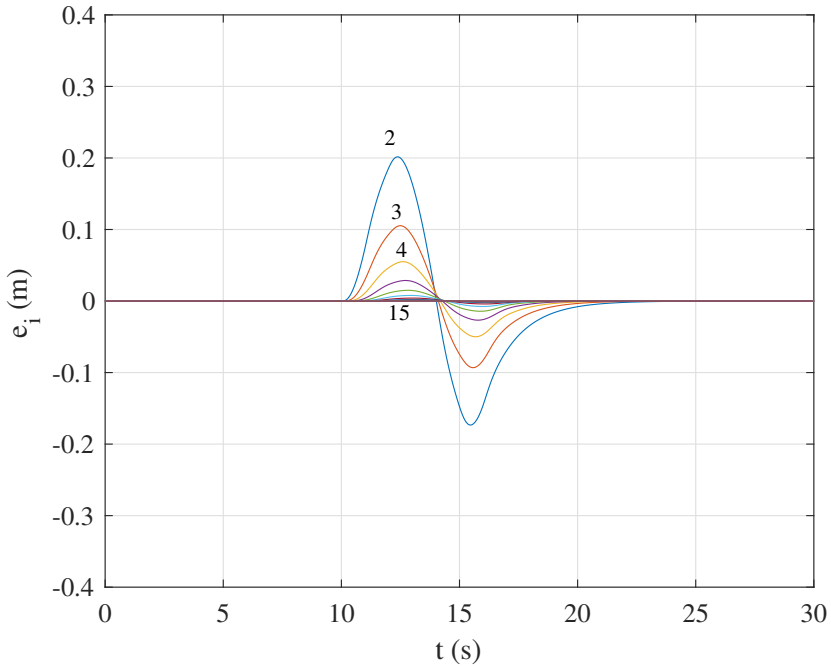

Figure 3.13: Evolution of spacing errors in a platoon of 15 vehicles with LPF and $k_a = 0.2$.

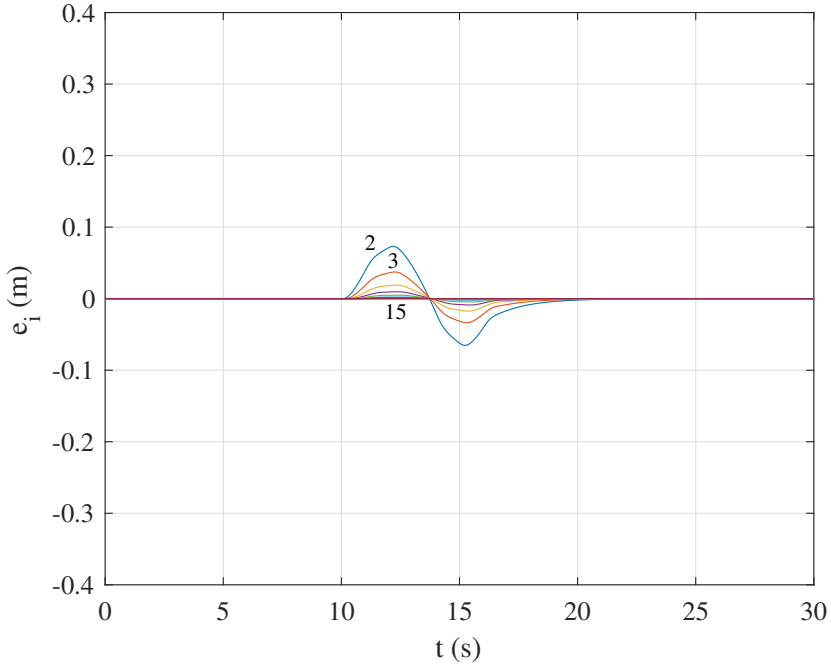

Figure 3.14: Evolution of spacing errors in a platoon of 15 vehicles with LPF and $k_a = 0.4$.

4. CONSTANT TIME HEADWAY CONTROLLERS*

In this chapter CTHP controllers that rely on communication are investigated to find the repective minimum employable time headway in presence of a parasitic lag [51]. The CTHP controller that requires acceleration of the preceding vehicle is investigated first in Section 4.1. Then CTHP controller that employes information from 'r' preceding vehicle followed by controller that employes information from the preceding and the 'r^{th}' preceding vehicle are studied in Section 4.2. Some preliminary analysis involving a CTHP controller that utilizes information from preceding and following vehicle is presented in Section 4.3. Numerical simulation and representative sample of results, along with some useful observations are presented Section 4.4.

4.1 Controller Using Predecessor Vehicle Acceleration

Consider the following control law utilizing predecessor's acceleration information in addition to the position and velocity information in (2.10):

$$u_i = k_a a_{i-1} - k_v(v_i - v_{i-1}) - k_p(e_i + h_w v_i),\ k_a, k_v, k_p > 0. \tag{4.1}$$

Using the above controller and the perturbed dynamic model in (2.3) results in the following spacing error governing equation:

$$\tau \dddot{e}_i + \ddot{e}_i + (k_v + k_p h_w)\dot{e}_i + k_p e_i = k_a \ddot{e}_{i-1} + k_v \dot{e}_{i-1} + k_p e_{i-1}. \tag{4.2}$$

*Parts of this chapter have been reprinted with permission from "Effects of V2V communication on time headway for autonomous vehicles", S. Darbha, S. Konduri, and P. R. Pagilla, in Proceedings of American Control Conference, May 2017, copyright held and published by IEEE.

Taking the Laplace transform of the above differential equation, results in the following error propagation equation.

$$E_i(s) = H_e(s;\tau)E_{i-1} = \frac{k_a s^2 + k_v s + k_p}{\tau s^3 + s^2 + (k_v + k_p h_w)s + k_p} E_{i-1}(s). \tag{4.3}$$

Note that the denominator polynomial of the above transfer function,

$$D(s,\ \tau) = \tau s^3 + s^2 + (k_v + k_p h_w)s + k_p$$

is Hurwitz for every $\tau \in (0, \tau_0]$ if and only if

$$k_v + k_p h_w > \tau_0 k_p \iff h_w > \tau_0 - \frac{k_v}{k_p}. \tag{4.4}$$

The above equation is a basic requirement of stability and it imposes a limit on the allowable time headway; in particular, a smaller value of k_p leads to a smaller lower bound for h_w. However, $\|H_e(jw;\tau)\|_\infty \leq 1$, imposes a more stringent requirement on the allowable time headway as summarized in the following theorem:

Theorem 3. *A platoon with individual vehicle dynamics* (2.3) *and the control law* (4.1) *is robust string stable if*

$$h_w \geq h_{\min} = \frac{2\tau_0}{1 + k_a}. \tag{4.5}$$

Proof. For proof the necessity condition $\|H(j\omega)\|_\infty \leq 1$ is used to find $h_{\min}$. Then the sufficiency condition is proved by finding gains that will guarantee non-negative impulse response $h(t) \geq 0$.

In order to show necessity, $k_a \in (0, 1]$ is proved first. Define

$$\omega_0 := \sqrt{\frac{k_v + h_w k_p}{\tau}}.$$

If $k_a > 1$, consider the frequency ω_0, and any $\tau < \min\{h_w, \tau_0\}$. Then $\omega_0^2 > k_p > \frac{k_p}{k_a}$. Hence, $(\omega_0^2 - \frac{k_p}{k_a}) > \omega_0^2 - k_p > 0$, and

$$\|H_e(j\omega_0;\tau)\|^2 = k_a^2 \frac{(\frac{k_p}{k_a} - \omega_0^2)^2 + \frac{k_v^2}{k_a^2}\omega_0^2}{(k_p - \omega_0^2)^2} \geq k_a^2 > 1.$$

Therefore, $k_a \in (0, 1]$ and $1 - k_a^2 \geq 0$. Now the bound on $h_{\min}$ can be derived. Consider

$$H_e(s) := \frac{N(s)}{D(s)} = \frac{k_a s^2 + k_v s + k_p}{\tau s^3 + s^2 + (k_v + k_p h_w)s + k_p}.$$

Let $s = j\omega$, then,

$$\|H_e(j\omega;\tau)\|_\infty 2 = \frac{(k_p - k_a\omega^2)^2 + k_v^2\omega^2}{(k_p - \omega^2)^2 + \omega^2(k_v + h_w k_p - \tau\omega^2)^2}.$$

Let us define

$$N(\omega^2;\tau) := (k_p - k_a\omega^2)^2 + k_v^2\omega^2, \text{ and}$$
$$D(\omega^2;\tau) := (k_p - \omega^2)^2 + \omega^2(k_v + h_w k_p - \tau\omega^2)^2,$$

then

$$\|H_e(j\omega;\tau)\|_\infty \leq 1 \iff N(\omega^2;\tau) - D(\omega^2;\tau) \geq 0, \ \forall\omega.$$

Substituting for N, D and simplifying,

$$\tau^2\omega^4 + \omega^2[(1 - k_a^2) - 2\tau(h_w k_p + k_v)] + (k_v + h_w k_p)^2 - k_v^2 - 2k_p(1 - k_a) \geq 0. \quad (4.6)$$

The above inequality is a bi-quadratic inequality. When $\tau = 0$, from the above inequality

$\|H_e(j\omega;\tau)\|_\infty \leq 1$, implies that

$$(k_v + h_w k_p)^2 - k_v^2 - 2k_p(1 - k_a) \geq 0. \tag{4.7}$$

When $\tau \neq 0$, the bi-quadratic inequality (4.6) holds for all $\omega \in \Re$ and $\tau \in (0, \tau_0]$ if and only if for every τ, if either the relation $(1 - k_a^2) - 2\tau(h_w k_p + k_v) \geq 0$ holds, or the discriminant of equation (4.6) is non-positive.

The relation $(1 - k_a^2) - 2\tau(h_w k_p + k_v) \geq 0$. together with the nominal case in (4.7) implies that

$$\begin{aligned} (k_v + h_w k_p)^2 &\geq k_v^2 + 2k_p(1 - k_a), \\ \Rightarrow (1 + k_a)(k_v + h_w k_p)^2 &- 4\tau k_p(k_v + h_w k_p) \\ &\geq k_v^2(1 + k_a) \geq k_v^2. \end{aligned}$$

Completing the square and noting that $k_v + h_w k_p > 0$, we get

$$k_v + h_w k_p \geq \frac{2k_p\tau}{1 + k_a} + \sqrt{\frac{4\tau^2 k_p^2}{(1 + k_a)^2} + k_v^2} \geq \frac{2k_p\tau}{1 + k_a} + k_v,$$

which implies,

$$h_w \geq \frac{2\tau}{1 + k_a}.$$

Since this should be true for every $\tau \in (0, \tau_0]$, it must be true in this case that the inequality (4.5) is true. The same result can also be shown by considering the discriminant of equation (4.6) is non-positive.

One has to show that gains k_p and k_v can be found when $h_w > h_{\min}$. It can be shown that for a given $\eta > 0$ and k_a, one can find k_p, k_v such that the following three conditions

hold in order for $\|H_e(j\omega;\tau)\|_\infty \leq 1$ for all $\tau \in (0, \tau_0]$, Stability: equation (4.4), nominal case $(\tau = 0)$: equation (4.7), and perturbed case $(\tau \neq 0)$: the family of polynomials given by equation (4.6), $\forall \quad \tau \in (0, \tau_0]$ is non-negative.

(a) Stability: If $h_w \geq \frac{2\tau_0}{1+k_a}(1+\eta)$, then $k_p \geq 0$ implies

$$h_w k_p = \frac{2\tau_0}{1+k_a}k_p + \frac{2\tau_0\eta}{1+k_a}k_p \geq \tau_0 k_p + \frac{2\tau_0\eta}{1+k_a}k_p > \tau_0 k_p.$$

The last inequality follows from

$$k_a \in (0,1] \Rightarrow 1 \leq 1+k_a \leq 2 \Rightarrow \frac{2}{1+k_a} \geq 1.$$

Since $k_v > 0$, it follows that $k_v + h_w k_p \geq \tau_0 k_p$. The stability condition is readily satisfied by the choice of $k_v, k_p > 0$, so it does not impose further restrictions on k_v and k_p.

(b) Nominal Case: Upon simplification of equation (4.7), condition (b) is equivalent to satisfying the inequality $h_w(2k_v + h_w k_p) \geq (1-k_a)$. The set of k_v, k_p that satisfy the above inequality when $h_w = \frac{2\tau_0(1+\eta)}{1+k_a}$ is given by:

$$\mathcal{S}_1 := \{(k_p, k_v) : k_p > 0,\ k_v > 0,\ \frac{k_v}{a_1} + \frac{k_p}{b_1} \geq 1.\},$$

where

$$a_1 := \frac{(1-k_a)^2}{4\tau_0(1+\eta)}, \quad b_1 := \frac{(1+k_a)^2(1-k_a)}{4\tau_0^2(1+\eta)^2}.$$

(c) Perturbed Case: The set of k_v, k_p satisfying the inequality $(1-k_a^2) - 2\tau_0(k_v + h_w k_p) \geq 0$, can be described by

$$\mathcal{S}_2 := \{k_p, k_v) : k_p > 0,\ k_v > 0,\ \frac{k_v}{a_2} + \frac{k_p}{b_2} \leq 1.\},$$

where

$$a_2 := \frac{1-k_a^2}{2\tau_0}, \quad b_2 := \frac{(1-k_a^2)(1+k_a)}{4\tau_0^2(1+\eta)}.$$

Clearly $\mathcal{S}_1, \mathcal{S}_2 \neq \emptyset$. To ensure that $\mathcal{S}_1 \cap \mathcal{S}_2 \neq \emptyset$, we need either $a_1 \leq a_2$ or $b_1 \leq b_2$. Considering the expressions for b_1 and b_2, we note that b_1 is always less than b_2. Hence, $\mathcal{S}_1 \cap \mathcal{S}_2 \neq \emptyset$ and one can find $(k_p, k_v) \in \mathcal{S}_1 \cap \mathcal{S}_2$.

Finally the sufficiency condition is also satisfied as shown in the following. This part involves finding one set of gains that belong to

$$\mathcal{S}_g = \{(k_p, k_v, k_a) | k_p, k_v, k_a > 0, h_e(t) \geq 0\},$$

where $h_e(t)$ is the impulse response of $H_e(s)$. □

4.1.1 Non-negativity of impulse response for string stability

The additional requirement of non-negativity of impulse response renders the problem difficult, as one must prove the following: Given $k_a \in [0, 1)$, there exist k_p, k_v such that $h(t) \geq 0$ for every $\tau \in [0, \tau_0]$ whenever $h_w \geq \frac{2\tau_0}{1+k_a}$. Although this problem appears to be simple, it is analytically difficult to solve and is related to the open problem of finding a fixed structure controller satisfying a transient specification (namely, the impulse response of the transfer function is non-negative). A transformation involving scaling with respect to τ_0 of the above problem leads it to a standard form (involving one less variable) where proving the following result suffices: Given $k_a \in [0, 1)$, there exist k_p, k_v such that $h(t) \geq 0$ for every $\tau \in [0, 1]$ whenever $h_w \geq \frac{2}{1+k_a}$. In this work, it is demonstrated numerically that a set of gains k_p, k_v can be found, for a given k_a that results in $h(t)$ being non-negative.

The basic idea of the transformation is as follows: Let $s = s'/\tau_0$, then the error propa-

gation transfer function becomes,

$$H_e(s'/\tau_0) = \frac{k_a s'^2/\tau_0^2 + k_v s'/\tau_0 + k_p}{\tau s'^3/\tau_0^3 + s'^2/\tau_0^2 + (k_v + k_p h_w)s'/\tau_0 + k_p}.$$

Multiplying both the numerator and the denominator with τ_0^2 results in,

$$H_e(s'/\tau_0) = \frac{k_a s'^2 + k_v s'\tau_0 + k_p \tau_0^2}{\tau s'^3/\tau_0 + s'^2 + (k_v + k_p h_w)s'\tau_0 + k_p \tau_0^2}.$$

Let $\tilde{\tau} = \tau/\tau_0$, $\tilde{k}_p = k_p\tau_0^2$, $\tilde{k}_v = k_v\tau_0$, $\tilde{h}_w = h_w/\tau_0$ then

$$\tilde{H}_e(s') := H_e(s'\tau_0) = \frac{k_a s'^2 + \tilde{k}_v s' + \tilde{k}_p}{\tilde{\tau} s'^3 + s'^2 + (\tilde{k}_v + \tilde{k}_p \tilde{h}_w)s' + \tilde{k}_p}, \tag{4.8}$$

where $\tilde{\tau} \in [0, 1]$ and $\tilde{h}_w = 2/(1 + k_a)$. The above representation considerably simplifies the analysis and it suffices to show that there exist gains $\tilde{k}_v$, $\tilde{k}_p$ such that $\tilde{h}_e(t) \geq 0$.

Since $\tilde{H}_e(s')$ is of the same form as $H(s)$ in Theorem 3, we can relabel all the variables ($\tilde{k}_v$ to be k_v, $\tilde{k}_p$ to be k_p, $\tau_0 = 1$ etc) and use them interchangeably. The values of k_p, k_v for a given k_a when $h_w \geq \frac{2\tau_0}{1+k_a}$ is determined using the following two results available in the literature:

1. When $\tau = 0$, let $-z_1$, $-z_2$ and $-p_1$, $-p_2$ denote the real and distinct location of zeros and poles of the above transfer function, respectively. Further let, $z_1 < z_2$ and $p_1 < p_2$. The impulse response is non-negative if [19],

$$p_1 \leq \frac{\tilde{h}_w \tilde{k}_p}{1 - k_a} \leq p_1 + p_2. \tag{4.9}$$

2. When $\tilde{\tau} \in (0, 1]$, let the three real and distinct poles of the transfer function be located at $-p_1$, $-p_2$, and $-p_3$, and let $p_3 > p_2 > p_1$. Then, the impulse response of

the system is,

$$\tilde{h}_e(t) = c_1 e^{-p_1 t} + c_2 e^{-p_2 t} + c_3 e^{-p_3 t},$$

where c_1, c_2 and c_3 are the residues obtained from the partial fraction expansion of the transfer function $\tilde{H}_e(s')$. The impulse response is non-negative if the residues satisfy [61]:

$$c_1 \geq 0, c_2 < 0 \text{ and } c_3 > \frac{p_2 - p_1}{p3 - p1} c_2. \tag{4.10}$$

Thus, for a given k_a, τ_0 and $\tilde{h}_w = 2/(1 + k_a)$, any set of $\{\tilde{k}_p, \tilde{k}_v\}$ that satisfy the relations in (4.9) and (4.10) will guarantee $\tilde{h}_e(t) \geq 0$.

In the case of $k_a = 0.95$, $\tau_0 = 1$, the following gains seem to indicate numerically that $h_e(t) \geq 0$:

$$\{k_v, k_p\} = \{0.082, 0.001\}.$$

Furthermore, these gains can be scaled back for any other τ_0 using $\tilde{k}_p = k_p \tau_0^2$ and $\tilde{k}_v = k_v \tau_0$ to guarantee non-negative impulse response of $H_e(s)$.

Note that the above theorem can be recast as follows:

Remark 2. *Let $h_e(t)$ be the unit impulse response of the error propagation transfer function $H_e(s)$. Then, there exists a set of gains (k_a, k_v, k_p) such that $\|h_e(t)\|_1 \leq 1$ for every $\tau \in [0, \tau_0]$.*

This characterization will be handy when studying other information architectures in the following sections. In the next section this analysis will be generalized to the CTHP controller which employs information from multiple vehicle look ahead.

4.2 With 'r' Predecessor Information

Consider the following generalization of the CTHP control law (2.10) with position, velocity and acceleration information from 'r' predecessor vehicles:

$$u_i(t) = \sum_{l=1}^{r} \left[k_{al} a_{i-l}(t) - k_{vl}(v_i(t) - v_{i-l}(t)) - k_{pl}(x_i(t) - x_{i-l}(t) + d_l + l h_w v_i(t)) \right], \tag{4.11}$$

where the gains k_{al}, k_{vl}, and k_{pl} are associated with feeding back the acceleration, velocity and position information associated with the l^{th} predecessor and d_l is the standstill distance between the i^{th} vehicle and its l^{th} predecessor. The above generalized control requires information that can be obtained only via vehicular communication. The goal is to investigate whether it is possible for the platoon to be robustly string stable while reducing the minimum employable time headway.

Substituting the control law (4.11) into (2.3), the governing equation for the i^{th} vehicle spacing error is given by

$$\tau \dddot{e}_i \; + \; \ddot{e}_i \; + \; \sum_{l=1}^{r} [(k_{vl} + l k_{pl} h_w)\, \dot{e}_i \; + \; k_{pl} e_i] \;\; = \;\; \sum_{l=1}^{r} (k_{al} \ddot{e}_{i-l} \; + \; k_{vl} \dot{e}_{i-l} \; + \; k_{pl} e_{i-l}).$$

The propagation of the spacing error to vehicle i from r predecessor vehicles is given by

$$E_i(s) = \sum_{l=1}^{r} H_{pl}(s) E_{i-l}(s),$$

where

$$H_{pl}(s) = \frac{k_{al} s^2 + k_{vl} s + k_{pl}}{\tau s^3 + s^2 + \sum_{l=1}^{r} [(k_{vl} + l k_{pl} h_w)\, s + k_{pl}]}. \tag{4.12}$$

The transfer function H_{pl} describes the effect of the spacing error in the $(i-l)^{th}$ vehicle

on the spacing error of the i^{th} vehicle. Using definition of induced norms [59], we have

$$\|e_i\|_\infty \leq \sum_{l=1}^{r} \|h_{pl}\|_1 \|e_{i-l}\|_\infty.$$

A sufficient condition for string stability is $\sum_{l=1}^{r} \|h_{pl}\|_1 \leq 1$. Since the objective is to demonstrate the benefits of V2V communication with some controller obeying the architecture considered, it suffices to choose the same set of gains so that one may use the result in Remark 2. For all l, let $k_{al} = k_a, k_{vl} = k_v, k_{pl} = k_p$, to define

$$H_0(s) := \frac{k_a s^2 + k_v s + k_p}{\tau s^3 + s^2 + (rk_v + \frac{r(r+1)}{2} k_p h_w)s + rk_p},$$

and the error propagation may be described by:

$$E_i(s) = H_0(s) \sum_{l=1}^{r} E_{i-l}(s).$$

Let $h_0(t)$ be the impulse response of $H_0(s)$ so that robust string stability is guaranteed if $\|h_0(t)\|_1 \leq \frac{1}{r}$. The interpretation of Theorem 3 given in Remark 2 can be used to get the following result:

Theorem 4. *A platoon with individual vehicle dynamics* (2.3) *and each vehicle receiving information from 'r' predecessors as given by the control action in* (4.11)*, where* $k_{al} = k_a$*,* $k_{vl} = k_v$*,* $k_{pl} = k_p$*, is robustly string stable when*

$$h_{\min} = \frac{4\tau_0}{(1+r)(1+rk_a)}. \tag{4.13}$$

Proof. Consider

$$rH_0 = \frac{rk_a s^2 + rk_v s + rk_p}{\tau s^3 + s^2 + (rk_v + \frac{r(r+1)}{2} k_p h_w)s + rk_p}.$$

Define $\bar{k}_a := rk_a,\ \bar{k}_v = rk_v,\ \bar{k}_p = rk_p,\ \bar{h}_w = \frac{r+1}{2}h_w$, and $\bar{H}_0(s) = rH_0(s)$, then

$$\bar{H}_0(s) = \frac{\bar{k}_a s^2 + \bar{k}_v s + \bar{k}_p}{\tau s^3 + s^2 + (\bar{k}_v + \bar{h}_w \bar{k}_p)s + \bar{k}_p}.$$

Comparing $H_e(s)$ from Theorem 3 with $\bar{H}_0(s)$, one can conclude that there exist a set of gains $(\bar{k}_a, \bar{k}_p, \bar{k}_v)$ such that $\|rh_0(t)\|_1 \leq 1$ for every $\tau \in [0, \tau_0]$ if

$$\begin{aligned} \bar{h}_w &\geq \frac{2\tau_0}{1+\bar{k}_a}, \\ \Rightarrow h_w &\geq \frac{2}{(1+r)}\frac{2\tau_0}{(1+rk_a)} = \frac{4\tau_0}{(1+r)(1+rk_a)}. \end{aligned}$$

□

4.2.1 With Immediate and 'r^{th}' Predecessor Information

Practical considerations on the communication bandwidth may force each vehicle to pick only a few predecessors to maintain a reliable communication; in such situations, one may want to use the immediate predecessor and a second predecessor (r^{th}vehicle) from the downstream of the platoon. When using immediate and r^{th}-predecessor information in the feedback, the control law can be rewritten as,

$$u_i = \sum_{l=1,r} \left[k_{al}a_{i-l} - k_{vl}(v_i - v_{i-l}) + k_{pl}(x_i - x_{i-l} + d_l + lh_w v_i)\right]. \tag{4.14}$$

The above control law is a special case of the r vehicle look ahead control law in (4.11) with two vehicle feedback, where the second vehicle is the r^{th} vehicle. If $k_{a1} = k_{ar} = k_a,\ \ k_{v1} = k_{vr} = k_v$, and $k_{p1} = k_{pr} = k_p$, define

$$H_0(s) := \frac{k_a s^2 + k_v s + k_p}{\tau s^3 + s^2 + (2k_v + 3k_p h_w)s + 2k_p},$$

so that the error propagation is given by:

$$E_i(s) = H_0(s)E_{i-1}(s) + H_0(s)E_{i-r}(s).$$

Let $h_0(t)$ be the impulse response of $H_0(s)$, then robust string stability is guaranteed if $\|h_0(t)\|_1 \leq \frac{1}{2}$. The proof of the following result is analogous to the proof of Theorem 4.

Corollary 1. *A platoon with individual vehicle dynamics* (2.3) *and the control law* (4.14)*, where* $k_{a1} = k_{ar} = k_a,\ \ k_{v1} = k_{vr} = k_v,\ k_{p1} = k_{pr} = k_p$*, is robust string stable when*

$$h_{\min} = \frac{4\tau_0}{(1+r)(1+2k_a)}. \tag{4.15}$$

Therefore, from the above theorems and its corollary it is clear that, with a CTHP controller utilizing 'r' predecessor vehicle look ahead information, one can possibly employ a smaller time headway while maintaining robustly string stable platoon.

Remark 3. *It is very important to note that, the lower bound on the time headway in the above theorem is derived from a sufficient condition for string stability. One may be able to find a smaller minimum employable time headway than the value given by equation* (4.13) *and* (4.15)*, while also guaranteeing string stability, however, at this point it is still unclear which analysis can be used to obtain such a result.*

4.3 With Immediate Predecessor and Follower Information

If the vehicles in the platoon use a bidirectional information flow graph shown in Figure 2.8(d) then one can employ information from both the predecessor and the follower vehicle in calculating the control input. When every vehicle can obtain position, velocity and acceleration information from its immediate predecessor and follower (shown in

Fig. 2.4) then the CTHP control input can be modeled as follows,

$$u_i = k_a^f a_{i-1} - k_v^f \dot{e}_i - k_p^f \delta_i + k_a^b a_{i+1} - k_v^b (v_i - v_{i+1}) - k_p^b (x_i - x_{i+1} - d - h_w v_i) \quad (4.16)$$

where k_a, k_v and k_p are positive feedback gains, the superscripts f and b denote the gains corresponding to the predecessor vehicle and the follower vehicle respectively. Let $K_p = k_p^f + k_p^b$, $K_v = k_v^f + k_v^b$, $K_a = k_a^f + k_a^b$, $\Delta_p = k_p^f - k_p^b$. Substituting the above controller in the vehicle dynamics given by (2.3), results in the following governing equation for the spacing error of the i^{th} vehicle:

$$\tau \dddot{e}_i + \ddot{e}_i + (K_v + h_w \Delta_p)\dot{e}_i + K_p e_i = k_a^f \ddot{e}_{i-1} + k_v^f \dot{e}_{i-1} + k_p^f e_{i-1} + k_a^b \ddot{e}_{i+1} + k_v^b \dot{e}_{i+1} + k_p^b e_{i+1} \quad (4.17)$$

Let the state vector be $X_i = [e_i, \dot{e}_i, \ddot{e}_i]^T$. The above governing equation can be rewritten as follows,

$$\begin{pmatrix} \dot{e}_i \\ \ddot{e}_i \\ \dddot{e}_i \end{pmatrix} = \begin{pmatrix} \dot{e}_i \\ \ddot{e}_i \\ \frac{1}{\tau}[-\ddot{e}_i + k_a^f \ddot{e}_{i-1} + k_a^b \ddot{e}_{i+1} - (K_v + \Delta_p h_w)\dot{e}_i \\ \quad + k_v^f \dot{e}_{i-1} + k_v^b \dot{e}_{i+1} - K_p e_i + k_p^f d_{i-1} + k_p^b e_{i+1}] \end{pmatrix} \quad (4.18)$$

Employing the bilinear $\mathcal{Z}$-transformation discussed in Section 2.2 of Chapter 2 and discretizing the above dynamics, results in the following spatially discretized state equation.

$$\frac{d}{dt} \begin{bmatrix} \tilde{e}(z,t) \\ \dot{\tilde{e}}(z,t) \\ \ddot{\tilde{e}}(z,t) \end{bmatrix} = \tilde{A}(z) \begin{bmatrix} \tilde{e}(z,t) \\ \dot{\tilde{e}}(z,t) \\ \ddot{\tilde{e}}(z,t) \end{bmatrix}, \quad (4.19)$$

where,

$$\tilde{A}(z) := \begin{bmatrix} 0 & 1 & 0 \\ 0 & 0 & 1 \\ \frac{-K_p+z^{-1}k_p^f+zk_p^b}{\tau} & \frac{-(K_v+\Delta_p h_w)+z^{-1}k_v^f+zk_v^b}{\tau} & \frac{-1+z^{-1}k_a^f+zk_a^b}{\tau} \end{bmatrix}.$$

Lemma 1 is used in the following theorem to show that the platoon is string stable when using information from the predecessor and the follower vehicle.

Theorem 5. *A platoon with individual vehicle dynamics* (2.3) *and controller given by* (4.16)*, is string stable.*

Proof. The proof involves first showing that for some value of θ there is one eigenvalue on the imaginary axis at zero and the other two are in the open left half plane. Then it is shown that the eigenvalue on the imaginary axis moves inside the left half plane for any change in θ.

From the discretized state equation in (4.19), the eigenvalues of the matrix $\tilde{A}(z)$ can be computed from its characteristic polynomial $|\lambda I - \tilde{A}| = 0$, where I is a 3×3 identity matix. Thus,

$$|\lambda I - \tilde{A}| = \lambda^3 + \lambda^2 \frac{1 - z^{-1}k_a^f - zk_a^b}{\tau} + \lambda \frac{K_v + \Delta_p h_w - z^{-1}k_v^f - zk_v^b}{\tau} + \frac{K_p - z^{-1}k_p^f - zk_p^b}{\tau} = 0 \quad (4.20)$$

Let $z = e^{j\theta}$ where $\theta \in [0, 2\pi]$, substituting for z in the above characteristic polynomial will result in

$$|\lambda I - \tilde{A}(e^{j\theta})| = \lambda^3 + \lambda^2 \frac{1 - e^{-j\theta}k_a^f - e^{j\theta}k_a^b}{\tau} + \lambda \frac{K_v + \Delta_p h_w - e^{-j\theta}k_v^f - e^{j\theta}k_v^b}{\tau} + \frac{K_p - e^{-j\theta}k_p^f - e^{j\theta}k_p^b}{\tau} = 0 \quad (4.21)$$

When $\theta = 0$ or 2π, $e^{j\theta} = 1$ and the above polynomial is reduced to:

$$|\lambda I - \tilde{A}| = \lambda^3 + \lambda^2 \frac{1 - K_a}{\tau} + \lambda \frac{\Delta_p h_w}{\tau} = 0. \tag{4.22}$$

The above polynomial has one root on the imaginary axis at $\lambda = 0$. Further, to satisfy the requirements of Lemma 1, one requires $K_a < 1$ and $\Delta_p > 0$. Thus at $\theta = 0, 2\pi$ all the conditions of Lemma 1 are satisfied. In the following it is shown that the root at $\lambda = 0$ does not move into the right half plane for a change in θ at $\theta = 0$. For simplicity let, $k_a^f = k_a^b = k_a$, $k_v^f = k_v^b = k_v$. Then using $e^{j\theta} = \cos\theta + j\sin\theta$, the polynmoial (4.21) is simplied to,

$$P(\lambda) = \lambda^3 + \lambda^2 \frac{1 - 2k_a \cos\theta}{\tau} + \lambda \frac{\Delta_p h_w + 2k_v(1 - \cos\theta)}{\tau} + \frac{K_p - e^{-j\theta} k_p^f - e^{j\theta} k_p^b}{\tau} = 0 \tag{4.23}$$

Let $\lambda' = \frac{\partial \lambda}{\partial \theta}$ and $\lambda'' = \frac{\partial^2 \lambda}{\partial \theta^2}$. Differentiating $P(\lambda)$ with respect to θ at $\theta = 0, \lambda = 0$ and setting the result equal to zero, will give the movement of the root with change in θ. Thus,

$$\begin{aligned} \frac{\partial P(\lambda)}{\partial \theta}\bigg|_{\theta=0,\lambda=0} &= \frac{\Delta_p h_w}{\tau}\lambda' + j\frac{\Delta_p}{\tau} = 0, \\ \lambda' &= \frac{-j}{h_w}. \end{aligned} \tag{4.24}$$

The first derivative does not provide any information on the movement of the real part of λ. Differentiating $\frac{\partial P(\lambda)}{\partial \theta}$ again w.r.t θ, at $\theta = 0, \lambda = 0$, and setting it equal to zero,

$$\begin{aligned} \frac{\partial^2 P(\lambda)}{\partial \theta^2}\bigg|_{\theta=0,\lambda=0} &= \frac{2(1 - 2k_a)}{\tau h_w^2} + \lambda'' \frac{\Delta_p h_w}{\tau} + \frac{K_p}{\tau} = 0, \\ \lambda'' &= -\frac{K_p + 2(1 - 2k_a)/h_w^2}{\Delta_p h_w}. \end{aligned} \tag{4.25}$$

Since $2k_a = K_a < 1$, we have $\lambda'' \leq 0$. Therefore, the root at $\lambda = 0$ moves to the left of the

imaginary axis with a change in θ. Hence, the platoon is string stable with a bidirectional communication. □

Remark 4. *It should be noted that the above theorem only shows that it is possible to obtain a string stable platoon when using bidirectional communication. It does not however provide any bound on the time headway. Determining this bound will require additional analysis which will be part of the future work.*

4.4 Numerical Simulations

Numerical simulations to corroborate the above results. The numerical values for the common parameters are given in Table 4.1. The velocity profile for the lead vehicles is shown in Fig. 4.1. Two time headway cases are considered; one that satisfies the minimum allowable time headway bound and the other that violates this limit.

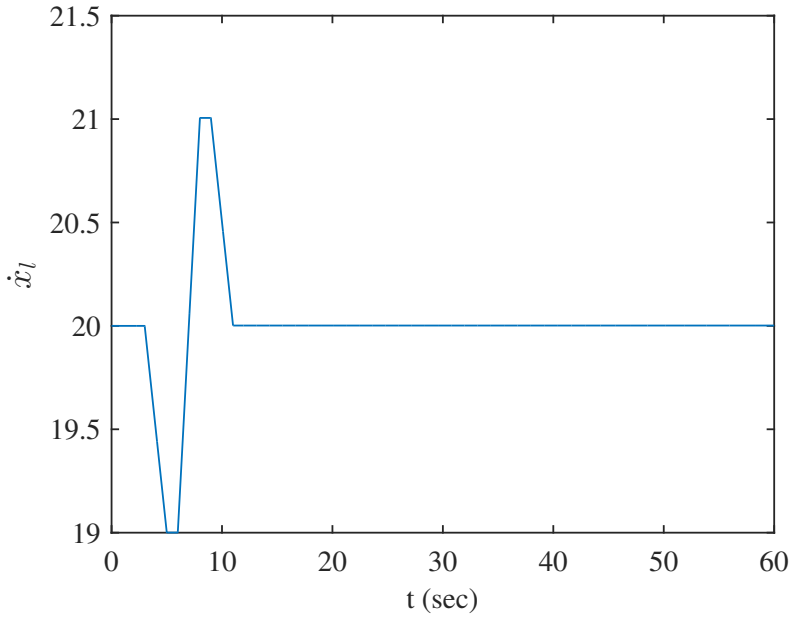

Figure 4.1: Velocity profile of the lead vehicle used in simulations.

Three values for 'r' are considered: $r = 1$, $r = 3$, and $r^{th} = 3$ where r^{th} indicates that information is used from the immediate and third predecessor; these three values correspond to the results in Theorems 3 and 4. Figures 4.2, 4.3, and 4.4 show the results for these three cases. Numerical values of the time headways used for these three cases are given in Table 4.2; the column entitled h_w (a) corresponds to values larger than the lower bound ($h_{\min}$) and the column h_w (b) corresponds to time headway values smaller than the lower bound. It is clear from the simulation results that smaller values of time headway

n	d	τ_0	k_p	k_v	k_a	v_r
15	5 m	0.5	45	0.8	0.25	20 m/s

Table 4.1: Numerical values

Figure	r	$h_{\min}$	h_w (a)	h_w (b)
Fig. 4.2	1	0.8	0.88	0.68
Fig. 4.3	3	0.28	0.5	0.27
Fig. 4.4	$r^{th} = 3$	0.33	0.58	0.31

Table 4.2: Numerical values corresponding to figures

than $2\tau_0$ can be employed with information obtained via V2V or I2V communication.

Figure 4.5 provides position and velocity gain values (with $k_a = 0.95$) that correspond to error propagation transfer function subjected to non-negative impulse response requirement. The gain values $\{\tilde{k}_v, \tilde{k}_p\}$ were determined using the discussions in Section III.D to ensure $\tilde{h}_e(t) \geq 0$ when $k_a = 0.95$, $\tau_0 = 0.5$ seconds, and $\tilde{h}_w = 2/(1 + k_a) = 1.02$. The approach involved utilization of a range of parameter values (gridding) for $\tilde{k}_v$ and $\tilde{k}_p$ and

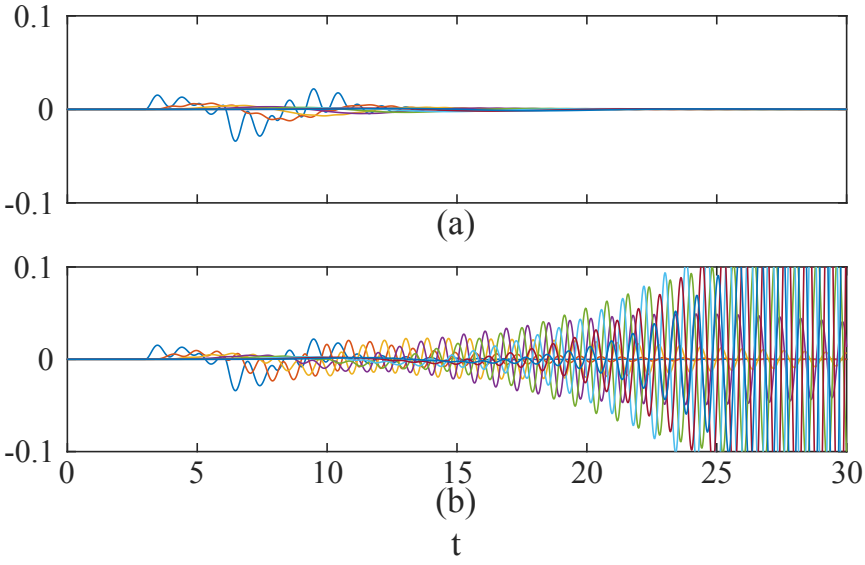

Figure 4.2: Evolution of spacing error using CTHP controller with $r = 1$, (a) $h_w > h_{\min}$ and (b) $h_w < h_{\min}$.

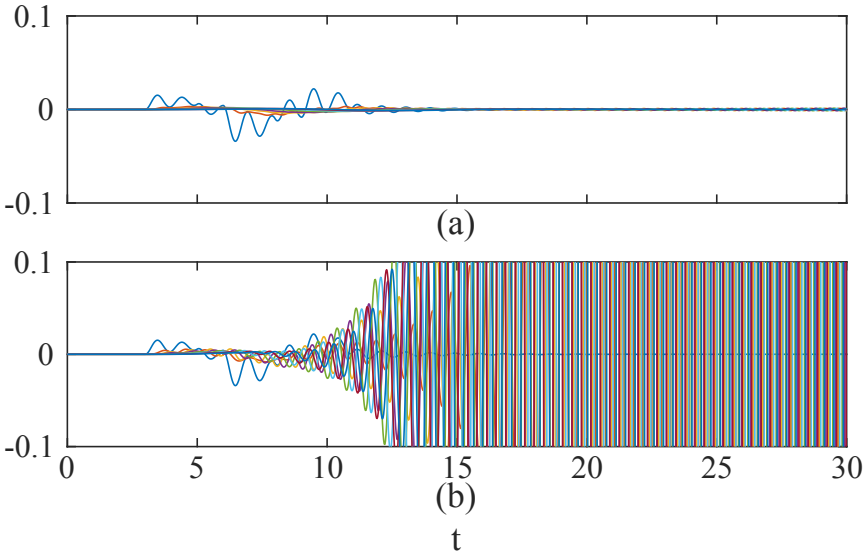

Figure 4.3: Evolution of spacing error using CTHP controller with $r = 3$, (a) $h_w > h_{\min}$ and (b) $h_w < h_{\min}$.

checking if the conditions for non-negative impulse response requirement were met. In Fig. 4.5, the blue dots correspond to $\tilde{h}_e(t) \geq 0$ when $\tilde{\tau} = 0$; the red dots correspond to

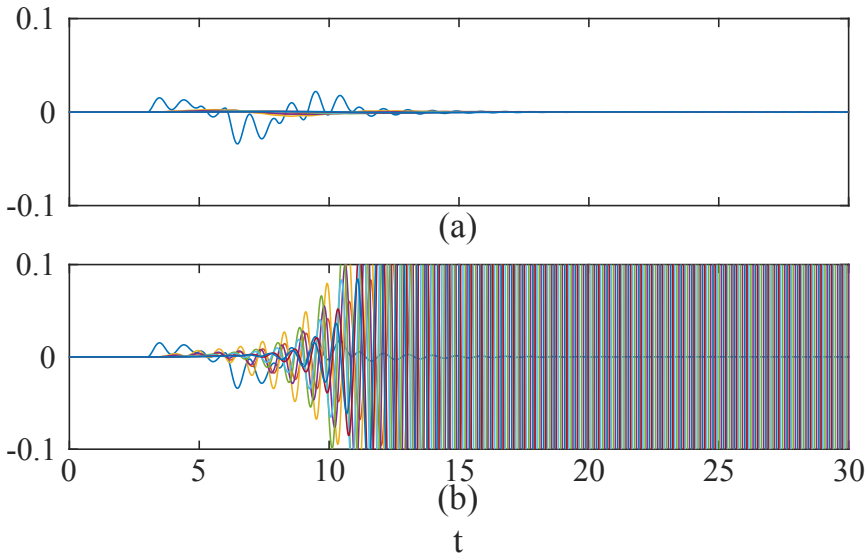

Figure 4.4: Evolution of spacing error using CTHP controller with $r^{th} = 3$, (a) $h_w > h_{\min}$ and (b) $h_w < h_{\min}$.

real poles for the time-scaled spacing transfer function ($\tilde{H}_e(s)$) and $\tilde{\tau} \in [0, 1]$; the orange circles correspond to the three conditions, $\tilde{\tau} \in [0, 1]$, real poles for $\tilde{H}_e(s)$, and $\tilde{h}_e(t) \geq 0$. Therefore, in Fig. 4.5, the orange shaded region provides the permissable position and velocity gain values. Fig. 4.6 provides the impulse responses for one particular set of gains in this region and various values of parasitic lags ($\tilde{\tau} \in [0, 1]$ in the intervals of 0.1 s, for gains $\tilde{k}_p = 0.001, \tilde{k}_v = 0.085$).

Simulations were also conducted to compare the platoon response when using predessor and follower information vs only the predecessor information. The parameters used in the simulation are $N = 15$, $d = 5$ m, $v_0 = 29$ m/s, $\tau = 0.1$ seconds, $k_p^f = 1$, $k_p^b = 0.99k_p^f$, $k_v^f = k_v^b = 2.5$, $k_a^f = k_a^b = 0.5$, $h_w = 0.15$. The lead vehicle undergoes a velocity maneuver starting at 10 seconds into the simulation, a deceleration followed by acceleration of magnitude 1 m/s^2. The evolution of spacing errors with the bidirectional and predecessor information are shown in Fig. 4.7, where dotted line represents the first follower and dashed line the last vehicle in platoon. Notice that the spacing errors

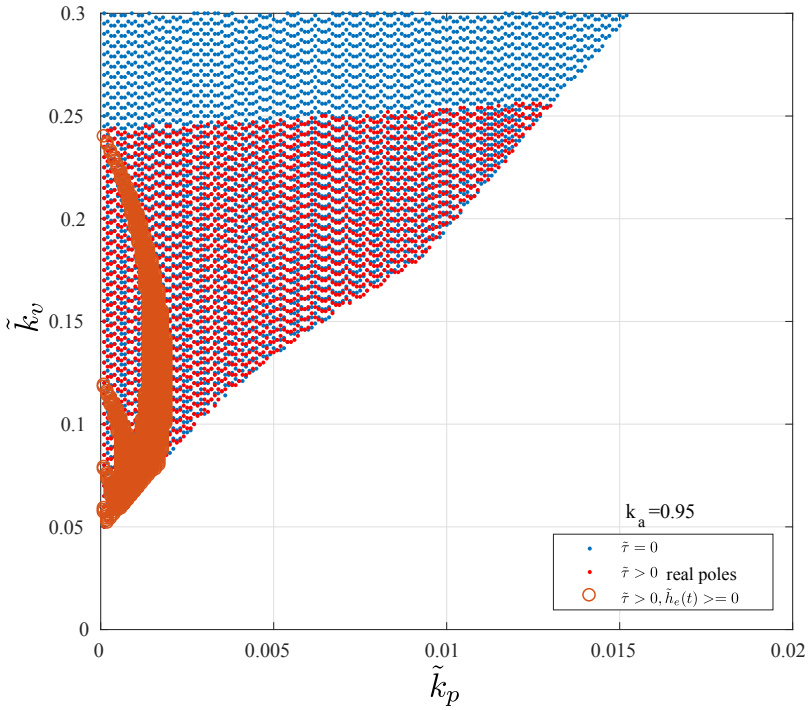

Figure 4.5: Gains $\tilde{k}_p, \tilde{k}_v$ that satisfy $\tilde{h}_e(t) \geq 0$ when $k_a = 0.95$ and $\tilde{h}_w = 1.02$.

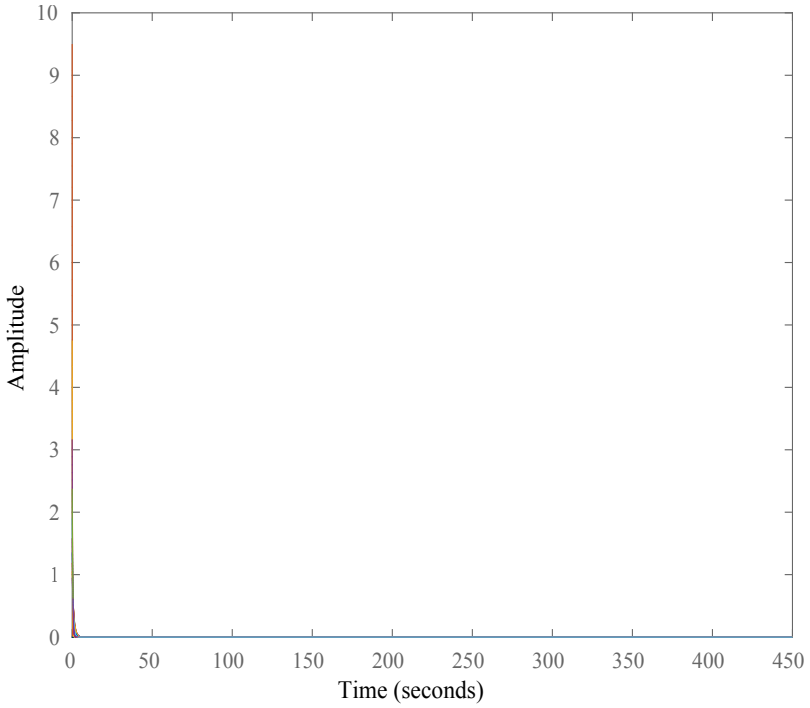

Figure 4.6: Impulse responses $\tilde{h}_e(t)$ for $\tilde{\tau} \in [0, 1]$ in 0.1 intervals for $\{k_a, \tilde{k}_v, \tilde{k}_p\} = \{0.95, 0.082, 0.001\}$ and $\tilde{h}_w = 1.02$.

attenuate with both bidirectional and predecessor information controller, however when the maneuver is complete at 14 seconds, the bidirectional converges smoothly while the predecessor information controller has an overshoot. Similar response can be observed for time headways as small as 0.05 seconds.

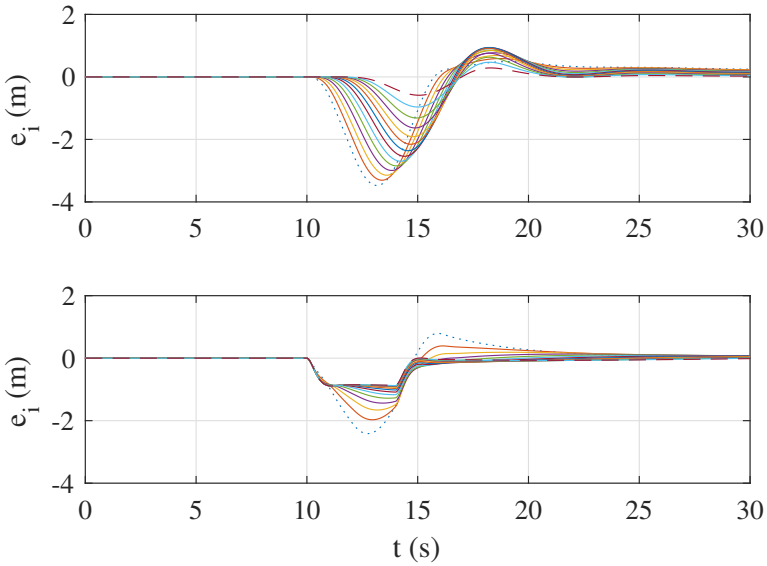

Figure 4.7: Spacing error evolution with bidirectional and predecessor information controllers with $h_w = 0.15$.

4.5 Observations

The communication models considered in this work and their respective minimum employable time headway are summarized in the Table 4.3. The following observations are made based on the results of Theorems 3, 4 and its corollary. These observations may be helpful in making design choices for implementing CACC systems with information from multiple vehicles in the feedback.

- When information from only immediate predecessor is used, and acceleration feed-

back gain is selected to be zero, the lower bound in inequality (4.5) reduces to h_{min} given in equation (4.5).

- In the immediate predecessor feedback if the acceleration feedback gain k_a is chosen arbitrarily close to one, the minimum employable time headway in eqn. (4.5) reduces to

$$h_{\min} = \tau_0. \tag{4.26}$$

Hence, choosing $k_a = 1$, the lower limit on h_w can be halved and platoon can be string stable for any headway greater than the maximum parasitic lag.

- If information from two predecessor vehicles is utilized with equal gains selected for position, velocity and acceleration feedback, and if the acceleration feedback gains are chosen such that their sum is close to unity, then the bound on minimum employable time headway reduces to

$$h_{\min} = \frac{2\tau_0}{3}. \tag{4.27}$$

The above bound on time headway is the same as the bound provided in [39]; this bound was obtained via numerical simulations.

- For $r \geq 3$, when equal gains are selected for position and velocity feedback, the lower bound on minimum time headway is $h_{\min} \leq \tau$. Thus the vehicle only needs to use information from at least three predecessor vehicles in order to overcome the limitation imposed by the parasitic lags in a vehicle. This is intuitive because if the vehicle has access to information of vehicles downstream, then it has knowledge of future events, which is not possible with information from only the immediate predecessor vehicle.

- One can also reduce the lower limit on the employable time headway even if predecessor vehicle(s) acceleration is not used in the feedback. If $k_{al} = 0$ and equal gains are chosen for position and velocity feedback errors, the inequality (4.13) is reduced to

$$h_w \geq \frac{4\tau_0}{r+1}. \tag{4.28}$$

- The inequality shown in (4.13) is free of the velocity feedback gain k_{vl} indicating that string stability of the platoon is not dependent on the velocity error. However, it is required if one were to obtain zero steady state errors to velocity maneuvers.

- Using the information from the immediate and r^{th}predecessor can have similar effect as using 'r' vehicles in the feedback. If acceleration gains are chosen such that their sum is close to one, the bound in (4.15) is reduced to

$$h_{\min} = \frac{2\tau_0}{(r+1)}.$$

  Picking a large r will in reduce the bound on employable minimum time headway, however, using a large r will inevitably result in communication overhead due to the long distances the information has to travel.

While theoretically using either large number of vehicles or the r^{th}predecessor in the feedback improves the capacity of the highway by reducing the lower bound on the minimum employable time headway, this may cause a lot of communication overhead. Furthermore, current state of the art uses near field communication technology [2] which imposes severe restriction on the value of r that can be used. In light of this a good compromise will be to use information from two or three predecessor vehicles that are close to the vehicle. For example, one can use information from the two immediate predecessors or the immediate and the 3-rd predecessor. In the cases where communication bandwidth is restricted, using

Communication Type	$h_{\min}$
Immediate predecessor	$2\tau_0/(1+k_a)$
r predecessors	$4\tau_0/(1+r)(1+rk_a)$
With $rk_a \approx 1$	$2\tau_0/(1+r)$
With $rk_a = 0$	$4\tau_0/(1+r)$
With $rk_a \approx 1, r = 2$	$2\tau_0/3$
With $rk_a \approx 1, r = 3$	$\tau_0/2$
Immediate and r^{th} predecessor	$4\tau_0/(1+r)(1+2k_a)$
With $2k_a \approx 1$	$2\tau_0/(1+r)$

Table 4.3: Communication type vs the minimum employable time headway.

only information from the immediate predecessor will also provide considerable benefits over using information from just the onboard sensors.

5. NUMERICAL STUDIES: EFFECT OF BRAKE LIGHT INFORMATION AND QUANTIZATION

In the previous chapters it was demonstrated that vehicular communication with CTHP controllers can result in reduction of inter-vehicular spacing. However, one can only use vehicular communication if the controlled vehicle and its predecessor are both equipped with communication devices. There may be situations on highways where vehicles that are not equipped for communication are within the platoon. The traditional method to deal with such situations has been to fall back to an adaptive cruise control [2], which leads to an increase in the time headway between the vehicle and its predecessor. But, one may be able to use a smaller time headway than ACC if the vehicle has information about changes in predecessor's acceleration or at the very least the knowledge of whether the predecessor vehicle is applying brakes(deceleration) via observation of brake light. This knowledge may aid the vehicles' controller to react quickly and avoid collisions.

Even if all the vehicles of the platoon are equipped for communication, there are limitations on the bandwidth. This may compel the designers to transmit as little information as possible to ensure the integrity of the information exchanged. One of the techniques that reduces the total information transmitted is information quantization. Quantization involves mapping the information into discrete sets. Quantization will result in loss of some information, usually the least significant bits of the data. This may have detrimental effect on the string stability of the platoon if the discrete sets are very coarse, which needs to be examined.

In this chapter, numerical simulations are used to investigate the platoons behavior when using brakelight information and information quantization. In Section 5.1 the effect of using brake light information on the vehicles in the platoon is studied. The effect of

information quantization on the behavior of platoon is investigated in Section 5.2.

5.1 Predecessor Brakelight Information

In this section the predecessor vehicles' brake light status is included in the control input to observe if it is possible to use a smaller time headway than the bound given by (2.20), i.e., $2\tau_0$. The general form of ACC control input that also incorporates brake light information may be written as,

$$u_i = -k_v(v_i - v_{i-1}) - k_p(x_i - x_{i-1} + d + h_w v_i) + u_b \tag{5.1}$$

where u_b is the input due to the feedback from the brake light sensor. It is assumed that the vehicle can detect its predecessor's brake irrespective of the time of the day, and that the input u_b satisfies the following conditions.

- The input should be zero when the brake light is not on.
- It should act only if the brake light is on for more than a specified period of time (few milli seconds).

For simplicity it is further assumed that the second condition is satisfied always. Consider the input u_b as follows,

$$u_b = -k\frac{1 + sign(brake)}{2} \tag{5.2}$$

where k is positive value and the function $sign(brake)$ is -1 when the brake light is off and 1 when it is on. Thus, the above input is non-zero only when the predecessor brake light is detected. The gain k may be a constant or a variable, the effect of which will be discussed next.

Let a variable gain be as follows,

$$k = k_p h_{bl} v_i \tag{5.3}$$

where h_{bl} is an additional headway due to the brake light. Using the above gain, when brake light is on we can rewrite the control input as,

$$u_i = -k_v(v_i - v_{i-1}) - k_p(x_i - x_{i-1} + d + (h_w + h_{bl})v_i). \tag{5.4}$$

Hence, the gain in (5.3) essentially increases the time headway whenever the vehicle detects its predecessor has applied brakes, which results in an increase of the spacing between vehicles.

The reason for using such a gain is discussed in the following. The vehicles equipped with ACC require a time headway of $2\tau_0$ because this headway provides sufficient spacing for the vehicle to react to any disturbances in the preceding vehicle. But the objective is to use a $h_w < 2\tau$, and be able attenuate spacing errors using only the brake light status. Using the above formulation for gain k one can continue using a small time headway as long as no brake light is detected. If the brake light is detected, the time headway can be increased to a value satisfying the bound ($2\tau_0$), thus ensuring that the vehicle has time to react to any further disturbances. Numerical simulations are carried out to evaluate the behavior of platoon using this control action.

The parameters used in the simulations are, $N = 15$, $d = 5$ m, $v_0 = 29$ m/s, $k_p = 1$, $k_v = 5$, $\tau = 0.1$ seconds. This will result in a minimum time headway of 0.2 seconds according to the bound in equation (2.20). In all the simulations, the lead vehicle undergoes a deceleration maneuver between 10 to 14 seconds of the simulation time. The time headway of the vehicles is chosen to be $h_w = 0.17$ seconds, which is less than minimum value computed. The evolution of the vehicle's velocity and accelerations are presented for all the simulations. The first follower vehicle is represented as a dotted line ($\cdots$) and the last vehicle in the platoon is represented by a dashed line ($--$).

For the first simulation, the lead vehicle undergoes a constant deceleration of $u_l = -1$

m/s^2. During this time the control input due to the brake light is selected such that it adds 0.03 seconds to the time headway (a step change) bringing the total time headway of vehicle to 0.2 seconds ($h_{\min}$). Thus, $u_b = 0.03v_i,\ t \in (10, 14)$. The velocity and acceleration evolution are shown in the Figure 5.1. Notice that the response of the system is slightly oscillatory, however, both the velocity and acceleration responses show an overshoot at 14 seconds into the simulation. This is the point when the brake light is off and the time headway is reduced from 0.2 to 0.17 in a single step. The response of the platoon for the same deceleration profile but with a gradual reduction in time headway from 0.2 to 0.17 seconds after the end of deceleration (at 14 seconds) is shown in Figures 5.2 and 5.3. From these figures it is observed that the overshoot in velocity and acceleration is small and they settle to the final values more smoothly than compared to Figure 5.1.

The next set of simulations are conducted with a sinusoidal deceleration profile for the lead vehicle. Simulations are conducted with, (1) a step change in the time headway (as in the previous case) and (2) a headway change similar to the deceleration profile (sinusoidal) of the predecessor. The velocity and acceleration evolution are shown in Figures 5.4 through 5.7. It is observed that a step change in the headway, results in oscillatory response combined with increasing overshoots. For a sinusoidal deceleration and sinusoidal change in headway, the response is not as jerky as the earlier simulation where the headway is increased and decreased abruptly as a step.

The results of the above discussed simulations show a common pattern, which is, if the change in time headway follows a curve similar to that of the predecessor braking (constant or step, sinusoidal), then the velocity and acceleration evolve smoothly. The drawbacks of using brake light status in the control input are: the vehicle only has access to brake light state which does not give any information about the type of deceleration profile that the predecessor is following, and brake light status is not useful if the preceding vehicle is accelerating.

One can also employ a constant gain for the brakelight feedback in (5.2). In such a case, the input (5.1) *when brake light is on* can be rewritten as,

$$u_i = -k - k_v(v_i - v_{i-1}) - k_p(x_i - x_{i-1} + d + h_w v_i) \tag{5.5}$$

where k is a fixed value. This is similar to the control input given by (4.1). Physically the above controller would result in a constant deceleration of the vehicle if the brake light is detected. Note that using the above controller will require that at zero velocity, k should be set to zero, else the vehicle controller will saturate.

The parameters of the simulation remain the same as the previous simulations. The leader decelerates at 1 m/s^2 for four seconds starting at 10 seconds into simulation. With brake light deceleration gain of $k = 0.1$, and $h_w = 0.18$, the evolution of spacing errors and the accelerations are shown in Fig. 5.8. While the acceleration decreases in magnitude from first follower to the last, the spacing error shows the opposite trend by increasing in overshoot. The gain is further increased to $k = 0.3$ and the simulations are rerun with a time headway of 0.15 whose results are shown in figure 5.9. The errors are attenuated only when the time headway is chosen greater than 0.2 indicating that the use of signum function for brake light status may not be a good strategy.

5.2 Quantization of Information

To study the effect of quantization, the following simple quantization model that rounds the acceleration information is utilized:

$$a_{i-1} = q * floor\left(\frac{a_{i-1}}{q} + \frac{1}{2}\right), \tag{5.6}$$

where q is the quantization step. A small value of q implies that the quantization is very fine. If $q = 1$ then the real number a_{i-1} is simply rounded to the integer value that is the

floor of the given number. The quantized acceleration from the above equation can now be used in the CACC control input from equation (4.1).

All the simulations on information quantization use the parameters $N = 15$, $d = 5$ m, $v_0 = 29$ m/s, $k_p = 1$, $k_v = 2.5$, $\tau = 0.1$ seconds, and $k_a = 0.5$, which implies $h_{\min} = 0.133$. A fixed time headway of $h_w = 0.17$ seconds is used in the simulations. The lead vehicle undergoes a continuous sinusoidal disturbance of magnitude 3 m/s^2 at a frequency of one radian. When a small quantization step of $q = 0.1$ is used, the spacing errors attenuate, however, the control input evolution shows some noise, Figure 5.10.

As the quantization step increases, the spacing error attenuation reduces. Around a quantization value of $q = 0.6$, the spacing errors begin to amplify indicating loss of string stability, as seen in Figure 5.11. It was observed that, with an increase in the acceleration feedback gain, one can use a higher quantization value. The quantization value at which errors start to amplify is also correlated to the time headway chosen. Figure 5.12 shows the spacing error amplification for three different time headway choices and their corresponding quantization values. This implies that the platoon can sustain the string stability with a larger quantization value provided a large time headway value is chosen.

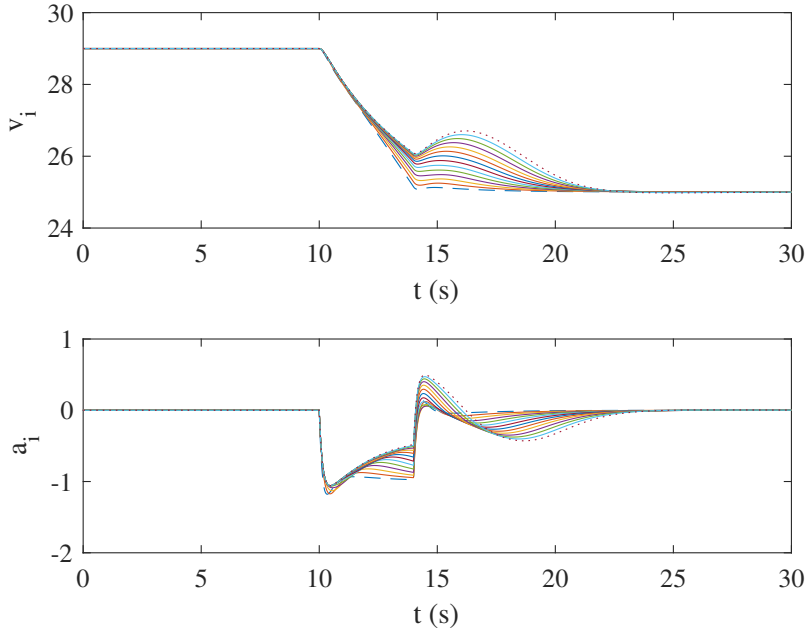

Figure 5.1: Constant deceleration and step change in h_w from 0.17 to 0.2 s.

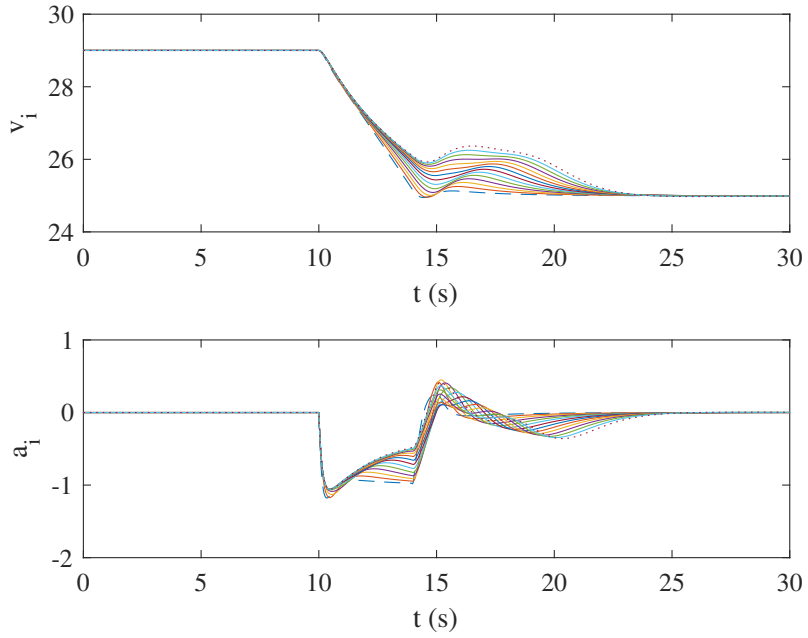

Figure 5.2: Constant deceleration and step change in h_w from 0.17 to 0.2 s followed by a gradual change in h_w from 0.2 to 0.17 s in 1 second.

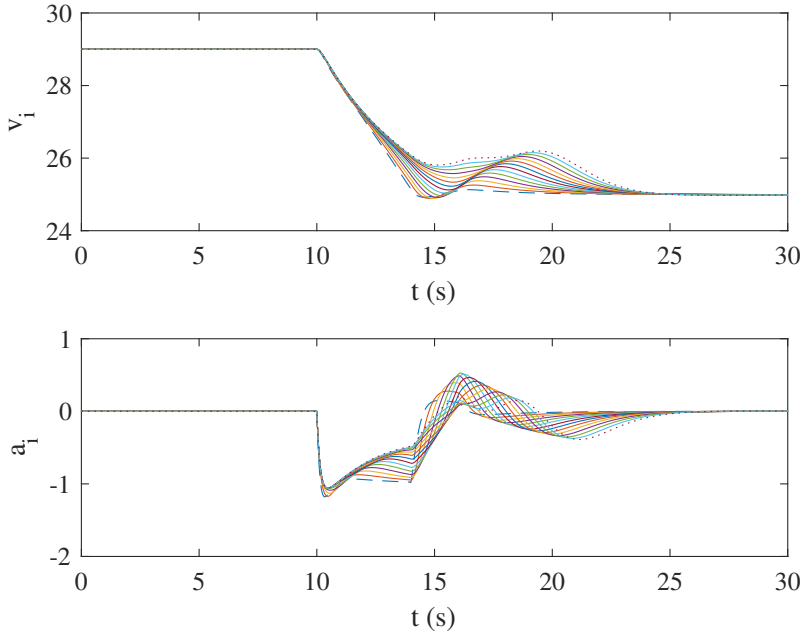

Figure 5.3: Constant deceleration and step change in h_w from 0.17 to 0.2 s followed by a gradual change in h_w from 0.2 to 0.17 s in 2 seconds.

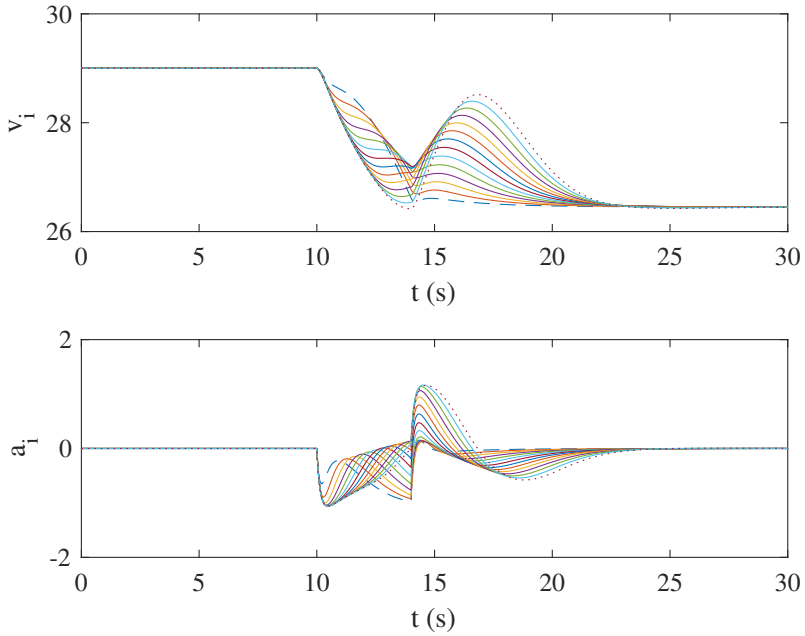

Figure 5.4: Sinusoidal deceleration and step change in h_w from 0.17 to 0.2 s.

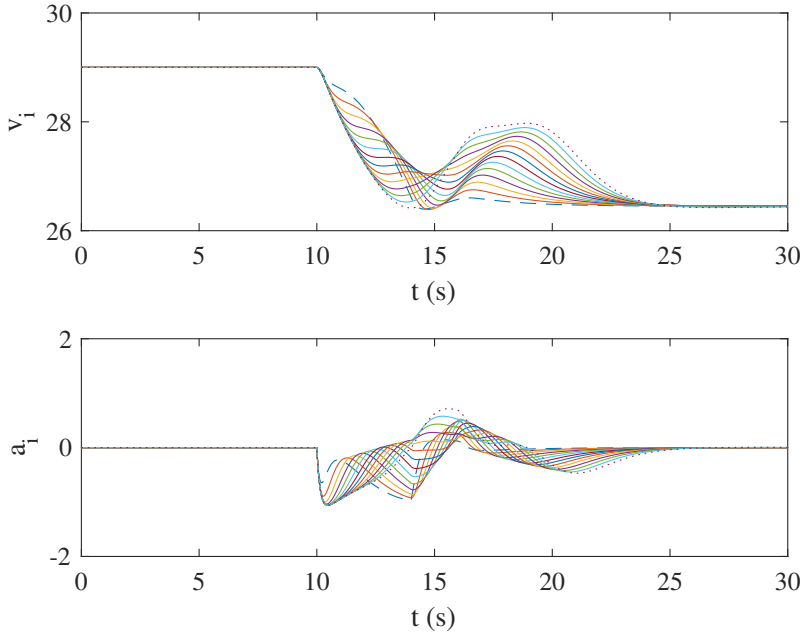

Figure 5.5: Constant deceleration and step change in h_w from 0.17 to 0.2 s followed by a gradual change in h_w from 0.2 to 0.17 s in 2 seconds.

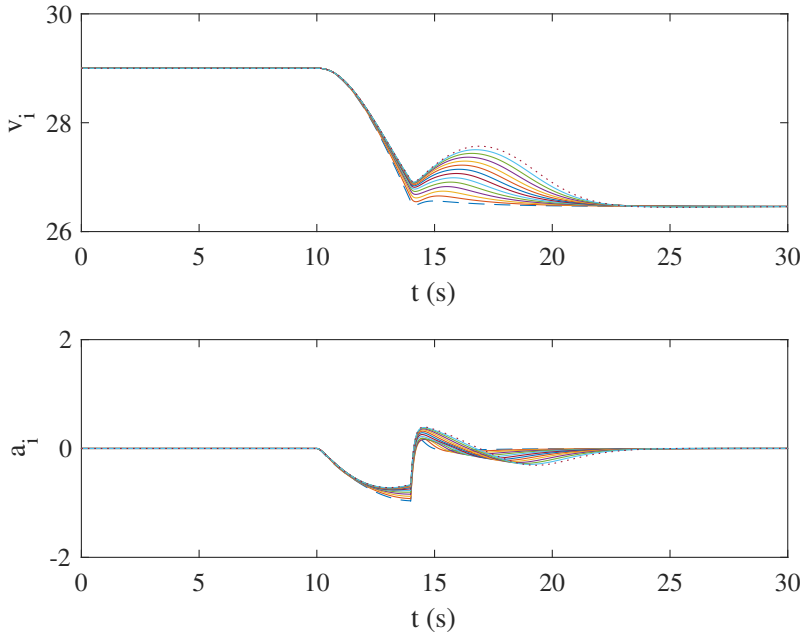

Figure 5.6: Sinusoidal deceleration and sinusoidal increase in h_w from 0.17 to 0.2 s.

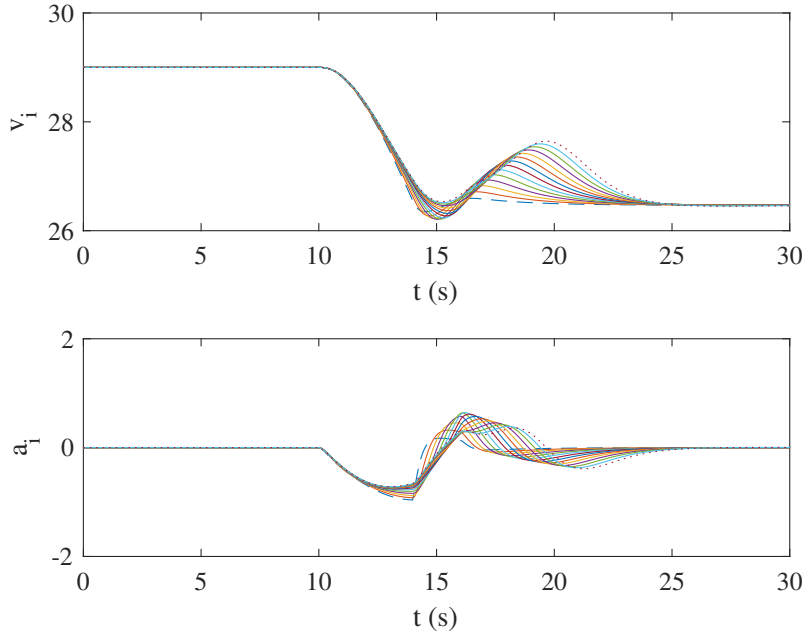

Figure 5.7: Sinusoidal deceleration and sinusoidal increase in h_w followed by a gradual change in h_w from 0.2 to 0.17 s in 2 seconds.

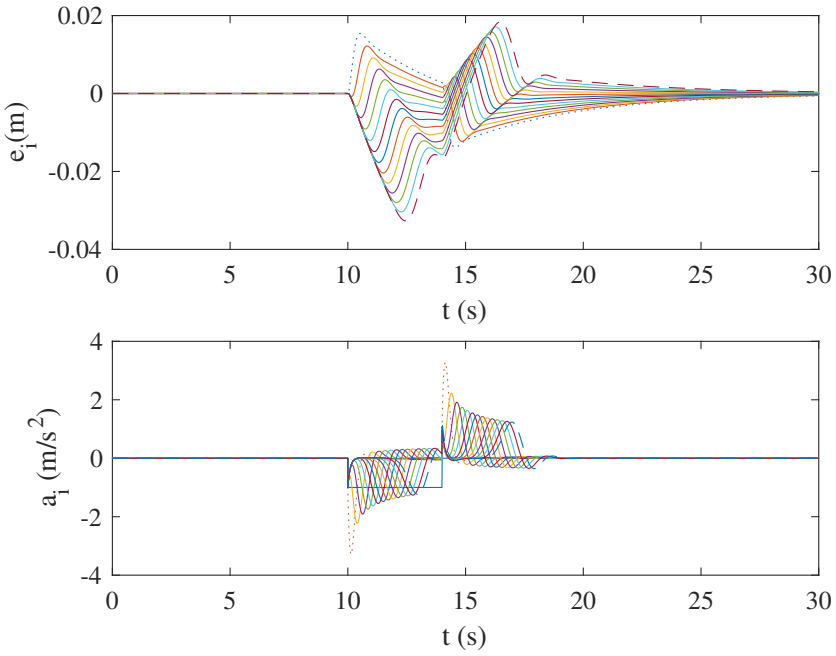

Figure 5.8: Evolution of spacing errors and vehicle acceleration with predecessor brake-light gain$= 0.1$, $h_w = 0.18$.

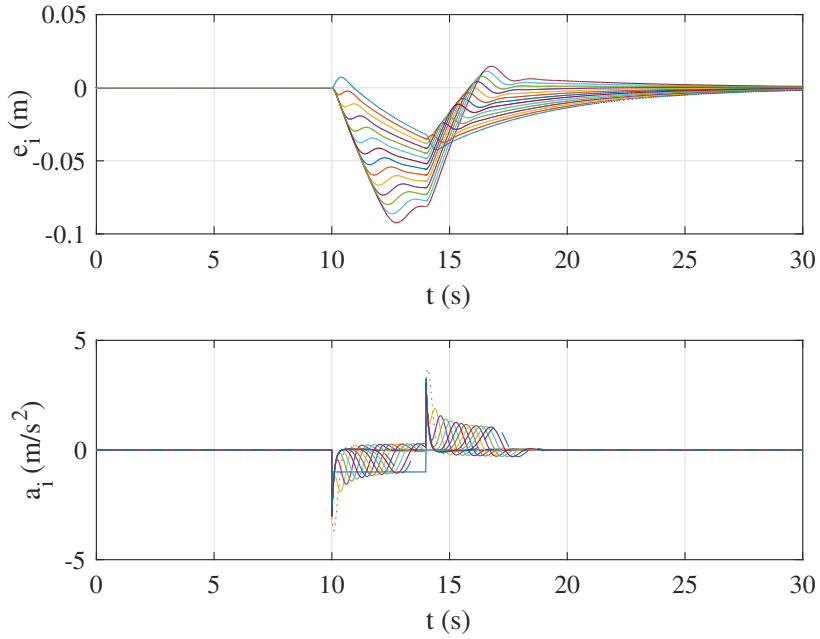

Figure 5.9: Evolution of spacing errors and vehicle acceleration with predecessor brake-light gain$= 0.3$,$h_w = 0.15$.

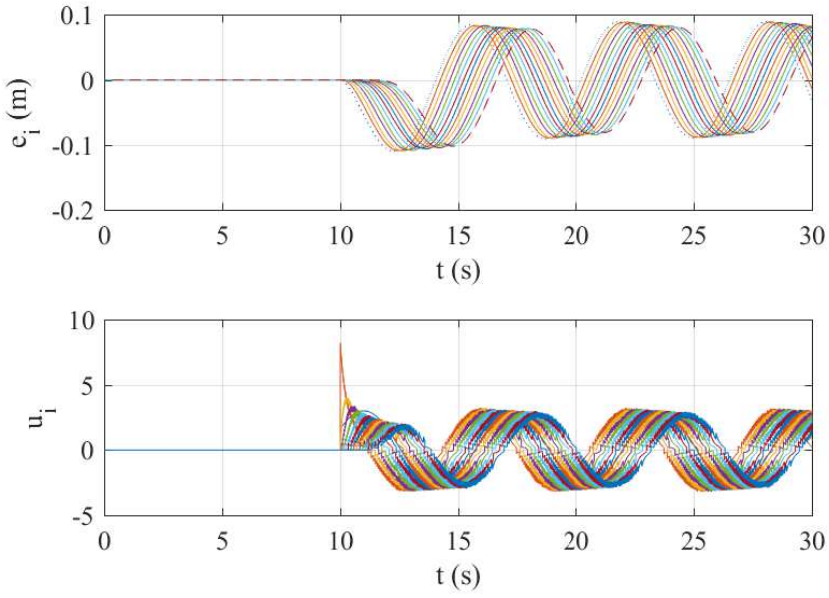

Figure 5.10: Evolution of spacing error and control input with an acceleration quantization step of 0.1

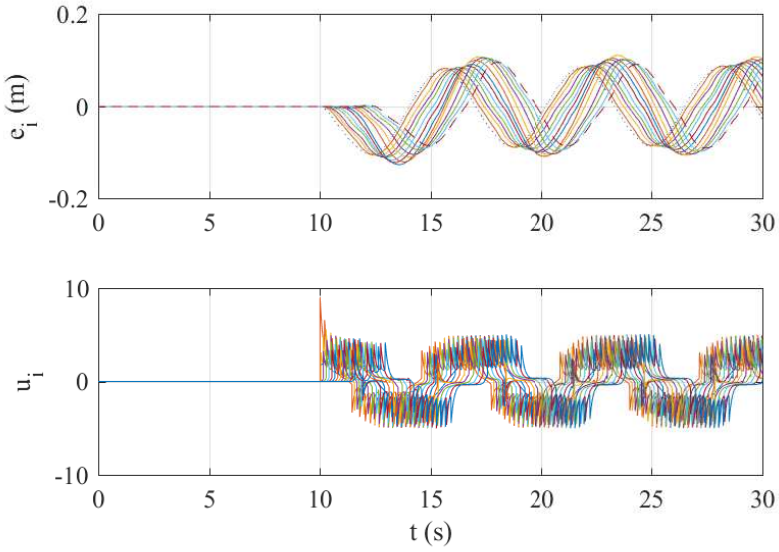

Figure 5.11: Evolution of spacing error and control input with an acceleration quantization step of 0.6

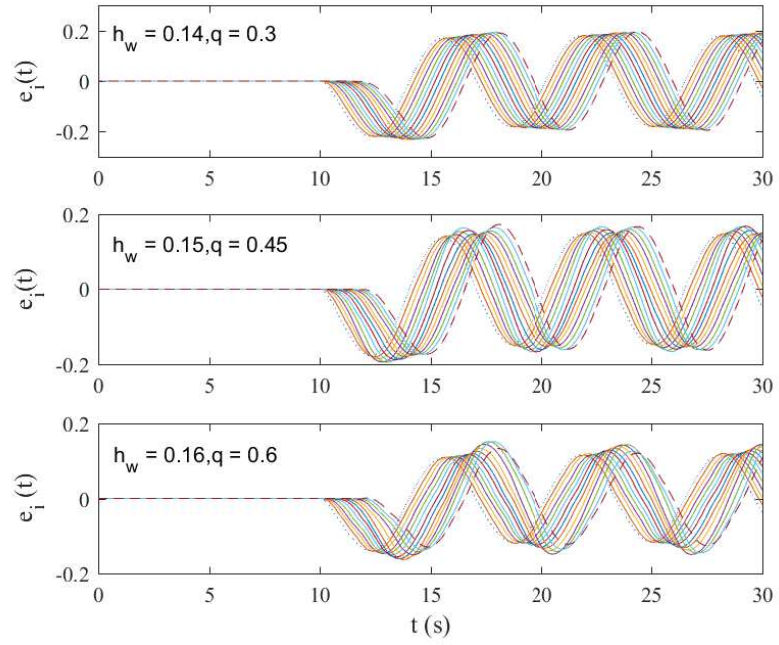

Figure 5.12: Spacing error evolution for time headway and corresponding quantization value.

6. FORMATIONS WITH RING COMMUNICATION GRAPH*

The information flow graphs that are used in the previous chapters have an independent leader vehicle. All the other vehicles in the platoon rely on the leader's movement either directly or indirectly, and this is beneficial for AVs traveling as string on highway. However, this may not be the best method to control vehicles that are traveling in two or three dimensional formations. In this chapter a special type of communication and information flow graph called the ring graph is investigated. The unique feature of this graph is that every vehicle maintains its position depending on one another vehicle in the formation.

A ring graph offers several advantages over a predecessor follower (path) type graphs or bidirectional graphs. For example, a ring graph has less communication overload compared to the leader predecessor follower. One distinct advantage of ring graphs over other graphs is that the closed loop system matrices resulting from employing controllers that utilize ring communication are circulant. Circulant matrices exhibit special properties, such as analytical expressions for eigenvalues as functions of system parameters, which can be exploited for controller design as well as for determining operating parameters; this is discussed in the next section. Further, the knowledge of the analytical expressions for the system eigenvalues facilitates scaling of platoons. In the following I apply the ring communication graph to a vehicle platoon using a constant time headway (CTHP) spacing controller along with acceleration feedback, and propose a TSP formulation to create ring communication graphs for any given vehicle formation shape and size [52].

*Parts of the this chapter have been reprinted with permission from "A combinatorial approach for developing ring communication graphs for vehicle formations", ASME J. Dyn. Sys., Meas., Control, Vol. 139(10), Pages 101014-1 to 101014-9. Copyright held by ASME.

6.1 Ring Communication in Platoons

The graph Laplacian of a ring graph is a circulant matrix in which each successive row is obtained by cyclically right shifting the previous row. Let c_q be the sequence of the elements of the first row of a circulant matrix C. Then, the eigenvalues of the circulant matrix are the coefficients of the Discrete Fourier Transform of the sequence c_q [62]. These properties can be exploited to determine the stability of formation controllers employing ring communications.

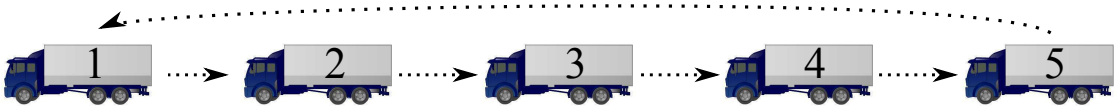

Figure 6.1: Basic ring communication in a platoon with 5 vehicles

A ring graph on a vehicle platoon in its most basic form may be visualized as shown in Fig. 6.1, where the directed arrows represent information flow and the ring is closed by communication from the last vehicle to the first vehicle; this is referred to as the 'basic' ring graph. Consider each vehicle as a point mass with double integrator dynamics as in Equation (2.3). Using the CTHP CACC control input from equation (4.1), the communication as shown in Fig. 6.1 and assuming that vehicles in the platoon are free of any parasitic lags, the closed loop dynamics of the platoon can be represented as,

$$E\dot{\mathbf{x}} = A\mathbf{x} - k_p\mathbf{b} \tag{6.1}$$

where

$$E = circ\left(\begin{bmatrix} 1 & 0 \\ 0 & 1 \end{bmatrix}, O_2, O_2, O_2, \begin{bmatrix} 0 & 0 \\ 0 & -k_a \end{bmatrix}\right),$$

$$\mathbf{x} = \begin{bmatrix} x_1 & \dot{x}_1 & x_2 & \cdots & x_5 & \dot{x}_5 \end{bmatrix}^T,$$

$$A = circ\left(\begin{bmatrix} 0 & 1 \\ -k_p & -\gamma \end{bmatrix}, O_2, O_2, O_2, \begin{bmatrix} 0 & 0 \\ k_p & k_v \end{bmatrix}\right),$$

$$\mathbf{b} = \begin{bmatrix} 0 & L_1 & 0 & L_2 & \cdots & 0 & L_5 \end{bmatrix}^T,$$

and $\gamma = (k_v + k_p h)$. Let

$$a_0 = \begin{bmatrix} 0 & 1 \\ -k_p & -\gamma \end{bmatrix}, \; a_{N-1} = \begin{bmatrix} 0 & 0 \\ k_p & k_v \end{bmatrix}.$$

Since E is a block circulant matrix, it can be block diagonalized and inverted [63]. Thus, the closed loop dynamics can be rewritten as,

$$\dot{\mathbf{x}} = \tilde{A}\mathbf{x} - \tilde{k}_p\mathbf{b} \tag{6.2}$$

where $\tilde{A} = E^{-1}A = circ(\tilde{a}_1, \tilde{a}_2, \cdots, \tilde{a}_N)$ with

$$\tilde{a}_i = b_{i-1}a_i + b_i a_N, \text{ and,}$$

$i = 1 : N, \; b_N = b_0$, and $\tilde{k}_p = E^{-1}k_p$. Note that $\tilde{A}$ is a block circulant matrix and can be block diagonalized to find the system eigenvalues. In the following discussion, $k_a = 0$ is chosen which implies that the matrix E is an identity matrix. Thus, the eigenvalues of the system matrix obtained after diagonalization are given by,

$$\begin{aligned} &\lambda_i^2 - (k_v\omega^{1-i} - \gamma)\lambda + (1 - \omega^{1-i}) = 0 \\ &\lambda_i = \frac{k_v\omega^{1-i} - \gamma \pm \sqrt{(k_v\omega^{1-i} - \gamma)^2 - 4(1 - \omega^{1-i})}}{2} \end{aligned} \tag{6.3}$$

where $\omega = e^{2\pi j/N}$ and $j = \sqrt{-1}$. When $i = 1$, $\lambda_1 = 0, -(k_v + \gamma)$ are two eigenvalues of the system. By choosing the gains $k_v = 1/h$ and $k_p = k/h$ with $k > 0$ [19], one can obtain the following eigenvalues:

$$\lambda_i = -k, -\frac{1 - \omega^{1-i}}{h}. \tag{6.4}$$

Note that for a formation of N vehicles, $N/2$ eigenvalues are located at $-k$ while the remaining are located on a closed locus that lies in the left half of the complex plane. Hence, the system is stable for all values of $k > 0$ and $h > 0$.

6.1.1 Alternative Ring Graphs

With the basic ring graph, as the size of the platoon increases, long distance communication may not be practically feasible due to an increase in the distance between the first and the last vehicle of the platoon. Limitations on the range of communication devices and obstacles between vehicles are some of the factors that may affect communication. An information hopping mechanism may be used but with each hop the time taken for information to reach the first vehicle from the last vehicle increases. Hence, alternative forms of ring graph which do not involve communication over large distances are desirable. An alternative form of a ring graph over a vehicle platoon is obtained by rearranging the communication ring while maintaining the physical positions intact. Fig. 6.2 shows a possible alternative configuration of ring graph over a platoon of five vehicles where each vehicle communicates with the $(i-2)^{nd}$ vehicle instead of the $(i-1)^{th}$ vehicle. Since eigenvalues of a matrix are unchanged by elementary row and column operations, the eigenvalues of the closed loop system matrix with alternative ring graphs are the same as those of the basic ring graph for the same formation size [64].

It is noted that in this work every vehicle computes its control input solely based on the information of the $(i-1)$-th vehicle in the communication ring. For example, for the

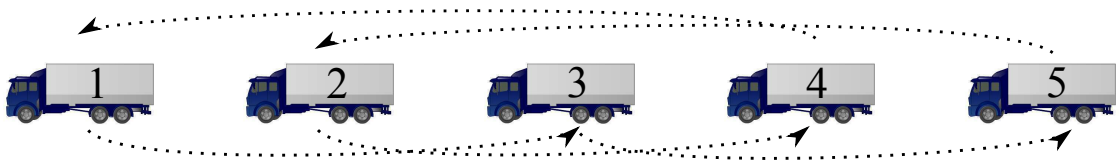

Figure 6.2: Alternate ring graph with communication structure $1 \rightarrow 3 \rightarrow 5 \rightarrow 2 \rightarrow 4 \rightarrow 1$
.

platoon with alternative ring communication shown in Fig. 6.2, Vehicle 2 maintains its position with respect to Vehicle 5 instead of Vehicle 1, and so on for the other vehicles. Thus, the communication time between any two communicating vehicles in the ring remains the same. This is not true for the basic ring communication shown in Fig. 6.1, since vehicle 1 needs information from Vehicle 5. Furthermore, if a communication protocol like the token ring protocol is used then vehicle transmits its own information only after it receives information, in which case alternative ring graphs offer the least possible cycle time thereby ensuring the quickest information refresh rate.

6.1.2 Communication Advantages of Alternative Ring Graphs

Consider a platoon of N vehicles with identical communication devices. Let T_c denote the time constant associated with transmitting information within every device's range and the time taken to process the received information before transmitting. The total time for completion of one cycle is the sum of all the individual communication times and the processing times, which depends on the communication protocol, physical devices used, etc.

In the basic ring graph (Fig. 6.1) for a vehicle platoon the physical distance between the first and the last vehicle in the ring increases with the formation size N. In order to communicate the information of the last vehicle to the first vehicle, it has to be hopped over other vehicles in the formation to meet the sensing range constraint of the communication device, and the number of such hops increases with formation size. For example, consider

a ten vehicle vehicle platoon shown in Fig. 6.3, with the transmitter range of 12 m (shaded region) and inter-vehicular spacing of 5 m ($\delta = 5$). Thus, the farthest each vehicle can communicate is two vehicles in either direction. The information hop from the last vehicle to the first vehicle is represented by dotted arrows in Fig. 6.3. The total time taken for one communication cycle with this basic ring graph (T_{basic}) is the sum of the time taken for the information to flow from the first to the last vehicle, $9T_c$, and the time taken for information to hop from the last vehicle to the first vehicle, $5T_c$, that is, $T_{basic} = 9T_c + 5T_c = 14T_c$. Consider an alternative ring graph shown in Fig. 6.4. The total time taken for one communication cycle with this alternative ring graph (T_{alt}) is the sum of ten individual communications, i.e., $T_{alt} = 10T_c$ [65]. Hence, the communication cycle time for the basic ring graph is larger than that of the alternative ring graph. This approach can be generalized as follows.

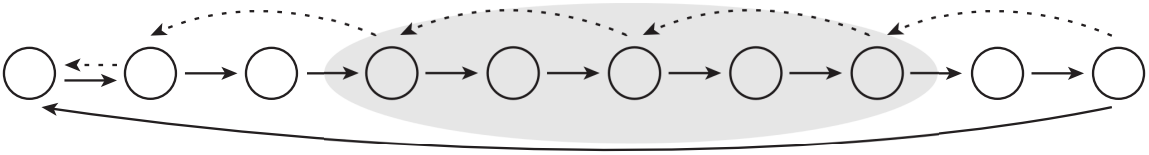

Figure 6.3: Information hopping from vehicle ten to one

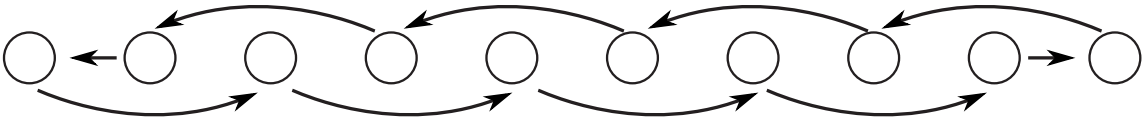

Figure 6.4: Platoon of ten vehicles with alternative ring graph

Let the effective communication range of transmitters be a sphere of radius ζ and M

be the number of vehicles the information can be transmitted in one single hop. For an N-vehicle formation, the number of hops required from the last vehicle to the first vehicle is $floor(N/M)$ where the function $floor(a)$ gives the largest integer smaller than a. The total cycle times for the basic ring graph with information hops and the optimal alternative ring graph with the communication range constraint, respectively, are given by

$$T_{basic} = \left(N - 1 + floor\left(\frac{N}{M}\right)\right) T_c, \quad \text{and}$$
$$T_{alt} = NT_c. \tag{6.5}$$

For a fixed M and a large N, $\lim_{N\to\infty} T_{alt}/T_{basic} = 1/2$.

In a platoon there are only two directions the information can flow from a vehicle, thus one can simply set $M \leq \zeta/\delta$. It is more difficult to establish a hop factor M in two or three dimensional formations. Let the sensor communication range be $\zeta = 12$ m as in the previous case for 2D and 3D formations, shown in Fig. 6.5. The shaded regions indicate the communication range of the respective vehicle. Then the problem of finding the number of vehicles to hop depends on the direction of communication. For instance, for the 3D formation there are no vehicles to hop on along the diagonals of the cube. Hence, there is a need for a formulation that will work with absolute distances between vehicles in the formation rather than the direction of communication. Further for the 2D and 3D formations, the formation of a ring is not as intuitive as in the case of the platoon.

Notice that for the simple examples shown in Fig. 6.5, there are numerous ways to form a ring graph. The problem of selecting a communication graphs is exacerbated for larger and irregular shaped formations. Since the closed loop system based on a ring communication graph has many desirable properties, a systematic method is needed to form ring graphs irrespective of the number of vehicles or dimension of the formation.

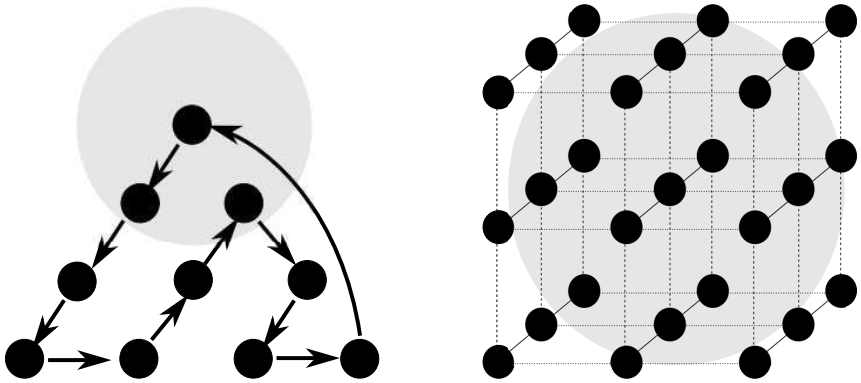

Figure 6.5: 2D and 3D formation example with communication range disc.

6.2 Ring Graph as a Canonical TSP

While it is straightforward to construct a basic ring graph over vehicles in cyclic pursuit or in a simple vehicle platoon, it is difficult to do so in two- and three-dimensional formations. Further, employing a basic ring graph in vehicle platoons requires the lead vehicle to receive information from the last vehicle, both of which may be separated by a large distance depending on the size of the platoon. This poses multiple implementation issues such as requiring large communication range for the sensors, presence of obstacles like buildings or tunnels, etc. Typically, a protocol such as the token ring protocol is used for communicating information from one vehicle to another. In such a case, the "freshness" of the information is directly related to the distance traveled by the token in the ring graph. It appeals to intuition to minimize the distance traveled by the token among all possible ring graphs that can be constructed. In this section, a combinatorial approach for developing ring graphs with given constraints is used. The key is in the formulation of the ring graph along with the constraints involved as a combinatorial search in a simple and tractable way. Once a good formulation is in place, any one of the available search algorithms can be used to find possible solutions. Using combinatorial search to draw graphs has been considered in the literature [66, 67].

Generating a ring graph over a formation can be viewed as finding a Hamiltonian cycle for a given connected graph or a tour for the TSP. Therefore, the algorithms available to find a Hamiltonian cycle may be used to find a ring graph. For this reason, the problem of finding a ring graph with constraints is modeled as the canonical TSP. In its classical form the TSP is the following: Given a list of cities and their pairwise distances, the problem of finding a minimum cost tour such that one starts from a city, visits all the cities, and returns to the starting city. There are a number of efficient algorithms to find exact and approximate solutions for the TSP, [68].

Let c_{ij} be defined as the distance between vehicles and $V = \{1, 2, \ldots, n\}$ be the set of indices of vehicles. The set of edges, E, of the information flow graph is the set of all ordered pairs of the form $(i, j),\ i, j \in V$ such that $i \neq j$. For every edge $(i, j) \in E$, let a binary decision variable x_{ij} denote whether the vehicle indexed by i communicates with a vehicle indexed by j. For every *strict* subset S of V, one can define the cut-set, $\delta(S)$ of S to be the set of edges which leave the set S, i.e., $\delta(S) := \{(i, j) : i \in S\}$.

Given a cost matrix consisting of pair-wise distances between vehicles, the problem is formulated as follows [68]:

$$\min \sum_{i=1}^{n} \sum_{j=1}^{n} c_{ij} x_{ij} \tag{6.6a}$$

$$\text{subjected to } \sum_{j \in \delta(i)} x_{ij} = 1,$$

$$\sum_{j \in \delta(i)} x_{ji} = 1,\ \forall i = 1, 2, \ldots, n, \tag{6.6b}$$

and

$$\sum_{j \in \delta(S)} x_{ij} \geq 1,\ \ \forall i \in \delta(S) \subset \{1, 2, \ldots, n\}. \tag{6.6c}$$

The set of constraints (6.6b) enforce degree constraints, i.e., the token must be received

and transmitted by every vehicle in the formation exactly once in a cycle of updating the information. The last of the inequality constraints, (6.6c), eliminates sub-tours, i.e., the possibility of two disjoint cycles forming on the set of vehicle nodes. A solution to this canonical TSP problem provides the optimal topology for the ring graph. It is important to note that the formulation remains the same irrespective of the shape and dimension of the formation.

Additional constraints may be added to the TSP formulation depending on the physical constraints on the system, such as the communication range of transmitters. Let the communication range be denoted by ζ [49,64]. To limit the distance between each communicating vehicle, let c_{ij} denote the distance between vehicles if it is within the communication range ζ; otherwise, let $c_{ij} = n\zeta$, where n is the number of vehicles in the formation. This modification in effect restricts the solution to only those scenarios where the communication range between each communicating pair is satisfied. The alternative ring graph obtained using the TSP formulation with a communication range $\zeta = 2\delta$ (where δ is the inter-vehicular spacing) on a ten vehicle platoon is shown in Fig. 6.4. The ring graphs obtained for the 2D and 3D formations discussed above are also shown in Fig. 6.6. It should be noted the solutions shown for each case are only two of many possible solutions that satisfy all the constraints.

6.3 Addition of Vehicles To The Formation and Removal of Vehicles From an Existing Formation

Another key implementation issue is encountered when one wishes to add/remove vehicles from a formation; this requires reconfiguration of the existing communication graph and potentially a different controller is needed to ensure that the formation is stable; this is typically referred to as the topology reconfiguration problem. Topology reconfiguration is a relatively challenging problem depending on the type of goals of reconfiguration such

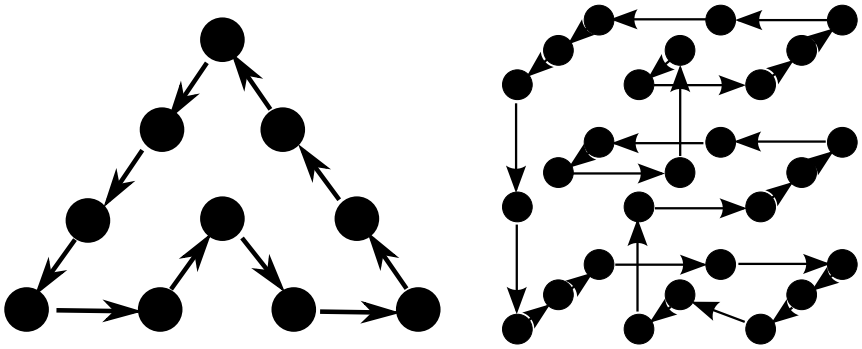

Figure 6.6: 2D and 3D formation with ring graph obtained from the TSP formulation

as type of communication graph, number of vehicles added or removed, etc. Topology reconfiguration is a well known research problem in computer networking. Reconfiguration in multi-agent formations was studied recently in [69]. The focus in the literature has been on problems where the number of vehicles is unchanged, but the information flow has to be reconfigured. These methods are not applicable to those situations where one has to add/remove vehicles.

When vehicles are added/removed to/from a formation, the closed loop properties of the system may change and the communication graph may need to be reconfigured. In contrast to other directed or undirected graphs, addition/removal of vehicles from/to a formation with ring communication graphs does not affect closed loop stability of the formation if the ring communication is maintained for the resulting reconfigured formation. It can be shown that by setting up the closed loop structure of the system as discussed in Section 6.1, one can ensure that the eigenvalues of the closed loop system remain on a fixed closed locus irrespective of the size of the formation. Reconfiguration of a communication graph is an NP-complete problem and exact solutions may require considerable resources to compute, however, heuristics can be used to find solutions that are near optimal. Stability of the reconfigured formation with ring graphs and heuristics to add/remove vehicles to/from the formation are discussed next.

Let G_o denote the initial configuration of the communication graph. Can we reconfigure the communication graph to a final configuration $G_f(V_f, E_f)$ such that we keep the same controller and preserve closed loop stability when adding or removing vehicles to the existing formation. The dimension change in the system matrix due to addition/removal of vehicles is handled in the following manner. A cap on the total number of vehicles is assumed and a relevant number of zero rows and columns are added based on this cap. With this approach one can model the change in the system matrix as a perturbation on the existing matrix. If fewer vehicles than the cap are added, the analysis can be restricted to the non-zero block of the system matrix. For example, with a five vehicle platoon, if the cap is at seven vehicles, then the initial closed loop system matrix with five vehicles is taken as

$$A^{'} = \begin{bmatrix} A & O_{5x2} \\ O_{2x5} & O_{2x2} \end{bmatrix}, \tag{6.7}$$

where $A := circ(a_0, O_2, O_2, O_2, a_5)$. The closed loop system matrix for the reconfigured system with seven vehicles is

$$A = circ(a_0, O_2, O_2, O_2, O_2, O_2, a_6). \tag{6.8}$$

By preserving the ring communication structure for the reconfigured formation, the eigenvalues are given by Eq. (6.4) and the bounds on these eigenvalues are the same the initial formation. For any of the other commonly used communication graphs (directed or undirected), there is no known mechanism to determine the eigenvalues of the reconfigured formation.

For example, the eigenvalues of a platoon with 10 and 13 vehicles using the same control gains ($h = 0.9$, $k_a = 0$, $k_v = 1/h$ and $k_p = 3/h$ in Eq. (4.1)) are shown in Fig. 6.7. One can also find the locus of the eigenvalues. Let λ denote any one of the eigenvalues of

the system matrix, and let $\omega = p + jq$ and $\lambda = x + jy$. Since ω and λ are both complex numbers, from equation (6.4) we have the following locus equation:

$$\begin{aligned} h(x^2 + y^2) + 2x &= 0 \\ \left(x + \frac{1}{h}\right)^2 + y^2 &= \left(\frac{1}{h}\right)^2 \end{aligned} \tag{6.9}$$

The locus is a circle centered on $(-1/h, 0)$ with radius $1/h$. Therefore, half of the eigenvalues are at $-k$ and the other half are on the circle given by the above equation.

Two methods may be employed for reconfiguring the ring communication graph: (1) using a search over the entire node set, and (2) insertion/removal heuristics using the existing topology. To search the entire node set one can use the TSP formulation from Section 6.2 for every addition or removal of vehicles to/from the formation. Then any available exact algorithms for solving combinatorial problems can be used to find solutions. However, this can be resource intensive and time consuming. Insertion heuristics are quicker as they alter the path locally to add nodes. The existing optimal topology is used as a starting point and new nodes are inserted into the topology following a particular insertion criterion. Some commonly used insertion criterion are the nearest insertion, farthest insertion, cheapest insertion, etc., [68].

Without loss of generality if one were to restrict the addition of new vehicles to the boundary of the existing formation, the insertion search can be highly localized. The nearest node search replaces parts of an existing path such that it passes through the newly added node. The algorithm starts with the existing optimal solution, finds the node n_c on the existing solution which is nearest to the newly added node m; see Fig. 6.8. The solution is then modified to include the new node either before or after the node n_c such that the cost of the entire cycle is minimal. The result of using this algorithm on the ten vehicle platoon with two additional nodes is shown in Fig. 6.9. The nearest node search algorithm

is faster owing to its simplicity and limited search space when compared to searching over the entire new formation.

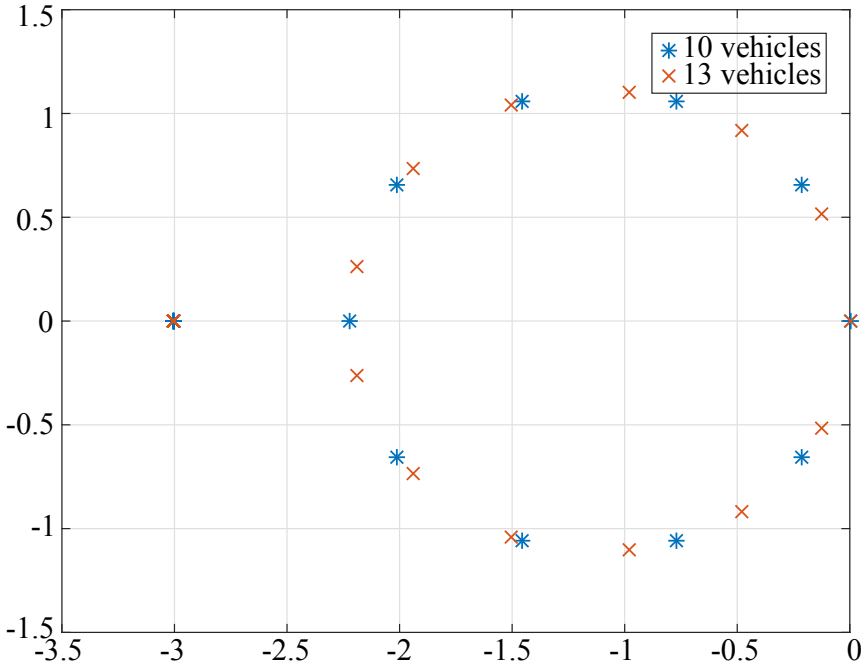

Figure 6.7: Eigenvalues of the platoons with ring graph with 10 and 13 vehicles

In general removal of nodes is more restrictive and there are not many heuristic methods available for reconfiguring the graph upon removal of nodes. However, a simple removal heuristic algorithm may be employed that works similar to the nearest neighbor insertion heuristic by locally altering the path around the node removed. Since, in vehicle formations, one only deals with Euclidean distances and the distances obey triangular inequality, the ratio of the tour cost resulting from removal heuristics to the optimal cost of $N-1$ nodes can be shown to be ≤ 1.5 [70].

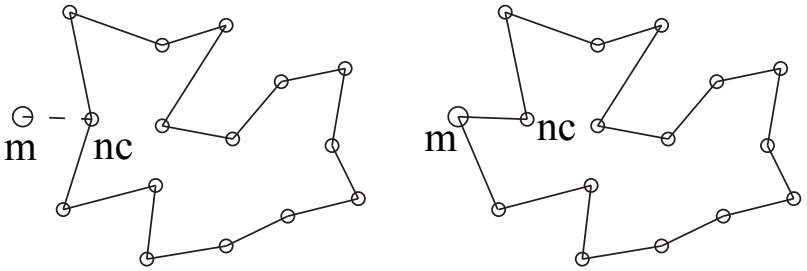

Figure 6.8: Graph reconfiguration after adding a single node, newly added node ‘m’ and its closest node along the path ‘nc’, Reconfigured graph passing through ‘m’

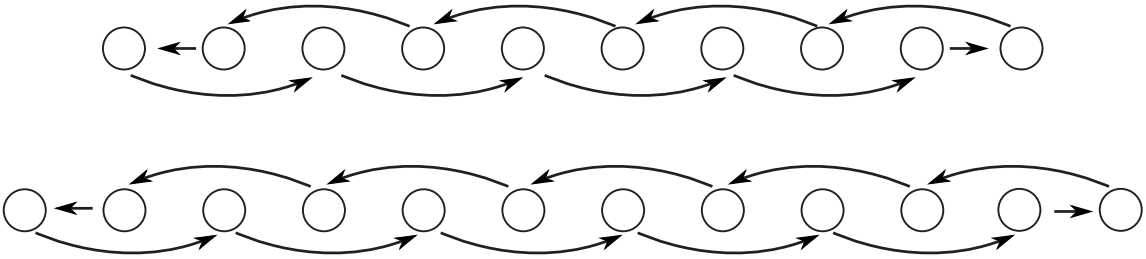

Figure 6.9: Reconfiguration using graph search: Initial configuration, and Reconfigured graph with additional two vehicles.

6.4 Formation Experiments using Ring Graphs

Experiments were conducted with a group of four fully autonomous differential drive robotic vehicles. Each robot has two independent wheels and a free caster. Each independent wheel is actuated by a motor rated at 12 V, with a no-load speed of 350 rotations per minute and a stall torque of 0.78 Nm. A pair of quadrature encoders with 1856 counts per revolution are used to measure the angular speed of the wheels and calculate the position of the robot. The robot control algorithms are implemented using an Arduino micro-controller along with motor drivers and ‘Xbee Series 1’ communication module and a desktop computer containing a ‘Xbee Series 1’ receiver [49, 71]. All the experiments are conducted in a decentralized manner with the on-board micro-controller on each robot performing the necessary computations to generate the control input and then transmit-

ting its identity information and position data using the communication module. A central desktop computer is used only to log the data and to send start/stop command signals. The communication cycle in the platoon follows the ring graph, i.e., each vehicle transmits information only after receiving.

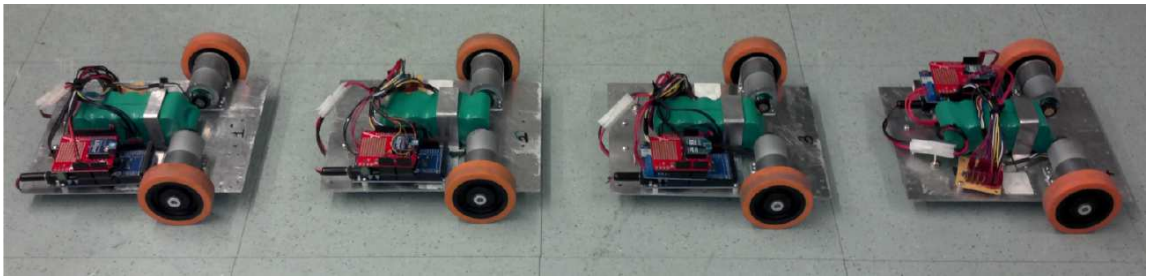

Figure 6.10: Picture of mobile robots.

The control algorithm consists of two loops as shown in Fig. 6.11, where q_{ref} and q_a are the reference and actual position vectors, V_d is the vector of desired velocities, V is the vector of motor voltages. The outer loop comprises of a nonlinear kinematic path controller as given in [72]; this outer loop takes the measurement of the robots' current position error and computes the desired linear and angular velocities as follows,

$$v_d = v_r \cos\theta_e + k_x x_e \tag{6.10a}$$

$$w_d = w_r + v_f(k_y y_e + k_\theta \sin\theta_e) \tag{6.10b}$$

where v, w are the linear and angular velocities, respectively, subscripts d, r denote the desired and reference values and k_x, k_y and k_θ are positive controller gains. The errors

x_e, y_e, θ_e are computed as,

$$\begin{bmatrix} x_e \\ y_e \\ \theta_e \end{bmatrix} = \begin{bmatrix} \cos\theta & \sin\theta & 0 \\ -\sin\theta & \cos\theta & 0 \\ 0 & 0 & 1 \end{bmatrix} \begin{bmatrix} x_r - x \\ y_r - y \\ \theta_r - \theta \end{bmatrix} \tag{6.11}$$

where the subscript r denotes the reference value. The references values of x, y and θ are obtained from the reference trajectory in the case of a single robot tracking and from the position of the $(i-1)^{th}$ robot and the desired inter-vehicular spacing in the case of a robot platoon. The output of the outer loop provides a velocity correction to the inner velocity loop. The inner loop consists of a simple proportional integral (PI) controller to control individual motor velocities as

$$V = K_p W_e + K_i \int_0^t W_e(\tau) d\tau \tag{6.12}$$

where $V = [V_l, V_r]^T$ is the voltage input for each motor, $W_e = [\omega_{e_l}, \omega_{e_r}]^T$ is the error vector of the left and right motor velocities, and K_p, K_i are the proportional and integral gains. All the experiments are conducted without acceleration and velocity error feedback.

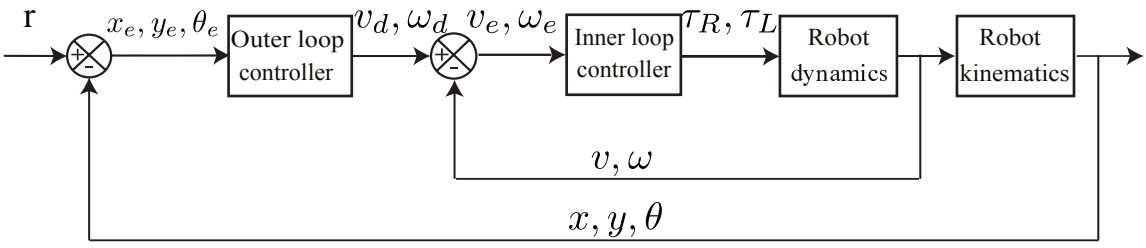

Figure 6.11: Two loop trajectory tracking controller.

Experiments were conducted to compare the ring graph in basic form versus the alternative form. In the first set of experiments, a vehicle platoon is formed with information flow given by basic and alternative ring graphs. The second set of experiments were conducted using the alternative ring graph by varying the initial spacing conditions. The reference linear velocity is chosen to be 0.457 m/s and the angular velocity is set to 0 rad/s. The velocity value is set only in robot 1 which communicates it to the rest of the platoon through the ring. The desired inter-vehicular spacing is however set in each individual robot. In the three experiments discussed in this paper, the vehicles start at zero velocity and accelerate for five seconds after which the coordination algorithm is activated. The desired platoon trajectory is a straight line with a fixed velocity and inter-vehicular spacing. The robots are arranged a apriori in a straight line formation. The initial acceleration stage was included to build up the velocity more smoothly. During this stage each robot has a reference straight line trajectory.

Results of the experiment with the basic ring graph and the results of experiments with an alternative ring graph are shown in Fig. 6.12(a). Comparing the results it can be seen that in both cases the platoon maintains its initial inter-vehicular spacing. These experiments show that an alternative ring graph can be used in the place of a basic ring graph with similar results.

6.4.1 Initial Spacing Not Equal to the Desired Spacing

Two sets of experiments were conducted, one with initial spacing less than the desired spacing and the other with initial spacing more than the desired spacing. In the first set, the initial spacing is set to 0.61 meters (2 ft) and the robots 1, 2, 3 and 4 are positioned at locations 1.83, 1.22, 0.61 and 0 meters on the base line. The desired spacing is set to 0.914 m (3 ft). In the second set of experiments, the initial spacing is set to 0.914 meters (3 ft) and the desired spacing to 0.609 meters (2 ft). The robots are positioned at

2.743, 1.828, 0.914 and 0 meters on the base line. The evolution of the position of the vehicles within the platoon is shown in Fig. 6.12(b). In both the cases the vehicles in the platoon adjust their relative positions as soon as the coordination controller is activated at 5 seconds into the experiment. Once the positions are adjusted, the inter-vehicular spacing error is maintained close to zero.

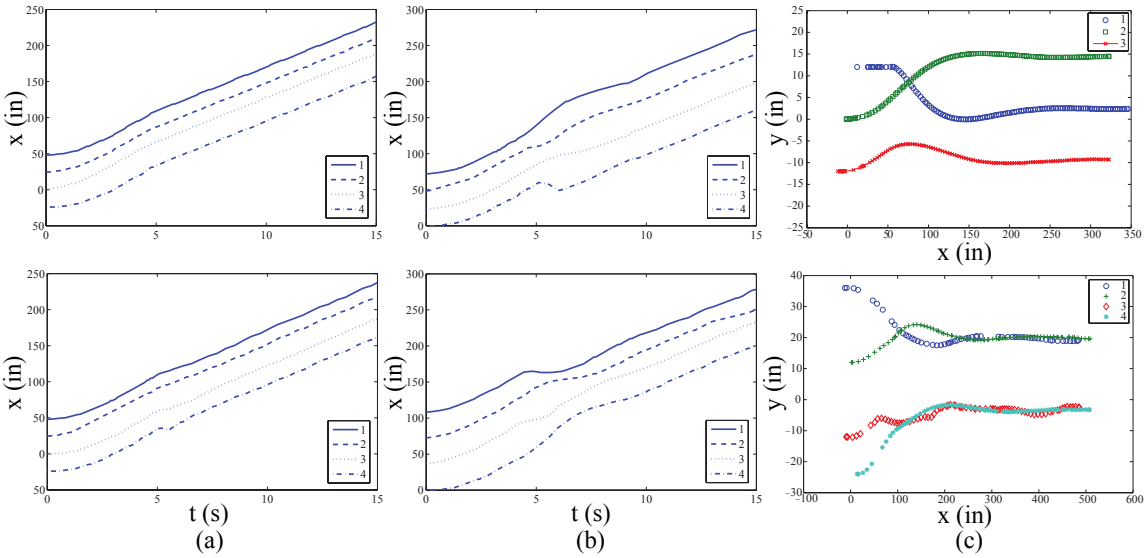

Figure 6.12: Evolution of position with (a) basic and alternative ring graphs, (b) initial position less and greater than desired spacing, and (c) triangle and square formation with non-zero initial position errors.

6.4.2 Experiments with Two Dimensional Formations

Formation experiments using the mobile robots were also carried out. The first set of experiments used three robots in a triangular formation with non-zero initial conditions. The robots start at initial positions with non-zero spacing error and converge to a triangular formation and continue forward. The initial positions of the three robots are $(0.3048, 0.3048)$, $(-0.3048, 0)$ and $(-0.3048, -0.3048)$ and the initial orientation is same

for all the three robots (0 deg). The position of the vehicles is shown in Fig. 6.12(c).

The second set of experiments were conducted using the four robots with a square formation of side length 0.6096 m. The reference linear velocity of the formation is taken as 0.457 m/s and the reference angular velocity is taken as 0 rad/s. The initial positions of the four robots are $(-0.3048, 0.9144)$,$(0, 0.3048)$,$(-0.3048, -0.3048)$ and $(0.3048, -0.6096)$. The trajectories of the four robots are shown in Fig. 6.12(c). The robots start at non-zero initial spacing errors, go through an orientation change to achieve and maintain the square formation.

7. CONCLUSIONS AND FUTURE WORK

7.1 Summary and Conclusions

The focus of this work was on investigating spacing policies and communication strategies that can aid in reducing the inter-vehicular spacing while ensuring robustness to parasitic lags. A substantial portion of this dissertation involves quantifying the advantages of using vehicular communication with CTHP controllers. String stability is used as a performance metric to study CTHP controllers that employ immediate predecessor acceleration and multiple predecessor information in the presence of parasitic lags. For each controller, the minimum employable time headway that can guarantee robust string stability is derived.

In Chapter 2, some brief background is presented for the vehicle model employed, information flow graphs, and string stability analysis methods. Spacing errors, string stability and robust string stability are defined and discussed. The string stability of vehicle platoons for some well known CSP and CTHP controllers from the literature is discussed. Minimum employable time headway ($h_{\min}$) is defined and $h_{\min}$ values of some CTHP controllers from the literature are reviewed.

In Chapter 3, properties of vehicle platoons with CSP controllers using information from 'r' preceding vehicles are studied. It is shown that with an 'r' vehicle look ahead CSP controller, the platoon is not robustly string stable irrespective of the acceleration feedback gain values selected. When the information from the immediate predecessor and the platoon leader are used, the platoon is robustly string stable; an upper bound for the lag in terms of the controller gain values is derived in this chapter. A design procedure for the selection of controller gains when using a CSP controller with leader and predecessor information such that the platoon is string stable in the presence of parasitic lags is also

presented. Results from numerical simulations are provided to corroborate the theoretical results derived.

In Chapter 4, robust string stability of controllers utilizing constant time headway policy is investigated to find the minimum employable time headway. All the controllers considered require V2V or I2V communication to obtain information of the predecessor vehicles. Three controllers that use CTHP are considered in this chapter: (1) a controller that uses acceleration, velocity and position information of the immediate predecessor, (2) a controller that uses information from multiple predecessors ('r' predecessors), and (3) a controller that uses information from immediate and 'r'-th predecessor. For all the three controllers considered, the minimum employable time headway is found as a function of controller gains and the vehicles' parasitic lags. Further, it is also shown that when using bidirectional communication the platoon is string stable. Numerical simulations are conducted to validate the theoretical analysis and the results are presented and discussed.

Based on the discussion and analysis from the first four chapters, one can make the following observations:

- In general, as shown by many authors in the literature, autonomous vehicle platoons with CACC provide better robustness to parasitic lags over ACC. Information about the downstream vehicles in the platoon that can be obtained from V2V or I2V communication is beneficial for safe operation of the platoon. However, one has to appropriately choose the spacing policy and the controller to guarantee robust string stability.

- Controllers based on constant spacing policy are not robust to parasitic lags even when using information from multiple vehicles in the platoon downstream. The only exception to this generalization is the CSP controller that uses information from the immediate predecessor and the platoon leader. In this case the platoon is robust to

sufficiently small parasitic lags, which can be increased by choosing small controller gains.

- The controllers based on constant time headway policy in general exhibit robustness to parasitic lags. Although CTHP controllers that use information only from onboard sensors (ACC) exhibit some robustness to lags, this level of robustness is too restrictive for practical applications. CTHP controllers that rely on information obtained from V2V or I2V communication show substantial improvement in robustness to parasitic lags.

- For a fixed time headway, using predecessor vehicle acceleration in CTHP controller can potentially double the maximum allowable parasitic lag (τ_0).

- The robustness is further improved when using information from multiple vehicles in the platoon downstream or using only information from the immediate predecessor and 'r'-th predecessor. However, using information from 'r' vehicles can add to communication overload of the networks if r is large. A good compromise is to employ the predecessor and 'r'-th vehicle information, as this provides better robustness than using information from just the immediate predecessor without adding excessive communication overhead.

In Chapter 5, some preliminary studies related to the use of predecessor brakelight information in the absence of vehicular communication are discussed. The effect of information quantization is also discussed. From the numerical results it is observed that one *may* employ the status of predecessor brakelight into the longitudinal control of vehicles to maintain a smaller time headway. Information quantization will have a detrimental effect on the platoon. However, a larger acceleration feedback gain or time headway can help mitigate some detrimental effects of quantization.

In Chapter 6, a combinatorial approach for developing ring communication graphs for vehicle formations is proposed by formulating the problem as a canonical TSP with constraints. Ring graphs for vehicle platooning, 2D and 3D formations with communication distance constraints and other constraints can be obtained using this formulation. The advantage of using ring communication graphs is that one can add vehicles to or remove vehicles from the formation without changing the controller for each vehicle and preserving the stability of the formation control algorithm. Platoon and formation experiments were performed with four mobile robots by using ring graphs in multiple formation shapes and different initial conditions.

7.2 Future Work

Some future research directions based on this work are as follows:

- The minimum employable time headway for CTHP controller that employ immediate predecessor in the feedback is computed using the frequency domain approach to string stability analysis. In order to guarantee that controller gains exists one has to show that the impulse response of the spacing error transfer function must be non-negative ($h(t) \geq 0$). In this dissertation, this was demonstrated using numerical simulations. Future work should focus on finding analytical bounds for selection of gains such that $h(t) \geq 0$ is guaranteed.
- The analysis of CTHP controllers using multiple predecessor information in the feedback involved using a sufficient condition for string stability. There is a possibility that vehicles can employ a smaller time headway than $\frac{4\tau}{(1+r)(1+rk_a)}$. It is unclear on how to approach the string stability problem with multiple predecessors in order to find a tight bound on $h_{\min}$, this should be investigated in the future.
- When employing bidirectional information exchange in CTHP controllers, the results derived in this work only show that it is possible to ensure string stability.

Bounds on minimum employable time headway should be derived.

- One of the key assumptions of the analysis in this dissertation is that the communication is free from delays or losses. There is a large volume of research in the literature that is focused on studying these effects, however, there is a limited understanding on how to apply analytical tools from time delay systems to vehicle platoons. Many works such as [39] have relied on using numerical simulations to provide some guidelines. Other works have only concentrated on studying effects of delays when using only the immediate predecessor information. Future work should investigate the effects of such communication uncertainties while choosing time headway.
- Another key assumption is that the vehicles in the string are all equipped for communication and are capable of implementing CACC controllers that were used in the analysis. However, methods to deal with vehicles that are not equipped with communication are limited [2]. Since highways for at least the near future will be used by vehicles with and without CACC (and ACC), analysis of this problem should be considered in the future.
- One of the limitations of this dissertation is the lack of experimental validation. Although there are instances in literature that involve extensive experiments, these are mainly limited to immediate predecessor information feedback. Experiments should be conducted with controllers using multiple predecessor information, especially using $r \geq 3$ and $h_w < \tau$ to study the behavior of vehicles.
- In the context of ring graphs, potential future work includes: (1) obtaining analytical expressions for eigenvalues and stability of the system using acceleration feedback, (2) studying how communication delays affect the stability of the formation, and (3) factoring these delays as constraints in developing the ring graph.

REFERENCES

[1] K. C. Dey, L. Yan, X. Wang, Y. Wang, H. Shen, M. Chowdhury, L. Yu, C. Qiu, and V. Soundararaj, "A Review of Communication, Driver Characteristics, and Controls Aspects of Cooperative Adaptive Cruise Control (CACC)," *IEEE Transactions on Intelligent Transportation Systems*, vol. 17, pp. 491–509, Feb 2016.

[2] C. Nowakowski, D. Thompson, S. E. Shladover, A. Kailas, and X.-Y. Lu, "Operational Concepts for Truck Cooperative Adaptive Cruise Control (CACC) Maneuvers," in *Transportation Research Board 95th Annual Meeting*, no. 16-4462, 2016.

[3] R. Warren, "Automated People-Movers," tech. rep., Transportation Research Board, 2012.

[4] J. Eickholt, "The Future of Transportation," tech. rep., Siemens, 2015.

[5] M. Lowson, "PRT for Airport Applications," Tech. Rep. 05-0432, TRB 84th Annual Meeting, 2005.

[6] T. S. Catapult, "Planning and Preparing for Connected and Automated Vehicles," tech. rep., Catapult Transportation Systems, 2016.

[7] S. Shladover, "PATH at 20-History and Major Milestones," *IEEE Trans. Intell. Transport. Sys.*, vol. 8, pp. 584 –592, dec. 2007.

[8] A. Dávila and M. Nombela, "SARTRE: SAfe Road TRains for the Environment," September 2010.

[9] A. Lari, F. Douma, and I. Onyiah, "Self-Driving Vehicles and Policy Implications: Current Status of Autonomous Vehicle Development and Minnesota Policy Implications," *Minnesota Journal of Law, Science & Technology*, vol. 16(2), no. 5, pp. 735–769, 2015.

[10] T. Litman, "Autonomous vehicle implementation predictions," *Victoria Transport Policy Institute*, vol. 28, 2014.

[11] K. H. Johansson, "Cyber-Physical Control of Road Freight Transport," in *2016 IEEE International Conference on Autonomic Computing (ICAC)*, pp. 4–4, July 2016.

[12] R. Janssen, H. Zwijnenberg, I. Blankers, and J. de Kruijff, "Truck Platoon; Driving the Future of Transportation," tech. rep., TNO, Mar. 2015.

[13] "Fast Facts U.S. Transportation Sector Greenhouse Gas Emissions 1990-2014," Tech. Rep. EPA-420-F-16-020, Enivronmental Protection Agency, June 2016.

[14] B. Besselink and K. H. Johansson, "Control of platoons of heavy-duty vehicles using a delay-based spacing policy," *IFAC-PapersOnLine*, vol. 48, no. 12, pp. 364–369, 2015.

[15] R. Rajamani, *Vehicle Dynamics and Control*. Springer, 2012.

[16] J. Ploeg, A. F. A. Serrarens, and G. J. Heijenk, "Connect & drive: design and evaluation of cooperative adaptive cruise control for congestion reduction," *Journal of Modern Transportation*, vol. 19, no. 3, pp. 207–213, 2011.

[17] J. Hederick, M. Tomizuka, and P. Varaiya, "Control Issues in Automated Highway Systems," *IEEE Control Systems*, vol. 14, pp. 21–32, 1994.

[18] D. V. A. H. G. Swaroop, *String stability of interconnected systems: An application to platooning in automated highway systems*. PhD thesis, University of California, Berkeley, CA, 1994.

[19] D. Swaroop, J. Hedrick, C. Chien, and P. Ioannou, "A comparision of spacing and headway control laws for automatically controlled vehicles," *Vehicle System Dynamics*, vol. 23, no. 1, pp. 597–625, 1994.

[20] P. Seiler, A. Pant, and K. Hedrick, "Disturbance propagation in vehicle strings," *IEEE Transactions on Automatic Control*, vol. 49, pp. 1835–1842, Oct 2004.

[21] M. E. Khatir and E. J. Davison, "Decentralized control of a large platoon of vehicles using non-identical controllers," in *Proceedings of the 2004 American Control Conference*, vol. 3, pp. 2769–2776 vol.3, June 2004.

[22] D. Swaroop and J. K. Hedrick, "Constant Spacing Strategies for Platooning in Automated Highway Systems," *ASME. J. Dyn. Sys., Meas., Control.*, vol. 121, pp. 462–470, 1999.

[23] P. A. Ioannou and C.-C. Chien, "Autonomous intelligent cruise control," *IEEE Transactions on Vehicular Technology*, vol. 42, no. 4, pp. 657–672, 1993.

[24] J. B. Michael, D. N. Godbole, J. Lygeros, and R. Sengupta, "Capacity Analysis of Traffic Flow Over a Single-Lane Automated Highway SystemâŃŹ," *Journal of Intelligent Transportation System*, vol. 4, no. 1-2, pp. 49–80, 1998.

[25] H. E. Sungu, M. Inoue, and J.-i. Imura, "Nonlinear spacing policy based vehicle platoon control for local string stability and global traffic flow stability," in *European Control Conference*, pp. 3396–3401, 2015.

[26] I. G. Jin, S. S. Avedisov, and G. Orosz, "Stability of connected vehicle platoons with delayed acceleration feedback," in *ASME 2013 Dynamic Systems and Control Conference*, pp. V002T30A006–V002T30A006, American Society of Mechanical Engineers, 2013.

[27] K. C. Chu, "Decentralized Control of High-Speed Vehicular Strings," *Transportation Science*, vol. 8, pp. 361–384, Nov. 1974.

[28] S. Chang, "Temporal stability of n-dimensional linear processors and its applications," *IEEE Transactions on Circuits and Systems*, vol. 27, pp. 716–719, Aug 1980.

[29] X. Liu, A. Goldsmith, S. S. Mahal, and J. K. Hedrick, "Effects of communication delay on string stability in vehicle platoons," in *Procs. of IEEE Intelligent Transportation Systems*, pp. 625–630, August 2001.

[30] S. Oncu, N. van de Wouw, W. Heemels, and H. Nijmeijer, "String stability of interconnected vehicles under communication constraints," in *IEEE 51st Annual Conference on Decision and Control (CDC)*, pp. 2459–2464, IEEE, 2012.

[31] S. Klinge and R. H. Middleton, ""string stability analysis of homogeneous linear unidirectionally connected systems with nonzero initial conditions"," in *Procs. of IET Irish Signals and Systems Conference*, pp. 1–6, December 2009.

[32] D. Swaroop and J. K. Hedrick, "String stability of interconnected systems," *IEEE Transactions on Automatic Control*, vol. 41, pp. 349–357, Mar 1996.

[33] R. Rajamani and C. Zhu, "Semi-autonomous adaptive cruise control systems," *IEEE Transactions on Vehicular Technology*, vol. 51, pp. 1186–1192, Sep 2002.

[34] D. Swaroop and K. R. Rajagopal, "A review of constant time headway policy for automatic vehicle following," in *IEEE Proceedings of Intelligent Transportation Systems*, pp. 65–69, 2001.

[35] J. V. Werf, S. Shladover, M. Miller, and N. Kourjanskaia, "Effects of Adaptive Cruise Control Systems on Highway Traffic Flow Capacity," *Transportation Research Record: Journal of the Transportation Research Board*, vol. 1800, pp. 78–84, 2002.

[36] V. Milanes, S. E. Shladover, J. Spring, C. Nowakowski, H. Kawazoe, and M. Nakamura, "Cooperative Adaptive Cruise Control in Real Traffic Situations," *IEEE Transactions on Intelligent Transportation Systems*, vol. 15, pp. 296–305, Feb 2014.

[37] G. J. L. Naus, R. P. A. Vugts, J. Ploeg, M. J. G. van de Molengraft, and M. Steinbuch, "String-Stable CACC Design and Experimental Validation: A Frequency-Domain Approach," *IEEE Transactions on Vehicular Technology*, vol. 59, pp. 4268–4279, Nov 2010.

[38] L. I., A. Festag, and G. Fettweis, "Vehicular Communication Performance in Convoys of Automated Vehicles," in *IEEE ICC 2016 Ad-hoc and Sensor Networking Symposium*, IEEE, 2016.

[39] J. I. Ge and G. Orosz, "Dynamics of connected vehicle systems with delayed acceleration feedback," *Transportation Research Part C: Emerging Technologies*, vol. 46, pp. 46 – 64, 2014.

[40] D. Swaroop and S. M. Yoon, "Integrated lateral and longitudinal vehicle control for an emergency lane change manoeuvre design," *International Journal of Vehicle Design*, vol. 21, no. 2-3, pp. 161–174, 1999.

[41] S. Darbha and W. Choi, "A Methodology for Assessing the Benefits of Coordination on the Safety of Vehicles," *Journal of Intelligent Transportation Systems*, vol. 16, no. 2, pp. 70–81, 2012.

[42] D. Tian, J. Zhou, Y. Wang, Z. Sheng, H. Xia, and Z. Yi, "Modeling chain collisions in vehicular networks with variable penetration rates," *Transportation Research Part C: Emerging Technologies*, vol. 69, pp. 36 – 59, 2016.

[43] A. Chakravarthy, K. Song, and E. Feron, "Preventing Automotive Pileup Crashes in Mixed-Communication Environments," *IEEE Transactions on Intelligent Transportation Systems*, vol. 10, pp. 211–225, June 2009.

[44] S. Tak, S. Kim, and H. Yeo, "A Study on the Traffic Predictive Cruise Control Strategy With Downstream Traffic Information," *IEEE Transactions on Intelligent Trans-*

portation Systems, vol. 17, pp. 1932–1943, July 2016.

[45] S. Oncu and J. Ploeg and N. van de Wouw and H. Nijmeijer, "Cooperative Adaptive Cruise Control: Network-Aware Analysis of String Stability," *IEEE Transactions on Intelligent Transportation Systems*, vol. 15, pp. 1527–1537, Aug 2014.

[46] J. A. Marshall, M. E. Broucke, and B. A. Francis, "Formations of Vehicles in Cyclic Pursuit," *IEEE Trans. on Automat. Contr.*, vol. 49, pp. 1963–1974, November 2004.

[47] K. Galloway, E. Justh, and P. Krishnaprasad, "Geometry of cyclic pursuit," in *Procs. of IEEE Conference on Decision and Control*, pp. 7485 –7490, December 2009.

[48] J. A. Rogge and D. Aeyels, "Vehicle Platoons Through Ring Coupling," *IEEE Trans. on Automat. Contr.*, vol. 53, pp. 1370–1378, July 2008.

[49] S. Konduri, P. R. Pagilla, and S. Darbha, "Vehicle formations using directed information flow graphs," in *American Control Conference (ACC), 2013*, pp. 3045–3050, 2013.

[50] S. Konduri, P. R. Pagilla, and S. Darbha, "Vehicle Platooning with Multiple Vehicle Look-ahead Information," in *To be presented at IFAC World Congress 2017.*

[51] S. Darbha, S. Konduri, and P. R. Pagilla, "Effects of V2V Communication on Time Headway for Autonomous Vehicles," in *American Control Conference*, May 2017.

[52] S. Konduri, P. R. Pagilla, and S. Darbha, "A combinatorial approach for developing ring communication graphs for vehicle formations," *ASME. J. Dyn. Sys., Meas., Control.*, 2017.

[53] S. Konduri, P. R. Pagilla, and S. Darbha, "Reconfiguration of a vehicle formation with ring communication structure," in *European Controls Conference*, 2016.

[54] L. Xiao and F. Gao, "Practical String Stability of Platoon of Adaptive Cruise Control Vehicles," *IEEE Trans. Intell. Transport. Sys.*, vol. 12, pp. 1184–1194, Dec. 2011. Very useful for the benefits paper. Definitely cite.

[55] M. R. I. Nieuwenhuijze, "String Stability Analysis of Bidirectional Adaptive Cruise Control," 2010.

[56] S. Yadlapalli, S. Darbha, and K. Rajagopal, "Information flow and its relation to stability of the motion of vehicles in a rigid formation," *IEEE Trans. on Automat. Contr.*, vol. 51, pp. 1315 –1319, aug. 2006.

[57] S. Darbha and P. R. Pagilla, "Limitations of employing undirected information flow graphs for the maintenance of rigid formations for heterogeneous vehicles," *International Journal of Engineering Science*, vol. 48, no. 11, pp. 1164 – 1178, 2010.

[58] A. Firooznia, J. Ploeg, N. van de Wouw, and H. Zwart, "Co-Design of Controller and Communication Topology for Vehicular Platooning," *IEEE Transactions on Intelligent Transportation Systems*, vol. PP, no. 99, pp. 1–12, 2017.

[59] C. Desoer and M. Vidyasagar, *Feedback Systems: Input-output Properties*. Classics in Applied Mathematics, Society for Industrial and Applied Mathematics (SIAM, 3600 Market Street, Floor 6, Philadelphia, PA 19104), 1975.

[60] B. Bamieh, F. Paganini, and M. A. Dahleh, "Distributed control of spatially invariant systems," *IEEE Transactions on Automatic Control*, vol. 47, pp. 1091–1107, Jul 2002.

[61] S.-K. Lin and C.-J. Fang, "Nonovershooting and monotone nondecreasing step responses of a third-order siso linear system," *IEEE Transactions on Automatic Control*, vol. 42, pp. 1299–1303, Sep 1997.

[62] R. M. Gray, "Toeplitz and Circulant Matrices: A review," tech. rep., Stanford University, 2006.

[63] T. D. Mazancourt and D. Gerlic, "The inverse of a block-circulant matrix," *IEEE Trans. on Antennas and Propagation*, vol. 31, pp. 808–810, Sep 1983.

[64] S. Konduri, "Coordination of multiple autonomous vehicles with directed communication graphs," Master's thesis, Oklahoma State University, Stillwater, OK, USA, 2012.

[65] S. Konduri and P. R. Pagilla, "On vehicle formations with ring structured communication graphs," in *2013 IEEE International Conference on Control Applications (CCA)*, pp. 1206–1211, Aug 2013.

[66] T. M. J. Fruchterman and E. M. Reingold, "Graph Drawing by Force-directed Placement," *Softw. Pract. Exper.*, vol. 21, pp. 1129–1164, Nov. 1991.

[67] T. Dwyer, Y. Koren, and K. Marriott, "Drawing directed graphs using quadratic programming," *IEEE Trans. on Visualization and Computer Graphics*, vol. 12, pp. 536–548, July 2006.

[68] G. Reinelt, *The Traveling Salesman: Computational Solutions for TSP Applications*. Berlin, Heidelberg: Springer-Verlag, 1994.

[69] L. Navaravong, J. Shea, E. Pasiliao, and W. Dixon, "Optimizing network topology to reduce aggregate traffic in a system of mobile robots under an energy constraint," in *IEEE International Conference on Communications*, pp. 16–20, June 2012.

[70] C. Archetti, L. Bertazzi, and M. G. Speranza, "Reoptimizing the traveling salesman problem," *Networks*, vol. 42, no. 3, pp. 154–159, 2003.

[71] S. Konduri, E. O. C. Torres, and P. R. Pagilla, "Dynamics and Control of a Differential Drive Robot With Wheel Slip: Application to Coordination of Multiple Robots," *ASME. J. Dyn. Sys., Meas., Control*, vol. 139, Nov 2016.

[72] Y. Kanayama, Y. Kimura, F. Miyazaki, and T. Noguchi, "A stable tracking control method for an autonomous mobile robot," in *IEEE International Conference on Robotics and Automation*, pp. 384 –389 vol.1, may 1990.